

**ON EMERGENT SONIC GEOMETRY THROUGH THE
LINEAR PERTURBATION OF RELATIVISTIC BLACK
HOLE ACCRETION**

By
MD. ARIF SHAIKH
PHYS08201205006

Harish-Chandra Research Institute, Prayagraj

*A thesis submitted to the
Board of Studies in Physical Sciences
In partial fulfillment of requirements
for the Degree of*
DOCTOR OF PHILOSOPHY
of
HOMI BHABHA NATIONAL INSTITUTE



June, 2019

Homi Bhabha National Institute¹

Recommendations of the Viva Voce Committee

As members of the Viva Voce Committee, we certify that we have read the dissertation prepared by Md. Arif Shaikh entitled "On emergent sonic geometry through the linear perturbation of relativistic black hole accretion " and recommend that it may be accepted as fulfilling the thesis requirement for the award of Degree of Doctor of Philosophy.

Chairman - Prof. S. Naik

S. Naik

Date: 18/11/19

Guide /Convener - Prof. Tapas Kumar Das

Tapas Kumar Das

Date: 18/11/2019

Examiner - Prof. Subir Ghosh

S. Ghosh

Date: 18/11/2019

Member 1- Prof. Pinaki Majumdar

Pinaki Majumdar

Date: 18.11.19.

Member 2 - Prof. Ujjwal Sen

Ujjwal Sen

Date: 18.11.19

Member 3 - Prof. Santosh Kumar Rai

Santosh Kumar Rai

Date: 18.11.19

Final approval and acceptance of this thesis is contingent upon the candidate's submission of the final copies of the thesis to HBNI.

I/We hereby certify that I/we have read this thesis prepared under my/our direction and recommend that it may be accepted as fulfilling the thesis requirement.

Date: 18.11.2019

Place: Prayagraj

Tapas Kumar Das

Prof. Tapas Kumar Das
Guide

¹ This page is to be included only for final submission after successful completion of viva voce.

STATEMENT BY AUTHOR

This dissertation has been submitted in partial fulfillment of requirements for an advanced degree at Homi Bhabha National Institute (HBNI) and is deposited in the Library to be made available to borrowers under rules of the HBNI.

Brief quotations from this dissertation are allowable without special permission, provided that accurate acknowledgement of source is made. Requests for permission for extended quotation from or reproduction of this manuscript in whole or in part may be granted by the Competent Authority of HBNI when in his or her judgment the proposed use of the material is in the interests of scholarship. In all other instances, however, permission must be obtained from the author.

Md Arif Shaikh
Md. Arif Shaikh

DECLARATION

I, hereby declare that the investigation presented in the thesis has been carried out by me. The work is original and has not been submitted earlier as a whole or in part for a degree / diploma at this or any other Institution / University.

Md Arif Shaikh

Md. Arif Shaikh

List of Publications arising from the thesis

Journal

1. “Relativistic sonic geometry for isothermal accretion in the Schwarzschild metric”, Md Arif Shaikh, Ivleena Firdousi and Tapas Kumar Das, *Classical and Quantum Gravity*, **2017**, *34*, 155008.
2. “Relativistic sonic geometry for isothermal accretion in the Kerr metric”, Md Arif Shaikh, *Classical and Quantum Gravity*, **2018**, *35*, 055002.
3. “Linear perturbations of low angular momentum accretion flow in the Kerr metric and the corresponding emergent gravity phenomena”, Md Arif Shaikh and Tapas Kumar Das, *Physical Review D*, **2018**, *98*, 123022.
4. “Effective sound speed in relativistic accretion discs around Schwarzschild black holes”, Md Arif Shaikh, Susovan Maity, Sankhasubhra Nag and Tapas Kumar Das, *New Astronomy*, **2019**, *69*, 48-57.

List of Publications not included in the thesis

Journal

1. “Acoustic geometry obtained through the perturbation of the Bernoulli’s constant”, Satadal Datta, Md Arif Shaikh and Tapas Kumar Das, *New Astronomy*, **2018**, *63*, 65-74.

Conferences

1. “Emergence of relativistic sonic geometry through perturbation of matter in black hole metric”, 35th meeting of Astronomical Society of India (ASI), Jaipur, 6–10 March 2017. (Poster presentation)
2. “Relativistic sonic geometry for isothermal accretion in Kerr metric”, 29th meeting of Indian Association of General Relativity and Gravitation (IAGRG), IIT Guwahati, 18–20 May 2017. (Poster presentation)

3. "Emergence of curved sonic manifold for isothermal accretion in black hole metric", Young Astronomers Meet, IUCAA, Pune, 11–15 September 2017. (Oral presentation)
4. "Relativistic acoustic geometry in general relativistic accretion disc around Kerr black holes", Exploring the Universe: Near Earth Space Science to Extra-Galactic Astronomy, S N Bose National Centre for Basic Sciences, Kolkata, 14–17 November 2018. (Oral presentation)

Md Arif Shaikh

Md Arif Shaikh

ACKNOWLEDGEMENTS

I take this opportunity to thank my supervisor Prof. Tapas K. Das for his constant guidance, support and encouragement throughout the last five years. I am extremely grateful for the innumerable discussions between us ranging from purely academic to non-academic topics which have enriched me not only as a researcher but as a human being also. It would not have been possible for me to finish the thesis without the support and flexibility that I enjoyed as a PhD student.

Besides my supervisor, I would like to thank the members of the thesis committee: Prof Satchitananda Naik, Prof. Pinaki Majumdar, Prof. Ujjwal Sen and Prof. Santosh Kumar Rai, for their insightful comments and encouragement. I also thank all the faculties of the physics department at HRI who have helped me to learn a lot during the course work. I thank my M.Sc project instructors, Prof J. K. Bhattacharjee, Prof. Rajesh Gopakumar, Prof. Pinaki Majumdar and Prof. Ashoke Sen.

I would like to thank Prof Sankhasubhra Nag for many interesting discussions during several visits to Sarojini Naidu College for Women, Kolkata. I thank Prof. P. Ajith for several visits to ICTS, Bengaluru during which I have learnt a lot.

I thank my friends, seniors and juniors at HRI who have made my stay at HRI for the last seven years enjoyable. I especially thank the members of the astrophysics group: Satadal, Susovan, Pratik da and Safikul da. I thank my friend Riasen for always being there to help me out.

I thank Maa and my other family members for always being there for me and supporting me.

I thank my wife for being so loving, caring and supportive, for bearing my constant and boring complaints and for always being there to encourage me and motivate me to achieve more.

Contents

Summary	1
List of Figures	4
List of Tables	5
1 Aspects of analogue gravity	7
1.1 Acoustic spacetime in Newtonian transonic fluids	8
1.1.1 Linearization of fluid equations	9
1.1.2 The acoustic spacetime metric and horizon	10
1.1.3 Causal structure of the acoustic spacetime	13
1.1.4 Acoustic surface gravity	20
1.2 Black hole accretion as analogue gravity model	21
2 Aspects of black hole accretion	25
2.1 Accretion flow geometry	25
2.2 Stationary low angular momentum accretion flow	27
2.3 Linear perturbation, stability analysis and analogue gravity	29
3 Relativistic sonic geometry for isothermal accretion in the Schwarzschild metric	31
3.1 Governing equations	32
3.2 Velocity potential, mass accretion rate and the relativistic Bernoulli's constant	33
3.2.1 Velocity potential	33

3.2.2	Relativistic Bernoulli's constant	34
3.2.3	Mass accretion rate	36
3.3	The acoustic metric from linear perturbation analysis	39
3.3.1	Linear perturbation of Michel flow	40
3.3.2	Linear perturbation of axially symmetric flow	45
3.3.3	Acoustic metric	50
3.4	Location of the acoustic horizon	54
3.4.1	Michel flow	54
3.4.2	Axially symmetric flow	55
3.5	Causal structure	56
3.5.1	Causal structure for Michel flow	57
3.5.2	Causal structure for axially symmetric flow	61
3.6	Acoustic surface gravity	66
3.6.1	Acoustic surface gravity for Michel flow	66
3.6.2	Acoustic surface gravity for axially symmetric flow	67
3.7	Critical points and the transonic points in VE model	68
4	Relativistic sonic geomtry for isothermal accretion in the Kerr metric	71
4.1	Basic set up	72
4.2	Linear perturbation of velocity potential, mass accretion rate and the relativistic Bernoulli's constant	74
4.2.1	Linear perturbation of velocity potential	75
4.2.2	Linear perturbation of mass accretion rate	76
4.2.3	Linear perturbation of relativistic Bernoulli's constant	79
4.3	Acoustic metric	81
4.4	Location of the acoustic event horizon	82
4.4.1	Choice of parameters $[T, \lambda_0, a]$	83
4.4.2	Dependence of the acoustic event horizon of $[T, \lambda_0, a]$	86
4.5	Causal structure of the acoustic spacetime	90
4.6	Acoustic surface gravity	95
4.7	Effect of the presence of dissipative mechanism	98

5	Relativistic sonic geomtry for adiabatic accretion in the Kerr metric	99
5.1	Introduction	99
5.2	Basic equations governing the flow	100
5.3	Accretion flow geometry	101
5.4	Linear perturbation analysis and the acoustic geometry	102
5.4.1	Linear perturbation of mass accretion rate	104
5.4.2	The acoustic metric	107
5.5	Location of the acoustic event horizon	107
5.6	Causal structure of the acoustic spacetime	108
5.6.1	Equations for u'_0 and c'_{s0}	109
5.6.2	Mono-transonic case	112
5.6.3	Multi-transonic case	113
5.7	Acoustic surface gravity	118
5.8	Higher order perturbations and non-stationary flow	118
6	Linear stability analysis of stationary accretion flow in the Kerr metric	121
6.1	Standing wave analysis	122
6.2	Traveling wave analysis	124
7	Effective sound speed in relativistic accretion discs around Schwarzschild black holes	129
7.1	Introduction	129
7.2	Governing equations	134
7.3	Accretion disc models and critical points	134
7.3.1	Models of accretion disc under vertical equilibrium	136
7.3.2	Novikov-Thorne (NT)	138
7.3.3	Riffert-Herold (RH)	139
7.3.4	Abramowicz-Lanza-Percival (ALP)	140
7.4	Acoustic spacetime metric	141
7.4.1	Acoustic metric for adiabatic flow	143
7.4.2	Acoustic metric for isothermal flow	145

7.5	Effective speed of acoustic perturbation	146
7.6	In closing	149
8	Concluding remarks	153
8.1	Non-linear perturbations and acoustic spacetime	153
8.2	Effective sound speed in accretion disc around Kerr black holes . . .	156
8.3	Brief summary	156
	Bibliography	159

Summary

Linear perturbation of relativistic accretion on to black holes leads to the emergence of an embedded curved acoustic geometry. The acoustic perturbations are governed by this emergent sonic geometry. Such emergent acoustic spacetime could be studied to gain knowledge about different interesting properties of curved spacetime as the metric possesses many properties which are analogous to the kinematic properties of general relativistic spacetime. Such analogous properties which are found in an acoustic spacetime includes a sonic horizon and corresponding acoustic Hawking radiation in the form of a thermal spectrum of sound quanta emitting from the sonic horizon. Below we list the main results of our study:

- The emergence of acoustic geometry is independent of the physical quantity in terms of which we obtain the perturbation equation that is compared to the equation of massless scalar field in curved spacetime. For particular geometrical configuration of the accreting matter, linear perturbation of the velocity potential, the mass accretion rate and the relativistic Bernoulli's constant give rise to the same acoustic spacetime metric up to a conformal factor.
- The acoustic spacetime metric depends on the geometrical configuration of the accreting matter quite sensitively. The acoustic spacetime metric for constant height flow and conical flow are the same but differs for accretion disc under hydrostatic equilibrium along the vertical direction.
- Location of the acoustic horizon coincides with the critical points of the stationary accretion flow. Critical points are defined as the place where the gradient of the 'advective velocity' has 0/0 form. Depending on the geomet-

rical configuration of the accreting matter, the critical points and hence the acoustic horizon may or may not be isomorphic to the transonic surface. For constant height flow and the conical flow, acoustic horizon and the transonic surface are coincidental but for a disc, under vertical equilibrium, they are located at different points.

- The causal structure of the acoustic spacetime constructed by the null sound rays clearly shows the location of acoustic horizon and tilting of the sound cones.
- Axially symmetric accretion flow could encounter a stationary shock. In such cases, the flow becomes multi-transonic. The flow starts subsonically at large radial distance and becomes supersonic at the outer sonic point. After that, it encounters a shock and becomes subsonic. The subsonic flow then again becomes supersonic at the inner sonic point. The causal structure of the acoustic spacetime corresponding to such multi-transonic shocked accretion flow shows that the shock location could be interpreted as an acoustic white hole horizon.
- The acoustic surface gravity is proportional to the gradient of the ‘advective velocity’ minus the gradient of the sound speed evaluated at the acoustic horizon.
- Standing and travelling wave analysis of the perturbation equation implies that the stationary accretion solutions are stable under linear perturbation.
- For disc under vertical equilibrium, the transonic surface is not identical to the acoustic horizon. This is due to the fact that the speed of the acoustic perturbation in such a system is not exactly equal to the local sound speed. It is possible to define an effective sound speed which is the speed of the propagation of the acoustic perturbation. The transonic surface defined in terms of this effective sound speed coincides with the acoustic horizon.

List of Figures

1.1	An artistic impression of cascading sound cones in the geometrical limit	13
1.2	An artistic impression of trapped waves in the physical acoustic limit	14
1.3	Tilting of sound cones in moving fluid	14
1.4	A left-going velocity profile	16
1.5	Acoustic black hole and causal structure of acoustic spacetime in left-going velocity profile	17
1.6	A right-going velocity profile	18
1.7	Acoustic black hole and causal structure of acoustic spacetime in right-going velocity profile	19
3.1	Mach number vs radius plot and the corresponding causal structure of the acoustic spacetime in Michel flow	60
3.2	Phase portraits for multi-transonic axisymmetric accretion and it's corresponding causal structures	64
4.1	Parameter space allowing multiple critical points for different temperatures	84
4.2	Variation of inner acoustic horizon with black hole spin for different sets of temperature and angular momentum	87
4.3	Variation of outer acoustic horizon with black hole spin for different sets of temperature and angular momentum	89
4.4	Phase portraits for shocked multi-transonic axially symmetric isothermal accretion for different sets of values of temperature, angular mo-	

List of Tables

7.1	Values of β for different disc structure models	142
-----	---	-----

1

Aspects of analogue gravity

It was the seminal work of Unruh [1] that led to a new area of research known as the analogue gravity phenomenon. In the last few decades, the field has expanded hugely and encompasses a diverse list of physical systems where analogue gravity phenomena could be studied. An analogue model of gravity possesses interesting properties which are analogue counterparts of properties found in general relativity. The most important of such properties is the existence of an acoustic event horizon similar to the gravitational event horizon of a black hole in general relativity. An acoustic event horizon is the boundary of an acoustic black hole or the so-called “dumb hole” [2] from which acoustic waves cannot escape to the outside similar to the case of the event horizon of a black hole from which light can not escape to the outside.

By studying the behaviour of quantum fields in the background (classical) curved spacetime near the event horizon, Hawking predicted that a black hole is not entirely black and it actually radiates as a black body with a thermal spectrum of Planckian distribution with a temperature T_H [3]. This is a striking result which comes out as a consequence of treating the fields as quantum fields and thus provides a way to test the ultimate theory of quantum gravity which is yet to be well understood. Though this result of Hawking was derived in the context of black hole spacetime, such Hawking-like effect is not exclusive to black holes in general relativity. Hawking-like effect could be seen in other systems (where there is no effect of general relativity)

also. As the Hawking radiation is a kinematic effect, the only requirement for the Hawking-like effect is the existence of a Lorentzian metric with some sort of a horizon[4].

Analogue gravity systems, because of the presence of the acoustic spacetime and the acoustic event horizon, thus provides a platform where Hawking-like effect, henceforth called analogue Hawking radiation, could be observed. Unruh, in his paper [1], showed that in a Newtonian (non-relativistic flat spacetime) system of transonic fluid there exists an acoustic horizon and a thermal spectrum of acoustic quanta may be radiated from the acoustic horizon in the same way Hawking radiation is emitted from the event horizon of black holes. The analogue Hawking temperature T_{AH} of the emitted radiation is given by the same formula as in Hawking radiation with the only difference that the black hole surface gravity is replaced by acoustic surface gravity κ which is proportional to the gradient of the velocity of the transonic fluid at the acoustic horizon. Thus by exploring analogue gravity systems, we are able to look into different aspects of curved spacetime in a laboratory set up. Below, we provide a brief account of the emergence of acoustic spacetime in a Newtonian fluid system.

1.1 Acoustic spacetime in Newtonian transonic fluids

The following treatment is borrowed from [5]. We consider a barotropic, inviscid and irrotational fluid in Newtonian background. Such a fluid is governed by the continuity equation

$$\partial_t \rho + \nabla \cdot (\rho \vec{v}) = 0, \quad (1.1)$$

and the Euler equation

$$\partial_t \vec{v} + (\vec{v} \cdot \nabla) \vec{v} + \frac{1}{\rho} \nabla p + \nabla \phi + \nabla \Phi = 0. \quad (1.2)$$

where, \vec{v} is the velocity of the fluid, ρ is the density of the fluid, p is the pressure of the fluid, ϕ is the gravitational potential and Φ is the potential for any external

force. Eq. (1.2) can be rewritten in the following form

$$\partial_t \vec{v} - \vec{v} \times (\nabla \times \vec{v}) + \frac{1}{\rho} \nabla p + \nabla \left(\frac{1}{2} v^2 + \phi + \Phi \right) = 0. \quad (1.3)$$

The fluid being irrotational, the second term in the above equation vanishes. Further, we can introduce a potential field ψ in the fluid which is defined by the relation $\vec{v} = -\nabla\psi$. ψ is generally called the velocity potential. Also due to the assumption that the fluid is barotropic, i.e., the density is a function of the pressure only, we can define the specific enthalpy of the fluid as

$$h(p) = \int_0^p \frac{dp'}{\rho(p')}. \quad (1.4)$$

Eq. (1.4) implies that $\nabla h = (1/\rho)\nabla p$. Thus, the Euler Eq. (1.3) reduces to

$$-\partial_t \psi + h + \frac{1}{2} (\nabla \psi)^2 + \phi + \Phi = 0. \quad (1.5)$$

1.1.1 Linearization of fluid equations

We linearize the fluid equations given by Eq. (1.1) and (1.5) about some stationary background (ρ_0, p_0, ψ_0) . We write the fluid variables as sum of its background value plus some small fluctuations of linear order,

$$\begin{aligned} \rho &= \rho_0 + \rho_1 \\ p &= p_0 + p_1 \\ \psi &= \psi_0 + \psi_1 \end{aligned} \quad (1.6)$$

Using the above equation in the Eq. (1.1) and (1.5) and collecting the terms that are linear in the fluctuations gives the following equations

$$\partial_t \rho_1 + \nabla \cdot (\rho_1 \vec{v}_0 + \rho_0 \vec{v}_1) = 0 \quad (1.7)$$

$$-\partial_t \psi_1 + \frac{p_1}{\rho_0} - \vec{v}_0 \cdot \nabla \psi_1 = 0. \quad (1.8)$$

In deriving the Eq. (1.8), we have used the linearization of the specific enthalpy with the use of the barotropic equation of state, i.e.,

$$h(p) = h(p_0 + p_1) = h_0 + \frac{p_1}{\rho_0}. \quad (1.9)$$

We have also assumed that the external as well as the gravitational force are constant hence there are no fluctuations from those terms. Eq. (1.8) gives p_1 in terms of ψ_1 and the background variables. Now the local sound speed is defined by the relation

$$c_{s0}^2 = \frac{\partial p}{\partial \rho}, \quad (1.10)$$

and from the barotropic relation we have $p_1 = c_{s0}^2 \rho_1$. Thus, from Eq. (1.8) we obtain ρ_1 in terms of ψ_1 and other background variables as

$$\rho_1 = \frac{\rho_0}{c_{s0}^2} (\partial_t \psi_1 + \vec{v}_0 \cdot \nabla \psi_1). \quad (1.11)$$

Now using the above equation in the linearized continuity equation, i.e., Eq. (1.7) provides the following wave equation

$$-\partial_t \left[\frac{\rho_0}{c_{s0}^2} (\partial_t \psi_1 + \vec{v}_0 \cdot \nabla \psi_1) \right] + \nabla \cdot \left[\rho_0 \nabla \psi_1 - \frac{\rho_0}{c_{s0}^2} \vec{v}_0 (\partial_t \psi_1 + \vec{v}_0 \cdot \nabla \psi_1) \right] = 0. \quad (1.12)$$

The above wave equation describes the propagation of the linearized scalar field ψ_1 . Once this equation is solved for ψ_1 , one can easily find ρ_1 and p_1 also. Thus the above wave equation completely describes the propagation of acoustic perturbation in the fluid.

1.1.2 The acoustic spacetime metric and horizon

Eq. (1.12) can be written in a compact form if we define a symmetric 4×4 matrix $f^{\mu\nu}$ as

$$f^{\mu\nu} = \frac{\rho_0}{c_{s0}^2} \begin{bmatrix} -1 & \vdots & -v_0^j \\ \dots & \cdot & \dots \\ -v_0^i & \vdots & (c_{s0}^2 \delta^{ij} - v_0^i v_0^j) \end{bmatrix}. \quad (1.13)$$

Then Eq. (1.12) can be rewritten as

$$\partial_\mu (f^{\mu\nu} \partial_\nu \psi_1) = 0. \quad (1.14)$$

Here, μ, ν runs from 0 to 1 and the i, j runs from 1 to 3 and $(1 + 3)$ dimensional spacetime coordinates are given by $x^\mu = (t, x^i)$. Now, the equation of propagation of a scalar field φ in curved spacetime metric $g_{\mu\nu}$ is given by the equation

$\partial_\mu(\sqrt{-g}g^{\mu\nu}\partial_\nu\varphi) = 0$, where g is the determinant of the metric $g_{\mu\nu}$. Thus an acoustic spacetime time metric $G_{\mu\nu}$ is could be defined by the relation

$$\sqrt{-G}G^{\mu\nu} \equiv f^{\mu\nu}, \quad (1.15)$$

where G is the determinant of the acoustic metric $G_{\mu\nu}$. G can be determined by taking determinant of both of the sides in Eq. (1.17) which gives

$$(\sqrt{-G})^4 G^{-1} = \det(f^{\mu\nu}) \Rightarrow G = \det(f^{\mu\nu}). \quad (1.16)$$

From the Eq. (1.13), we find $\det(f^{\mu\nu}) = -\rho_0^4/c_{s0}^2$ and there $G = -\rho_0^4/c_{s0}^2$ and $\sqrt{-G} = \rho_0^2/c_{s0}$. Therefore, we also find the inverse metric $G^{\mu\nu}$ to be given by

$$G^{\mu\nu} = \frac{1}{\rho_0 c_{s0}} \begin{bmatrix} -1 & \vdots & -v_0^j \\ \dots & \cdot & \dots \\ -v_0^i & \vdots & (c_{s0}^2 \delta^{ij} - v_0^i v_0^j) \end{bmatrix}. \quad (1.17)$$

and the acoustic metric $G_{\mu\nu}$ itself is found by intervtng the above matrix and is given by

$$G_{\mu\nu} = \frac{\rho_0}{c_{s0}} \begin{bmatrix} -(c_{s0}^2 - v_0^2) & \vdots & -v_0^j \\ \dots & \cdot & \dots \\ -v_0^i & \vdots & \delta^{ij} \end{bmatrix}. \quad (1.18)$$

Thus, the acoustic line element could be given as

$$ds^2 = G_{\mu\nu} dx^\mu dx^\nu = \frac{\rho_0}{c_{s0}} [-(c_{s0}^2 - v_0^2) dt^2 - 2\vec{v}_0 \cdot d\vec{x} dt + (d\vec{x})^2]. \quad (1.19)$$

Defining a new time coordinate τ by

$$d\tau = dt + \frac{\vec{v}_0 \cdot d\vec{x}}{c_{s0}^2 - v_0^2}, \quad (1.20)$$

the line element could be written as [2, 5]

$$ds^2 = \frac{\rho_0}{c_{s0}} \left[-(c_{s0}^2 - v_0^2) d\tau^2 + \left(\delta_{ij} + \frac{v_0^i v_0^j}{c_{s0}^2 - v_0^2} \right) dx^i dx^j \right]. \quad (1.21)$$

It is assumed that the vector $\frac{\vec{v}_0}{c_{s0}^2 - v_0^2}$ is integrable. From the above expression of the line element, it is clear that the corresponding acoustic metric is static, i.e., it

is stationary (time-independent) and the time-translation Killing vector is hyper-surface orthogonal as there is no time-space cross terms. If the background flow is spherically symmetric then Eq. (1.21) can be further written in terms of the spherical polar coordinates as [1]

$$ds^2 = \frac{\rho_0}{c_{s0}} \left[-(c_{s0}^2 - v_0^2) d\tau^2 + \frac{c_{s0}^2}{c_{s0}^2 - v_0^2} dr^2 + r^2(d\theta^2 + \sin^2\theta d\phi^2) \right]. \quad (1.22)$$

The above line element has the similar form of the Schwarzschild metric.

The acoustic event horizon is defined as the boundary of the region from which null geodesics (here phonons) cannot escape. For the line element in Eq. (1.22), the acoustic event horizon is located at $v_0^2 = c_{s0}^2$. Thus the event horizon is the transonic surface of the fluid flow. The ergosphere is defined as the surface where the norm of the time-like Killing vector changes the sign and the Killing vector becomes space-like in the region inside the ergosphere. If the background fluid flow is steady, then the acoustic metric is time-independent and hence there exist a time-like Killing vector $\xi^\mu = \delta_t^\mu$. Norm of the time-like Killing vector ξ^μ is given as

$$\xi_\mu \xi^\mu = G_{\mu\nu} \xi^\mu \xi^\nu = G_{\mu\nu} \delta_t^\mu \delta_t^\nu = G_{tt} = -\frac{\rho_0}{c_{s0}^2} (c_{s0}^2 - v_0^2). \quad (1.23)$$

Thus the norm changes sign at $v_0^2 = c_{s0}^2$. Therefore, any region of supersonic flow can be regarded as ergo-region. For a general spacetime time metric, the ergosphere and the event horizon are not the same. However, for a static metric, these two surfaces coincide. For example, in general relativity, in the static Schwarzschild spacetime, event horizon and the ergosphere are basically the same surfaces. However, in the stationary but non-static Kerr spacetime, the ergosphere and the event horizon are two different surfaces. The event horizon of the Kerr black hole resides inside the ergosphere. Therefore, for an acoustic spacetime metric which is non-static, the event horizon would be different from the ergosphere and one has to use particular tools to define the event horizon (for example, see [6] for such details). For our present work, the acoustic metrics are found to be static and thus we can easily locate the acoustic event horizon. If spacetime is stationary, asymptotically flat and the event horizon has spherical topology, then the event horizon could be located easily in a suitable coordinate system [7]. In such spacetime, the event horizon is a

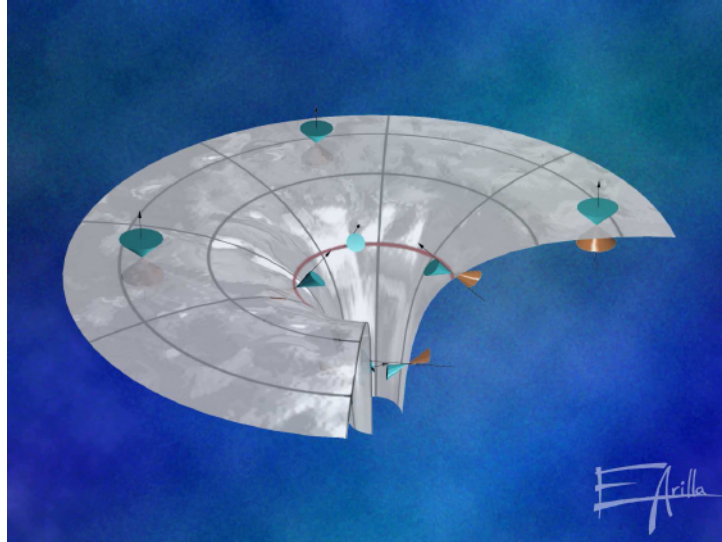


Figure 1.1: An artistic impression of cascading sound cones in the geometrical limit. Supersonic flow tilts the sound cone past the vertical at the horizon and forms an acoustic black hole. *Image courtesy: [8].*

$r = \text{constant}$ hypersurface which is null. We shall use such an approach to locate the event horizon in our work.

Fig. 1.1 shows an artistic impression of cascading sound cones in the geometrical limit. Supersonic flow tilts the sound cone past the vertical at the horizon and forms an acoustic black hole. Fig. 1.2 shows an artistic impression of trapped waves in the physical acoustic limit. Supersonic flow forces the waves to move downstream inside the acoustic horizon. Fig. 1.3 shows how the sound cone is tilted as the fluid becomes supersonic from the subsonic state. Fig. 1.1, 1.2, 1.3 have been taken from [8].

1.1.3 Causal structure of the acoustic spacetime

The tilting of the sound cone can be visualised by constructing the causal structure of the spacetime following the same procedures as found in general relativity. Some of the following treatments are taken from [9] and more detailed discussions on the causal structure of the acoustic Spacetime could be found there. For simplicity, let us consider the case where the perturbation propagates only in the x -direction. The

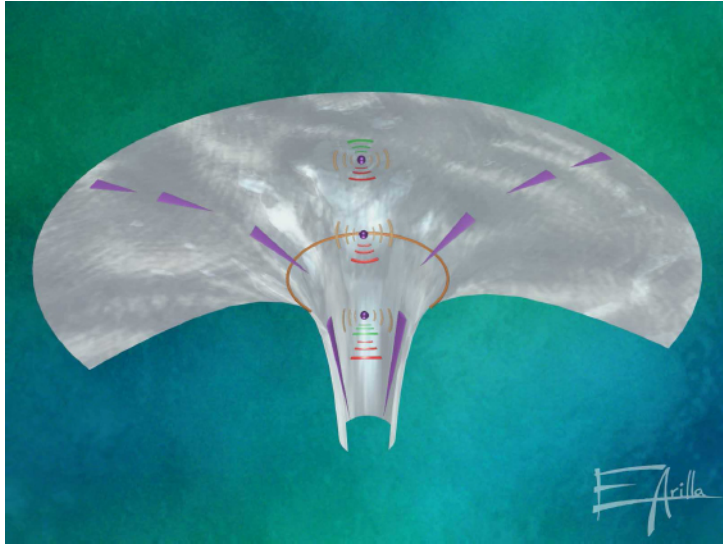


Figure 1.2: An artistic impression of trapped waves in the physical acoustic limit. Supersonic flow forces the waves to move downstream inside the acoustic horizon. *Image courtesy: [8].*

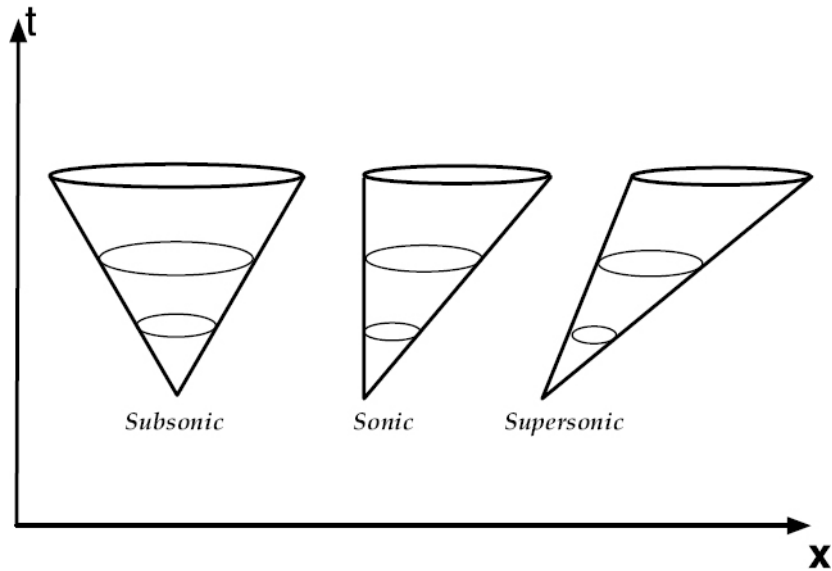


Figure 1.3: Moving fluid tilts the sound cone as it moves and tilts past the vertical when it becomes supersonic. *Image courtesy: [8].*

line element in Eq. (1.19) becomes

$$ds^2 = \frac{\rho_0}{c_{s0}} [-(c_{s0}^2 - v_0^2)dt^2 - 2v_0 dx dt + dx^2]. \quad (1.24)$$

The sound-cones are constructed from the null geodesics and the null geodesics are obtained by equating ds^2 to zero which gives

$$\left. \frac{dt}{dx} \right|_{\pm} = \frac{v_0 \pm c_{s0}}{v_0^2 - c_{s0}^2} = \frac{1}{v_0 \mp c_{s0}}. \quad (1.25)$$

Now let's assume that $v_0 > 0$, then the slope $(dt/dx)_- > 0$ and regular for all x . However, $(dt/dx)_+ < 0$ for subsonic flow and $(dt/dx)_+ > 0$ for supersonic flow. Similarly if $v_0 < 0$, then $(dt/dx)_+ < 0$ and regular for all x and $(dt/dx)_- > 0$ for subsonic flow and it is < 0 for supersonic flow. Thus at the sonic point, the sound-cone tilts past the vertical. Fig. 1.2 shows a schematic diagram of the tilting of the sound cone.

For a given velocity profile v_0 of the background flow, one can draw the causal structure explicitly. In order to draw the causal structure, let us first introduce the null coordinates as the following

$$du = dt - \frac{dx}{(v_0 + c_{s0})}, \quad (1.26)$$

$$dw = dt - \frac{dx}{(v_0 - c_{s0})}. \quad (1.27)$$

In terms of the null coordinates u, w , the line element in Eq. (1.24) becomes

$$ds^2 = -\frac{\rho_0}{c_{s0}}(c_{s0}^2 - v_0^2)dudw. \quad (1.28)$$

The null geodesics will be given by $u = \text{constant}$ and $w = \text{constant}$ lines. For example, let us consider the following representative left-going velocity profile as provided in [9]

$$v_0(x) = -\frac{2c_{s0}}{\exp(2x/a) + 1}, \quad (1.29)$$

where $a > 0$. To simplify further, we take the sound speed to be a constant which is true for isothermal flow. The velocity profile is plotted in Fig. 1.4 for $a = 2.0$, $c_{s0} = 0.5$. At $x = 0$, $|v_0| = c_{s0}$ and hence $x = 0$ is the acoustic horizon for this particular

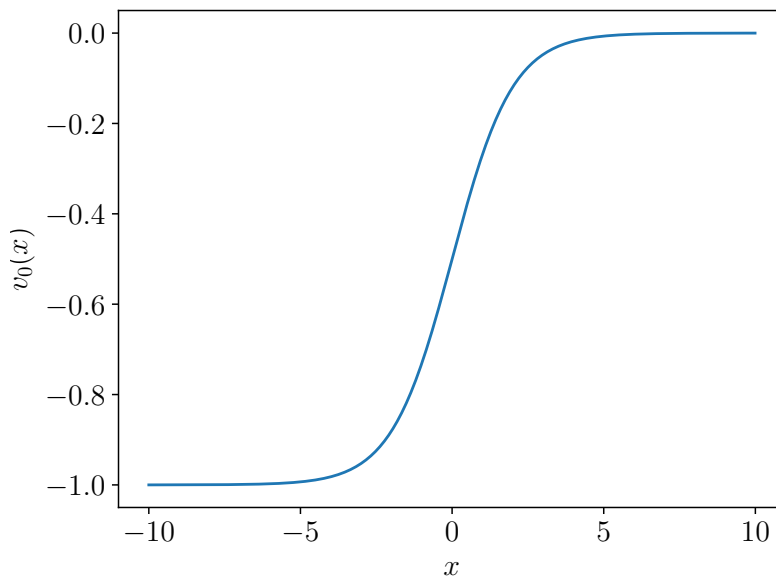


Figure 1.4: A simple and representative left-going velocity profile as given by Eq. (1.29) with $a = 2.0$, $c_{s0} = 0.5$.

velocity profile. Now integrating the Eq. (1.26) and (1.27) with the velocity profile in Eq. (1.29) gives

$$u = t - \frac{x}{c} - \frac{a}{c} \ln |1 - \exp(-2x/a)|, \quad (1.30)$$

$$w = t + \frac{x}{c} + \frac{a}{3c} \ln(1 + 3 \exp(-2x/a)). \quad (1.31)$$

In Fig. 1.5, we construct the causal structure of the acoustic spacetime metric given in Eq. (1.24) with a left-going velocity profile given in Eq. (1.29) with $a = 2.0$, $c_{s0} = 0.5$. The solid lines represent the $u = \text{constant}$ null rays and the dashed lines represent the $w = \text{constant}$ null rays. As can be noticed, the sound cones tilt past the vertical as the fluid crosses the horizon at $x = 0$. The region $x < 0$ represents an acoustic black hole. In the $x < 0$ region, x decreases along both the null rays as t increases.

Extending the analogy further, we can construct an acoustic white hole also. Similar to the general relativity, an acoustic white hole can be defined as a region where sound waves cannot enter. For illustration we again take a simple representative right-going velocity profile as presented in [9]

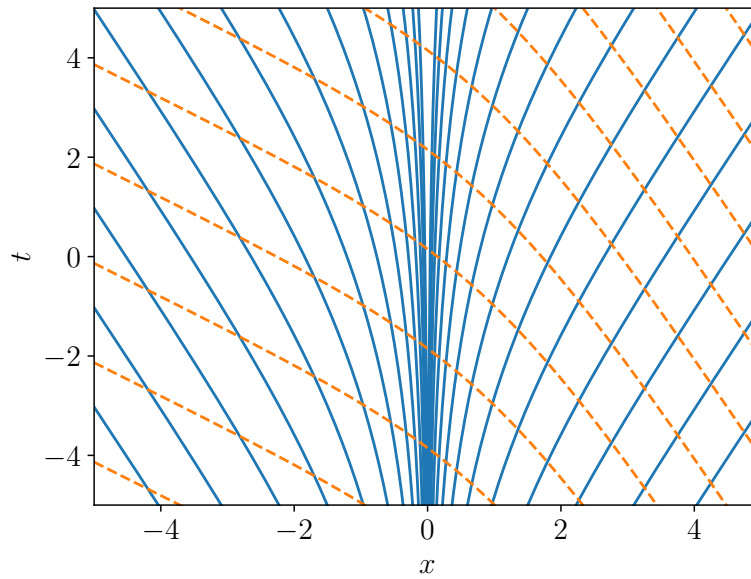


Figure 1.5: Acoustic black hole: causal structure of the acoustic spacetime metric given in Eq. (1.24) with a left-going velocity profile given in Eq. (1.29) with $a = 2.0, c_{s0} = 0.5$. The solid lines represent the $u = \text{constant}$ null rays and the dashed lines represent the $w = \text{constant}$ null rays. u, w are given in Eq. (1.30) and (1.31), respectively. As can be noticed, the sound cones tilt past the vertical as the fluid crosses the horizon at $x = 0$. The region $x < 0$ represents an acoustic black hole. In the $x < 0$ region, x decreases along both the null rays as t increases.

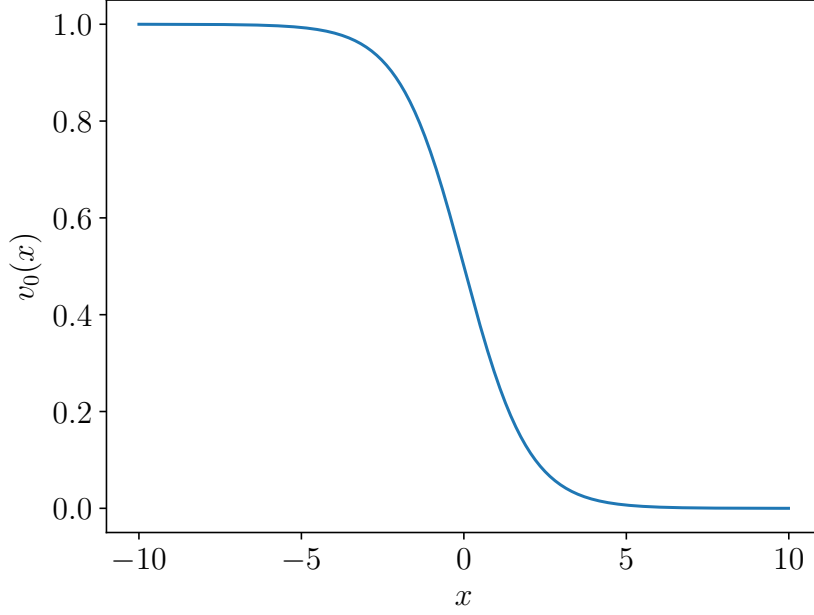


Figure 1.6: Right-going velocity profile presented in Eq. (1.32) with $a = 2.0$, $c_{s0} = 0.5$.

$$v_0(x) = \frac{2c_{s0}}{\exp(2x/a) + 1}. \quad (1.32)$$

The null coordinates for this velocity profile is given by

$$u = t - \frac{x}{c} - \frac{a}{3c} \ln(1 + 3\exp(-2x/a)), \quad (1.33)$$

$$w = t + \frac{x}{c} + \frac{a}{c} \ln|1 - \exp(-2x/a)|. \quad (1.34)$$

Fig. 1.6 represents a right-going velocity profile as given by Eq. (1.32) with $a = 2.0$, $c_{s0} = 0.5$. Fig. 1.7 represents the corresponding causal structure of the acoustic spacetime. $u = \text{constant}$ null rays are represented by the solid lines and the $w = \text{constant}$ null rays are represented by the dashed lines. $x = 0$ is the acoustic horizon. For $x < 0$, along both the null rays x increases as t increases. $x < 0$ region represents an acoustic white hole.

With a suitable velocity profile, it is possible to construct a causal structure where both an acoustic black hole and acoustic white hole horizon could be present. One can proceed further and draw the Penrose diagrams for the acoustic spacetime metric also. For details of such a study, we refer the readers to [9].

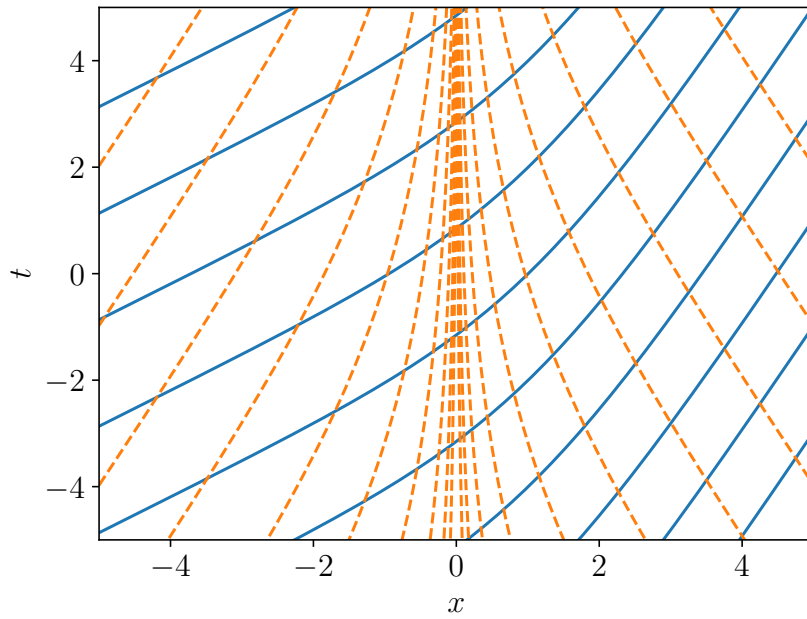


Figure 1.7: Acoustic white hole: causal structure with a right-going velocity profile (Eq. (1.32) with $a = 2.0, c_{s0} = 0.5$). Solid lines represent the $u = \text{constant}$ null rays and dashed lines represent the $w = \text{constant}$ null rays. The acoustic horizon is located at $x = 0$. The region $x < 0$ represent an acoustic white hole. For $x < 0$, for both null rays, x increases as t increases.

1.1.4 Acoustic surface gravity

The acoustic surface gravity plays a role similar to that of the surface gravity in general relativity, i.e., it acts as a gateway to calculate the analogue Hawking temperature. Depending on the nature of the acoustic metric, the calculation of surface gravity may be easy or more involved. For a static spacetime, the Killing horizon associated with the time-translation Killing vector $\chi^\mu = \delta_t^\mu$ coincides with event horizon [10]. Thus χ^μ is tangent to the null generators of the horizon. Because the event horizon and Killing horizon coincide, we have $\chi_\mu \chi^\mu = 0$ at the horizon. Therefore, the χ^μ is orthogonal to itself and hence normal to the horizon. Also the normal to the surface $\chi_\mu \chi^\mu = 0$ is given by $\partial_\alpha(\chi_\mu \chi^\mu)$. Thus there must be a scalar κ such that on the horizon [10, 11]

$$\partial_\alpha(-\chi_\mu \chi^\mu) = 2\kappa \chi_\alpha. \quad (1.35)$$

This is one of the procedures to calculate the surface gravity in general relativity and the scalar κ is the surface gravity of the black hole. The same applies to the static acoustic spacetime metric also. It is to be remembered that the above equation is to be evaluated at the horizon. If the metric is stationary but not static, then we have found a suitable vector field which satisfies the above properties and then the surface gravity can be obtained in terms of that vector using Eq. (1.35), e.g., see [5]. However, here as well as in the subsequent analysis, all the metrics are found to be static and hence we can use the Eq. (1.35) to calculate the acoustic surface gravity.

For the acoustic metric in Eq. (1.19), we find the norm of the Killing vector to be¹

$$\chi_\mu \chi^\mu = G_{tt} = \frac{\rho_0}{c_{s0}}(v_0^2 - c_{s0}^2). \quad (1.36)$$

and

$$\chi_\alpha = G_{\alpha\mu} \chi^\mu = G_{\alpha\mu} \delta_t^\mu = G_{\alpha t} = -\frac{\rho_0}{c_{s0}} v_{0\alpha}. \quad (1.37)$$

¹It should be noted that in order to calculate the surface gravity using Eq. (1.35), we have to use a coordinate system where the metric elements are non-singular. For example, we can not use the line elements in Eq. (1.21) or (1.22) to calculate the surface gravity.

Thus Eq. (1.35) gives

$$\nabla \left[\frac{\rho_0}{c_{s0}} (v_0^2 - c_{s0}^2) \right] = -2\kappa \frac{\rho_0}{c_{s0}} \vec{v}_0, \quad (1.38)$$

which is to be evaluated at the horizon. Now taking dot product of both sides with respect to the unit vector along \vec{v} gives the following equation in terms of a normal derivative

$$\frac{\partial}{\partial n} \left[\frac{\rho_0}{c_{s0}} (v_0^2 - c_{s0}^2) \right] = -2\kappa \frac{\rho_0}{c_{s0}} v_0, \quad (1.39)$$

which finally gives the acoustic surface gravity as

$$\kappa = \left| \frac{\partial}{\partial n} (c_{s0} - v_0) \right|. \quad (1.40)$$

It may be noticed that there is no dependence on the density term. This is due to the conformal invariance of the surface gravity. In Unruh's work [1], the sound speed is assumed to position independent. Such assumption reduces Eq. (1.40) to the formula found in [1].

1.2 Black hole accretion as analogue gravity model

Most of the analogue gravity models are based in condensed matter systems. Due to the fact that a condensed matter system is a quantum mechanical system, it is the appropriate place to explore the analogue Hawking radiation and other quantum mechanical aspects of the curved spacetime. However, it is to be mentioned that the notion of an acoustic metric and an acoustic horizon was first introduced by Moncrief [12] in the context of linear stability analysis of spherically symmetric accretion in the Schwarzschild metric. Thus, though Unruh [1] first pointed out that thermal spectrum of sound waves is emitted from the acoustic horizon, the notion of an acoustic spacetime metric and acoustic horizon predates Unruh's work and finds its place in accretion physics. In last two decades, there have been several works which illustrate the fact that an accreting black hole can be regarded as an example of a classical analogue gravity model and investigates different properties of the acoustic spacetime Newtonian, Pseudo-Newtonian or even in general relativistic background [13].

In order that a fluid system possesses an acoustic spacetime which has an acoustic horizon, the fluid must be transonic. In the case of black hole accretion, this criterion is always satisfied. This is because black hole accretion is intrinsically transonic in nature. The sound speed in an accretion system reaches its maximum value $c/\sqrt{3}$ at the event horizon, c being the velocity of light. However, the fluid matter could reach a velocity which is very close to the velocity of the light. Thus near the horizon, the fluid is always transonic. Black accretion systems are a very unique kind of classical analogue gravity system because here we have two kinds of horizons. One is the event horizon of the black hole and another is the acoustic horizon which lies outside the event horizon of the black hole. Thus the accreting matter actually passes through two different kinds of horizons, first it encounters the sonic horizon and then it encounters the event horizon.

Even though the detailed analysis of quantum Hawking-like effects may not be possible in a purely classical analogue system, the study of the acoustic surface gravity may have significant importance in such systems. The acoustic surface gravity itself is an important entity to study as it may help to understand the flow structure as well as the acoustic spacetime. Therefore, the acoustic surface gravity may be studied independently without studying the analogue Hawking-like phenomena characterized by the analogue Hawking temperature which may be too small to be detected experimentally in such system. The acoustic surface gravity plays an important role to study the non-negligible effects associated with the analogue Hawking effects which could be examined through the modified dispersion relations. Such studied has been performed in purely analytical work as well as experimental setup ([14–19]).

The deviation of the Hawking-like effect in the dispersive medium depends very sensitively on the gradient of dynamical velocity. In most of the above-mentioned studies, the velocity gradient is estimated by prescribing a particular velocity profile using certain assumptions. On the other hand in our current work, the values of the space gradient of the dynamical flow velocity have been computed very accurately. Thus it is obvious that the non-universal feature of the Hawking-like effect could be

further modified by studying the black hole accretion system as an analogue gravity system. Therefore, it is obvious that though the accreting black hole system may not provide any direct signature of the Hawking-like effect, it can still be considered as a very important as well unique theoretical construct to study analogue gravity phenomena.

Studying the features of the acoustic spacetime embedded in the accretion system provides a different point of view of the accretion process. It would be shown that the acoustic horizons and the transonic surface of the stationary accretion flow are related actually very intricately. In fact, we shall see that the acoustic horizon and the critical points of accretion flow are identical. In the next chapter, we introduce some basic aspects of stationary accretion on to black holes and will discuss the flow models we consider in our work.

2

Aspects of black hole accretion

2.1 Accretion flow geometry

The simplest model of accretion was given by Bondi [20] and is usually known as Bondi flow or Bondi accretion. Bondi flow describes spherically symmetric accretion of hydrodynamic fluid within Newtonian framework. The general relativistic version of the Bondi flow was given by Michel [21] and is considered to be the most simplest general relativistic accretion configuration onto compact astrophysical objects. However, in most realistic astrophysical systems, the accreting matter has some amount of angular momentum which breaks the spherical symmetry of the flow. In such cases, the accreting matter forms a disc around the accretor and such a disc is known as an accretion disc. In order to describe the accretion flow in the form of an accretion disc, usually three different kind of geometric configurations of the matter is considered in the literature (see [22] and references therein for further details). These three flow geometries are flow with constant thickness, wedge shaped flow with conical geometry and flow in hydrostatic equilibrium along vertical direction.

- *Flow with constant thickness:* In this model of accretion disc, the thickness of the accretion disc is assumed to be constant. In other words, the height of the accretion disc does not change with the radial distance measured from the center of the accretor along the equatorial plane. This kind of geometry

resembles a right circular cylinder of a fixed height with the axis of symmetry along the z -axis. This is the simplest possible flow geometry one can choose to describe accretion disc in astrophysics. As one can see, the height of the disc, being constant, does not change when we linearly perturb different flow variables in the linear perturbation analysis we perform in the following chapters. If we denote the local height of the disc (half of the thickness of the disc), as measured from the equatorial plane along the vertical direction, by H then for this model $H = \text{constant}$.

- *Wedge shaped flow with conical geometry:* In the Bondi flow [20] or Michel flow [21], the flow geometry is spherically symmetric and the introduction of angular momentum destroys the spherical symmetry of the flow making the flow axially symmetric. However the flow can still be assumed to be quasi-spherical in the sense that though it deviates from the absolute spherical symmetry, the ratio of the height of the disc and the radial distance remains constant. In other words the local flow height H is given by $H \propto r$, where r is the radial distance. The proportionality constant is obtained from the solid angle subtended by the flow at the center. In this case also the height does not depend on accretion variables such as velocity and density. Therefore here also the height remains unaffected while we do the linear perturbation analysis.
- *Flow in hydrostatic equilibrium along vertical direction:* This model of flow geometry is the most complicated one. In this model the flow is assumed to be in hydrostatic equilibrium along vertical direction. The flow thickness is therefore a function of radial distance as well as other accretion variables. In the following chapters, we shall discuss this model of accretion disc in more details and work with few different mathematical expressions for the disc height as could be found in accretion literature.

2.2 Stationary low angular momentum accretion flow

In our work, we consider an inviscid flow, i.e., there is no viscous dissipation in the accreting fluid. Such a flow can be described by two conservation equations. The first one is the continuity equation which ensures the conservation of mass and the second one is the Euler equation which ensures the conservation of energy-momentum. These equations are in general time-dependent and non-linear in nature. In order to simplify, it is convenient to consider the scenario where the accretion flow has obtained a steady state, i.e., the accretion variables, e.g., the velocity components and density, are time-independent or remain nearly unchanged over the period of observation.

For such steady state accretion flow, the two conservation equations, where the time derivatives now vanish, could be integrated to obtain two first integrals of motion. The continuity equation, upon integration, gives the mass accretion rate which is the rate of infall of accreting matter and is a constant of motion of the flow. Similarly, integrating the relativistic Euler equation gives the relativistic Bernoulli's constant which for flow with adiabatic equation of state is basically the specific energy of the flow.

We consider the accretion flow to possess low angular momentum. For accretion flow with high angular momentum, there should be some driving mechanism to make the accreting matter fall onto the accretor. In absence of such mechanism, the matter may settle into stable Keplerian orbits and accretion onto the accretor would not be possible. Viscosity plays an important role in driving the accretion flow. Viscosity transports angular momentum from the inner part of the accretion disc to the outer part of the disc. Thus, such a outward transportation of the angular momentum lowers its angular momentum and helps it to fall onto the accretor.

In our work, we consider the flow to be inviscid and therefore there is no viscous driving force. Neither we incorporate any other force in our governing equations which would ensure that the accreting matter never settles into stable Keplerian orbits and always falls towards the accretor. This motivates us to consider low angular

momentum flow. If the angular momentum is sufficiently small, then the matter would never settle into stable orbits and always falls towards the accretor. Thus low angular momentum accretion is possible without external driving mechanism like the viscous force.

The question which may arise is why we do not take into account viscosity in the first place. Apart from the fact that inclusion of viscosity makes the study of general relativistic accretion much more complicated, the main reason we exclude viscosity from our model is that it has been observed that the presence of viscosity breaks the Lorentzian symmetry of the acoustic metric and it is not possible to construct analogue spacetime for such flow [5].

It is believed that low angular momentum flow structure is a common feature for accretion onto the supermassive black hole at our Galactic centre (see [23] and references therein). Such sub-Keplerian weakly rotating flows may be observed in various astrophysical systems, for detached binary systems fed by accretion from OB stellar winds [24, 25], for instance. Also for semi-detached low-mass non-magnetic binaries [26], and for super-massive black holes fed by accretion from slowly rotating central stellar clusters ([27, 28] and references therein) such flows are common. Even for a standard Keplerian accretion disc, turbulence may produce such low angular momentum flow (see, e.g., [29] and references therein).

Because of the inner boundary conditions posed by the presence of the event horizon, black hole accretion is necessarily transonic [30] except for the possible cases of wind fed accretion of supersonic stellar winds [31]. In transonic accretion flow, the accreting matter starts subsonically with very small radial velocity at large distance. As the matter falls towards the accretor it loses gravitational potential and gains kinetic energy, i.e., the velocity increases as it nears the accretor. At a certain radial distance the accreting matter becomes supersonic and falls onto the black hole supersonically. For low angular momentum accretion, flow can also manifest multi-transonicity, i.e., one may observe the transition from the subsonic to supersonic flow at more than one places during the course of motion of the matter falling towards the horizon. Accretion solutions passing through more than

one sonic points may be connected through a discontinuous shock wave [30, 32–59]. In the subsequent chapters, we will study both shocked and as well as shockless accretion flow.

2.3 Linear perturbation, stability analysis and analogue gravity

To study the observational signature of black holes, one studies the dynamical and radiative properties of black hole accretion and constructs the characteristic black hole spectra [60, 61]. Such spectra is analyzed observationally to probe the space-time at close proximity of the event horizon of astrophysical black holes. One can use the stationary solutions to construct the black hole spectra ([42] and references therein). However, nonsteady features (time variability) and various kind of local as well as global fluctuations may be present in large astrophysical fluid flows. Such fluctuations may introduce undesired instability in the flow and in such cases, the stationary solutions may not be suitable to construct the black hole spectra.

In order to ensure that the stationary solutions are stable under time-dependent fluctuations, one performs a linear perturbation analysis. This is most basic task to check the stability of the stationary solutions. There are different ways to perform a linear stability analysis. Similar to many standard works in accretion literature [12, 62], we work with Eulerian perturbation which is perturbation relative to the inertial frame. Working with Eulerian perturbation is much simpler and the perturbation equation can be expressed in terms of the mass accretion rate [62] (variation of which can be measured observationally). One can also express the perturbation equation in terms of the relativistic Bernoulli's constant [63, 64] or the velocity potential [12]. Such perturbation equation can be studied to understand the nature of the solutions and hence the stability of the stationary solutions. In the following chapters, we will discuss the perturbation scheme in more details.

The perturbation equation is basically a wave equation which describes the propagation of the acoustic disturbance (perturbations) in the fluid. In fact, it was first

noticed by Moncrief [12], in context of linear stability analysis of general relativistic spherical accretion in Schwarzschild metric, that the wave equation mimics the wave equation of a massless scalar field in curved spacetime. Comparing these two wave equation, one can obtain an acoustic spacetime metric which describes the propagation of the acoustic perturbation in the accretion fluid. Thus the emergence of acoustic spacetime metric is a by product of stability analysis of the stationary accretion solutions. Our work combines these two apparently disjoint fields of study – the linear stability analysis of stationary accretion flow and the analogue gravity phenomenon. In this thesis we investigate the emergence of acoustic spacetime metric by performing linear perturbation of the accretion on to Schwarzschild and Kerr black holes and explore different properties of the acoustic spacetime. We then use the perturbation equations to study the linear stability of the stationary solutions in these systems. Thus, the main theme of our work is the linear perturbation of black hole accretion and the investigation of the emerging of acoustic spacetime.

Throughout our works, we will set $G = c = M_{\text{BH}} = 1$ where G is the universal gravitational constant, c is the velocity of light and M_{BH} is the mass of the black hole. The radial distance will be scaled by GM_{BH}/c^2 and any velocity will be scaled by c . We shall use the negative-time-positive-space metric convention.

3

Relativistic sonic geometry for isothermal accretion in the Schwarzschild metric¹

In this chapter, we investigate the emergence of the curved acoustic spacetime metric for isothermal accretion onto a Schwarzschild black hole. We consider the accretion flow to be inviscid and irrotational. We show that the linear perturbation of three different quantities – the velocity potential, the relativistic Bernoulli’s constant and the mass accretion rate – give rise to (conformally) the same acoustic metric. From the acoustic metric, we identify the location of the acoustic horizon and demonstrate it by constructing the causal structure of the acoustic spacetime. We discuss how one can compute the value of the acoustic surface gravity in terms of the accretion variables corresponding to the background solutions, i.e., the stationary integral solutions for different flow geometries. We show that the salient feature of the acoustic spacetime is independent of the physical variable we perturb but sensitively depends on the geometric configuration of the black hole accretion disc.

¹This chapter is based on the work titled “*Relativistic sonic geometry for isothermal accretion in the Schwarzschild metric*” by M. A. Shaikh, I. Firdousi and T. K. Das [64].

3.1 Governing equations

We consider the background spacetime to be stationary and spherically symmetric. The line element for such a spacetime has the general form

$$ds^2 = -g_{tt}dt^2 + g_{rr}dr^2 + g_{\theta\theta}d\theta^2 + g_{\phi\phi}d\phi^2, \quad (3.1)$$

where the metric elements $g_{\mu\nu}$ are functions of r and θ .² For Schwarzschild spacetime, the metric elements are given by

$$g_{tt} = g_{rr}^{-1} = (1 - 2/r), \quad g_{\theta\theta} = g_{\phi\phi}/\sin^2\theta = r^2. \quad (3.2)$$

In the units used here, the event horizon of the Schwarzschild black hole is located at $r = 2$. The energy momentum tensor for an ideal fluid is given by

$$T^{\mu\nu} = (p + \varepsilon)v^\mu v^\nu + pg^{\mu\nu}, \quad (3.3)$$

where v^μ is four-velocity of the fluid that satisfies the normalization condition $v_\mu v^\mu = -1$. p and ε are the pressure and the energy density of the fluid, respectively. For isothermal flow, $p \propto \rho$, where ρ is the rest-mass energy density. The total energy density ε is the sum of the rest-mass energy density and the internal energy density (due to the thermal energy), i.e., $\varepsilon = \rho + \varepsilon_{\text{thermal}}$.

The continuity equation is given by

$$\nabla_\mu(\rho v^\mu) = 0, \quad (3.4)$$

where the covariant divergence is defined as $\nabla_\mu v^\nu = \partial_\mu v^\nu + \Gamma_{\mu\lambda}^\nu v^\lambda$ with the Christoffel symbols $\Gamma_{\mu\lambda}^\nu = \frac{1}{2}g^{\nu\sigma}[\partial_\lambda g_{\sigma\mu} + \partial_\mu g_{\sigma\lambda} - \partial_\sigma g_{\mu\lambda}]$. The energy momentum conservation equation is given by

$$\nabla_\mu T^{\mu\nu} = 0. \quad (3.5)$$

A substitution of of Eq. (3.3) in Eq. (3.5) provides the relativistic Euler equation

$$(p + \varepsilon)v^\mu \nabla_\mu v^\nu + (g^{\mu\nu} + v^\mu v^\nu)\nabla_\mu p = 0. \quad (3.6)$$

²To avoid any ambiguity, we would like to clarify here that the ‘00’ component of the metric tensor $g_{\mu\nu}$ is taken to be $-g_{tt}$ in this work

3.2. Velocity potential, mass accretion rate and the relativistic Bernoulli's constant

The specific enthalpy of the flow is defined as

$$h = \frac{p + \varepsilon}{\rho}. \quad (3.7)$$

For isothermal flow, the sound speed may be defined as [65]

$$c_s^2 = \frac{1}{h} \frac{\partial p}{\partial \rho}. \quad (3.8)$$

The relativistic Euler equation for isothermal fluid can thus be written in terms of the sound speed as

$$v^\mu \nabla_\mu v^\nu + \frac{c_s^2}{\rho} (v^\mu v^\nu + g^{\mu\nu}) \partial_\mu \rho = 0. \quad (3.9)$$

The above equation can be further expanded using the definition of the covariant derivative which provides

$$v^\mu \partial_\mu v^\nu + \Gamma_{\mu\lambda}^\nu v^\mu v^\lambda + \frac{c_s^2}{\rho} (v^\mu v^\nu + g^{\mu\nu}) \partial_\mu \rho = 0. \quad (3.10)$$

3.2 Velocity potential, mass accretion rate and the relativistic Bernoulli's constant

In this section, we define three different quantities, i.e., the velocity potential, the mass accretion rate and the relativistic Bernoulli's constant. Linear perturbation of the accretion flow could be performed to obtain the perturbation equation in terms of these three different quantities. Here we use the continuity equation, Euler equation or the irrotationality condition (derived below) and show how one can define these aforementioned three quantities.

3.2.1 Velocity potential

In Newtonian framework, vorticity $\vec{\omega}$ is defined as the curl of the velocity vector \vec{v} , i.e., $\vec{\omega} = \nabla \times \vec{v}$ [66]. Thus it represents the local rotation of the fluid elements in the flow. In general relativity, the vorticity is defined as [6, 67]

$$\omega_{\mu\nu} = h_\mu^\rho h_\nu^\sigma v_{[\rho;\sigma]}, \quad (3.11)$$

where $v_{\mu;\nu} = \nabla_\nu v_\mu$ and $v_{[\mu;\nu]} \equiv \frac{1}{2}[v_{\mu;\nu} - v_{\nu;\mu}]$ and $h^\mu{}_\nu$ is the projection operator which projects an arbitrary vector in space-time into its components in the subspace orthogonal to v^ν and it is given by $h^\mu{}_\nu = \delta^\mu{}_\nu + v^\mu v_\nu$. Vorticity geometrically measures the twisting of the congruence[68]. In general, a flow may have non vanishing vorticity $\omega_{\mu\nu}$. A flow is said to be irrotational if it has vanishing vorticity, that is $\omega_{\mu\nu} = 0$.

Eq. (3.11) can be rewritten using the definition of the projection operator as

$$\omega_{\mu\nu} = v_{[\mu;\nu]} + \frac{1}{2}v^\rho[v_\nu\nabla_\rho v_\mu - v_\mu\nabla_\rho v_\nu]. \quad (3.12)$$

The relativistic Euler equation given by Eq. (3.9) provides

$$v^\mu\nabla_\mu v_\nu = -\frac{c_s^2}{\rho}[\partial_\nu\rho + v^\mu v_\nu\partial_\mu\rho]. \quad (3.13)$$

Using the above equation in Eq. (3.12) and rearranging gives

$$\omega_{\mu\nu} = \frac{1}{2\rho c_s^2}[\partial_\nu(v_\mu\rho^{c_s^2}) - \partial_\mu(v_\nu\rho^{c_s^2})]. \quad (3.14)$$

For irrotational flow $\omega_{\mu\nu} = 0$ which provides

$$\partial_\nu(v_\mu\rho^{c_s^2}) - \partial_\mu(v_\nu\rho^{c_s^2}) = 0. \quad (3.15)$$

This is the condition of irrotationality of isothermal fluid flow and henceforth we will refer Eq. (3.15) as the irrotationality condition. In the derivation of the irrotationality condition, we have used the fact that for isothermal flow the sound speed c_s is constant since the flow temperature remains invariant throughout. The irrotationality condition given by Eq. (3.15) can be used to introduce a potential field which, in analogy to the Newtonian fluid flow, we call the velocity potential ψ . The velocity potential ψ is defined by the following relation

$$v_\mu\rho^{c_s^2} = \partial_\mu\psi. \quad (3.16)$$

3.2.2 Relativistic Bernoulli's constant

The relativistic Bernoulli's constant is obtained by integrating the temporal component of the relativistic Euler equation given by Eq. (3.10). We consider two different

kinds of accretion flow on to the Schwarzschild black hole. First one is the spherically symmetric accretion known as Michel Flow [21] and the second one is the axially symmetric flow. First, we consider the case of Michel flow. Due to the spherical symmetry, the four-velocity components are given by $v^\mu = (v^t, v^r, v^\theta = 0, v^\phi = 0)$. The temporal component of the Eq. (3.10) is obtained by using $\nu = t$ which can be written as

$$v^r \partial_r v^t + v^t \partial_t v^t + \Gamma_{\mu\lambda}^t v^\mu v^\lambda + \frac{c_s^2}{\rho} [(v^t)^2 - g^{tt}] \partial_t \rho + \frac{c_s^2}{\rho} v^r v^t \partial_r \rho = 0, \quad (3.17)$$

where the relevant Christoffel symbol is $\Gamma_{rt}^t = \frac{1}{2} g^{tt} \partial_t g_{tt}$. The normalization condition gives $g_{tt}(v^t)^2 - 1 = g_{rr}(v^r)^2$ which can be used to rearrange the above equation as

$$v^t \partial_t v^t + \frac{c_s^2}{\rho} \frac{g_{rr}(v^r)^2}{g_{tt}} \partial_t \rho + v^r v^t \partial_r \{\ln(v_t \rho^{c_s^2})\} = 0. \quad (3.18)$$

For stationary accretion flow, where the time derivatives vanish, the above equation can be integrated to obtain the first integral of motion which we call the relativistic Bernoulli's constant ξ_0 and is given by

$$\xi_0 = -v_{t0} \rho_0^{c_s^2} = \text{constant}, \quad (3.19)$$

where v_{t0} and ρ_0 are the stationary values of v_t and ρ , respectively. It should be noted that ξ_0 can not be identified with the actual specific energy which is not a constant for isothermal flow.

For axially symmetric flow, the velocity component $v^\phi \neq 0$. We assume that the four-velocity component along the vertical direction v^θ is negligible compared the radial component v^r , i.e., $v^\theta \ll v^r$. Using the normalization condition and the relevant Christoffel symbol, the temporal component of the relativistic Euler equation for axially symmetric flow could be written as

$$v^t \partial_t v^t + \frac{c_s^2}{\rho} \frac{\{g_{rr}(v^r)^2 + g_{\phi\phi}(v^\phi)^2\}}{g_{tt}} \partial_t \rho + v^r v^t \partial_r \left\{ \ln(v_t \rho^{c_s^2}) \right\} = 0. \quad (3.20)$$

Therefore, for stationary axially symmetric accretion flow, similar to the Michel flow, integrating the above equation gives the same expression for the relativistic Bernoulli's constant as given by Eq. (3.19), i.e., $\xi_0 = -v_{t0} \rho_0^{c_s^2} = \text{constant}$.

3.2.3 Mass accretion rate

The continuity equation given by Eq. (3.4) can be written as

$$\frac{1}{\sqrt{-g}}\partial_\mu(\sqrt{-g}\rho v^\mu) = 0, \quad (3.21)$$

where g is the determinant of the spacetime metric $g_{\mu\nu}$ and therefore $g = -r^4 \sin^2 \theta$. For spherically symmetric Michel flow, the ∂_θ and ∂_ϕ terms do not contribute and hence the continuity equation becomes

$$\frac{1}{\sqrt{-g}}\partial_t(\rho v^t \sqrt{-g}) + \frac{1}{\sqrt{-g}}\partial_r(\rho v^r \sqrt{-g}) = 0. \quad (3.22)$$

For stationary flow, the ∂_t term also vanishes. Integrating over the covariant volume element $\sqrt{-g}d^4x$ gives

$$\partial_r(\sqrt{-g}\rho_0 v_0^r) dr d\theta d\phi = 0. \quad (3.23)$$

Let us now write $g = \tilde{g} \sin^2 \theta$ where $\tilde{g} = -r^4$. Then the above equation gives

$\partial_r(\sqrt{-\tilde{g}}\rho_0 v_0^r \sin \theta) dr d\theta d\phi = 0$. One can integrate out the θ, ϕ parts which will give a purely geometrical factor $\tilde{\Omega}$. Finally, integrating over the radial part gives the mass accretion rate which is given by

$$-\dot{M} = \tilde{\Omega} \sqrt{-\tilde{g}} \rho_0 v_0^r \quad (3.24)$$

\dot{M} represents the mass flux per unit time for ingoing accretion solution. It should be noted that for non-comoving observer, the ‘dot’ does not mean a time derivative (since we are dealing with stationary solutions only), it simply implies that the amount of mass falling in through a certain surface remains invariant per unit time for steady state solutions. The negative sign implies the in fall of matter. Because of the fact that $\tilde{\Omega}$ is merely a geometrical factor, we can absorb it in the left hand side to redefine the mass accretion rate to be $\Psi_0 \equiv -\dot{M}/\tilde{\Omega} = \sqrt{-\tilde{g}}\rho_0 v_0^r$ without any loss of generality.

For axially symmetric accretion, under the assumption that $v^\theta \ll v^r$ and using the fact that for axial symmetry the derivative with respect to ϕ vanishes, the continuity equation given by Eq. (3.21) can be written as

$$\partial_t(\rho v^t \sqrt{-g}) + \partial_r(\rho v^r \sqrt{-g}) = 0. \quad (3.25)$$

It is convenient to do a vertical averaging of the above equation. We assume that the thickness of the accretion disc is small compared to the radial size of the accretion disc. For such accretion disc, a vertical averaging of any flow variables $f(t, r, \theta)$ can be performed by integrating it along the θ direction using the following approximation [69]

$$\int f(t, r, \theta) d\theta \approx H_\theta f(t, r, \theta = \frac{\pi}{2}), \quad (3.26)$$

where H_θ is the characteristic angular scale of the flow and depends on the model of accretion disc we are working with. In Sec. 2.1, we discussed three different geometrical configurations of the axially symmetric accretion flow, namely, the constant height flow (CH), the wedge-shaped conical flow (CF) and the flow under hydrostatic equilibrium along the vertical direction (VE). H_θ contains the information about the vertical structure of the disc and by doing so allows us to work fully in the equatorial plane. This is the motivation behind doing a vertical averaging. H_θ can be also thought as the appropriate weight function to get the correct flux of the infalling matter while integrating the continuity equation. Thus, after vertical averaging the continuity equation Eq. (3.25) becomes

$$\partial_t(\sqrt{-\tilde{g}}\rho v^t H_\theta) + \partial_r(\sqrt{-\tilde{g}}\rho v^r H_\theta) = 0. \quad (3.27)$$

For stationary solutions, therefore we have

$$\partial_r(\sqrt{-\tilde{g}}\rho_0 v_0^r (H_\theta)_0) = 0, \quad (3.28)$$

which, when integrated over r , gives

$$\sqrt{-\tilde{g}}\rho_0 v_0^r (H_\theta)_0 = \text{constant}. \quad (3.29)$$

$(H_\theta)_0$ represents the stationary value of H_θ . To get the rate of in fall of matter, we also need to integrate over the azimuthal angle ϕ which introduces a geometrical factor which can be absorbed without any loss of generality to define the mass accretion rate for stationary axially symmetric accretion flow as

$$\Psi_0 = \sqrt{-\tilde{g}}\rho_0 v_0^r (H_\theta)_0. \quad (3.30)$$

H_θ can be related to the local height or thickness of the accretion disc $H(r)$ as $H_\theta = H(r)/r$. In Sec. 2.1, we discussed that for CH the thickness of the disc is constant for all the radial distance, i.e., $H(r) = \text{constant}$. For CF the disc thickness is proportional to the radial distance, i.e., $H(r) \propto r$. Therefore, for CH we have $H_\theta = \text{constant}/r$ and for CF we have $H_\theta = \text{constant}$.

The expression for the disc height for VE is rather involved. For VE, the expression of the disc height is obtained by balancing the pressure gradient with the component of the gravitational force along the vertical direction. In the Newtonian framework, the balancing equation is obtained from the component of the Euler equation along the vertical direction and one can find out the expression for the disc height from this equation. However, for the general relativistic framework, it is a quite involved task. Therefore, historically there have different models of VE. The first of such models was given by Novikov and Thorne [70] which was further improved by Riffert and Harold [71]. In this chapter, we will use the expression as derived by Abramowicz *et al.* [72]. In Chap. 7, we will discuss in detail about these three models of VE disc heights.

In the Schwarzschild metric, the expression for the disc height in VE as obtained by Abramowicz *et al.* is given by the relation

$$H_\theta^2 v_\phi^2 f(r) = \frac{p}{\rho}, \quad (3.31)$$

where $f(r)$ is independent of the flow variables. From the above relation, it is clear that the disc height for VE depends on the flow variables v_ϕ, p and ρ . Therefore, when the fluid variables are perturbed, the disc height H_θ is also perturbed which is not the case for CH or CF where the disc height is independent of the flow variables. In the next section, we show how the acoustic spacetime metric is obtained by linearly perturbing three different quantities discussed in this section.

3.3 The acoustic metric from linear perturbation analysis

One of the main themes of our work is to show how the linear perturbation of the accretion flow equations gives rise to the emergence of the curved acoustic spacetime metric. In analogue gravity literature, the standard way to obtain the acoustic metric is to linearly perturb the fluid equation and obtain the perturbation equation in terms of the velocity potential of irrotational flow (for example, see [1, 5, 12]). However, one can derive the acoustic spacetime metric by obtaining the perturbation equation in terms of the relativistic Bernoulli's constant [63, 64, 73] or the mass accretion rate [13, 22, 53, 64, 73–77] also. In this chapter, we derive the acoustic spacetime metric by linearly perturbing all these three different quantities. First, we derive the acoustic spacetime metric for Michel flow and then for axially symmetric accretion flow for three different geometric configurations of the disc in a unified way. Before performing these perturbation analyses, we provide a general scheme that is followed in the analysis.

In order to perform linear perturbation analysis of the accretion solutions, we write down a full time-dependent accretion flow variable as the sum of a stationary time-independent part and a time-dependent small fluctuation. Using the same, we write down the velocity potential, mass accretion rate or the relativistic Bernoulli's constant about their stationary background value. Then these equations are substituted in the equations governing the flow, i.e., the continuity equation, Euler equation, irrotationality condition and the normalization condition and at every stage, the equations contain the terms that are up to linear order in perturbations and any terms of higher order in perturbations are discarded. This makes the perturbation analysis linear in nature. By rearranging the resulting equations we obtain the perturbation equation in terms of the velocity potential, mass accretion rate or the relativistic Bernoulli's constant. The perturbation equation is then compared to the equation of a massless scalar field in curved spacetime to obtain the acoustic spacetime metric.

For example, the perturbation equation in terms $x_1(t, r)$, where x_1 is small time-dependent fluctuation of the variable $x(t, r)$ about its stationary background value $x_0(r)$, is obtained to be of the form

$$\partial_\mu (f^{\mu\nu} \partial_\nu x_1) = 0. \quad (3.32)$$

where $f^{\mu\nu}$ is a symmetric 2×2 matrix with μ, ν running over t, r . On the other hand, the wave equation of a massless scalar field φ in a curved spacetime with metric $g_{\mu\nu}$ is given by

$$\partial_\mu (\sqrt{-g} g^{\mu\nu} \partial_\nu \varphi) = 0. \quad (3.33)$$

Comparing Eq. (3.32) and Eq. (3.33) one obtains the acoustic spacetime metric $G_{\mu\nu}$ from the relation

$$f^{\mu\nu} = \sqrt{-G} G^{\mu\nu}, \quad (3.34)$$

where G is the determinant of the acoustic spacetime metric $G_{\mu\nu}$. We will discuss the acoustic metric obtained by perturbing different quantities and compare them at end of the current section. There, we will provide the expressions of the acoustic metric that will be used in the rest of this chapter. Before that, we will find out the $f^{\mu\nu}$ for different cases.

3.3.1 Linear perturbation of Michel flow

For spherically symmetric Michel flow, the velocity components v^θ and v^ϕ are zero. Therefore, from the normalization condition $v_\mu v^\mu = -1$, we find the relation between v^t and v^r as

$$v^t = \sqrt{\frac{1 + g_{rr}(v^r)^2}{g_{tt}}}. \quad (3.35)$$

3.3.1.1 Perturbation of the velocity potential

It is possible to obtain the perturbation equation for the velocity potential for general flow in a general curved background spacetime without considering the

symmetries of the flow or the background spacetime. In [6], the acoustic metric for a general background spacetime metric $g_{\mu\nu}$ was derived by perturbing the velocity potential for an adiabatic flow. A flow is called adiabatic when the total heat content of the fluid system is conserved and is governed by the equation of state $p \propto \rho^\gamma$, where $\gamma = c_p/c_v$ is the adiabatic index of the fluid. c_p and c_v are the specific heats of the fluid at constant pressure and at constant volume, respectively. For adiabatic flow, the velocity potential ψ is defined as $h v_\mu = \partial_\mu \psi$. For isothermal flow the velocity potential is defined by the relation $\rho c_s^2 v_\mu = \partial_\mu \psi$ as given by Eq. (3.16). Here, first, we obtain the acoustic metric for isothermal flow without any symmetry by perturbing the velocity potential and then for the Michel flow with spherical symmetry.

We write the accretion variables about their stationary values as

$$\begin{aligned}\rho &= \rho_0 + \rho_1, \\ v^\mu &= v_0^\mu + v_1^\mu, \\ \psi &= \psi_0 + \psi_1,\end{aligned}\tag{3.36}$$

where the subscript ‘0’ represents the stationary time-independent part of the variables and the subscript ‘1’ represents the time-dependent fluctuations. The linear perturbation of the normalization condition provides

$$g_{\mu\nu} v_0^\mu v_1^\nu = 0.\tag{3.37}$$

We now use Eq. (3.36) to substitute ρ, v^μ, ψ in the Eq. (3.16) and retain only the terms that are upto first order in perturbations. This provides the following equations

$$\rho_0^{c_s^2-1} c_s^2 \rho_1 = v_0^\mu \partial_\mu \psi_1,\tag{3.38}$$

$$\rho_0^{c_s^2} v_1^\mu = -g^{\mu\nu} \partial_\nu \psi_1 - v_0^\mu v_0^\nu \partial_\nu \psi_1.\tag{3.39}$$

Similar substitutions of ρ, v^μ, ψ in the continuity equation given by Eq. (3.4) provides

$$\partial_\mu [\sqrt{-g} (v^\mu \rho_1 + \rho_0 v_1^\mu)] = 0.\tag{3.40}$$

Substituting ρ_1 and v_1^μ from the above equation using Eq. (3.38) and Eq. (3.39), respectively, provides the perturbation equation in terms of ψ_1 as

$$\partial_\mu \left[\frac{\sqrt{-g}}{\rho_0^{c_s^2-1}} \left\{ g^{\mu\nu} + \left(1 - \frac{1}{c_s^2}\right) v_0^\mu v_0^\nu \right\} \partial_\nu \psi_1 \right] = 0. \quad (3.41)$$

From the above equation we identify the symmetric matrix $f^{\mu\nu}$ as

$$f^{\mu\nu} = k_1(r) \left[c_s^2 g^{\mu\nu} + (1 - c_s^2) v_0^\mu v_0^\nu \right], \quad (3.42)$$

where $k_1(r) = -(\sqrt{-g})/(\rho_0^{c_s^2-1} c_s^2)$.

In the above derivation, we have not assumed any symmetry of the accretion flow or the background metric. We now consider the case of Michel flow with spherical symmetry. For the Michel flow, the Eq. (3.38) becomes

$$\rho_1 = \frac{1}{\rho_0^{c_s^2-1} c_s^2} (v_0^t \partial_t \psi_1 + v_0^r \partial_r \psi_1), \quad (3.43)$$

and Eq. (3.39) provides

$$v_1^t = \frac{1}{\rho_0^{c_s^2}} [(g^{tt} - (v_0^t)^2) \partial_t \psi_1 - v_0^r v_0^t \partial_r \psi_1] \quad (3.44)$$

$$v_1^r = \frac{1}{\rho_0^{c_s^2}} [(-g^{rr} - (v_0^r)^2) \partial_r \psi_1 - v_0^r v_0^t \partial_t \psi_1]. \quad (3.45)$$

Eq. (3.40) becomes

$$\partial_t [\sqrt{-g} (v_0^t \rho_1 + \rho_0 v_1^t)] + \partial_r [\sqrt{-g} (v_0^r \rho_1 + \rho_0 v_1^r)] = 0. \quad (3.46)$$

We now substitute ρ_1 , v_1^t and v_1^r in the above equation using Eq. (3.43), (3.44) and (3.45), respectively. This provides

$$\begin{aligned} & \partial_t [k_1(r) \{c_s^2 g^{tt} + (1 - c_s^2)(v_0^t)^2\} \partial_t \psi_1] + \partial_t [k_1(r) (1 - c_s^2) v_0^r v_0^t \partial_r \psi_1] \\ & + \partial_r [k_1(r) (1 - c_s^2) v_0^r v_0^t \partial_t \psi_1] + \partial_r [k_1(r) \{-c_s^2 g^{rr} + (1 - c_s^2)(v_0^r)^2\} \partial_r \psi_1] = 0, \end{aligned} \quad (3.47)$$

from which we obtain the symmetric 2×2 matrix as

$$f^{\mu\nu} = k_1(r) \begin{bmatrix} c_s^2 g^{tt} + (1 - c_s^2)(v_0^t)^2 & (1 - c_s^2) v_0^r v_0^t \\ (1 - c_s^2) v_0^r v_0^t & -c_s^2 g^{rr} + (1 - c_s^2)(v_0^r)^2 \end{bmatrix} \quad (3.48)$$

From the $f^{\mu\nu}$ matrix, the acoustic spacetime metric is obtained by using the relation given by Eq. (3.34).

3.3.1.2 Perturbation of the relativistic Bernoulli's constant

In Eq. (3.19), we have defined the relativistic Bernoulli's constant which is a conserved quantity for stationary flow. We now define another quantity $\xi = -v_t(t, r)\rho^{c_s^2}(t, r)$ which has the stationary part equal to the relativistic Bernoulli's constant ξ_0 . We perturb the density and velocity components upto linear order about their background stationary values as following

$$\begin{aligned}\rho(t, r) &= \rho_0(r) + \rho_1(t, r), \\ v^t(t, r) &= v_0^t(r) + v_1^t(t, r), \\ v^r(t, r) &= v_0^r(r) + v_1^r(t, r),\end{aligned}\tag{3.49}$$

where $\rho_1(t, r)$, $v_1^t(t, r)$ and $v_1^r(t, r)$ represent the first order perturbations. In terms of ξ , Eq. (3.18) can be recast in the form

$$v^t \partial_t v^t + \frac{c_s^2}{\rho} \frac{g_{rr}(v^r)^2}{g_{tt}} \partial_t \rho + \frac{v^r v^t}{\xi} \partial_r \xi = 0.\tag{3.50}$$

Using Eq. (3.49) in Eq. (3.50) and collecting only the terms which are linear in perturbations provides

$$-\frac{\alpha \xi_0}{v_0^r} \partial_t v_1^r - \frac{c_s^2}{\rho_0} \alpha \xi_0 \partial_t \rho_1 = \partial_r \xi_1,\tag{3.51}$$

where we have used $v_1^t = \alpha(r)v_1^r$ with $\alpha(r) = (g_{rr}v_0^r)/(g_{tt}v_0^t)$. Similarly, using Eq. (3.49) in the expression of ξ , one can write $\xi(t, r) = \xi_0 + \xi_1(t, r)$ where ξ_1 is given by

$$\xi_1 = \frac{\xi_0 \alpha}{v_0^t} v_1^r + \frac{\xi_0 c_s^2}{\rho_0} \rho_1.\tag{3.52}$$

Differentiating both sides of the above equation with respect to t provides

$$\frac{\xi_0 \alpha}{v_0^t} \partial_t v_1^r + \frac{\xi_0 c_s^2}{\rho_0} \partial_t \rho_1 = \partial_t \xi_1.\tag{3.53}$$

Now we express $\partial_t v_1^r$ and $\partial_t \rho_1$ solely in terms of $\partial_t \xi_1$ and $\partial_r \xi_1$ using Eq. (3.51) and Eq. (3.53) which gives

$$\partial_t v_1^r = \frac{1}{\delta} \frac{\xi_0 c_s^2}{\rho_0} [\partial_r \xi_1 + \alpha \partial_t \xi_1],\tag{3.54}$$

$$\partial_t \rho_1 = -\frac{1}{\delta} \frac{\xi_0 \alpha}{v_0^r v_0^t} [v_0^r \partial_r \xi_1 + v_0^t \partial_t \xi_1],\tag{3.55}$$

where $\delta = (-\xi_0^2 c_s^2 \alpha) / (\rho_0 v_0^r g_{tt} (v_0^t)^2)$. Also, substituting the density and velocity components in the continuity equation given by Eq. (3.23) using Eq. (3.49) provides the following equation

$$\partial_t [\sqrt{-g}(\rho_1 v_0^t + \alpha \rho_0 v_1^r)] + \partial_r [\sqrt{-g}(\rho_1 v_0^r + \alpha \rho_0 v_1^r)] = 0. \quad (3.56)$$

Differentiating both sides of the above equation with respect to t and substituting $\partial_t v_1^r$ and $\partial_t \rho_1$ using Eq. (3.54) and (3.55), respectively, gives

$$\begin{aligned} & \partial_t [k_2(r) \{c_s^2 g^{tt} + (1 - c_s^2)(v_0^t)^2\} \partial_t \xi_1] + \partial_t [k_2(r) v_0^r v_0^t (1 - c_s^2) \partial_r \xi_1] \\ & + \partial_r [k_2(r) v_0^r v_0^t (1 - c_s^2) \partial_t \xi_1] + \partial_r [k_2(r) \{-c_s^2 g^{rr} + (1 - c_s^2)(v_0^r)^2\} \partial_r \xi_1] = 0. \end{aligned} \quad (3.57)$$

The above equation is of the form $\partial_\mu (f^{\mu\nu} \partial_\nu \xi_1) = 0$. Therefore, the symmetric 2×2 matrix $f^{\mu\nu}$ is obtained to be

$$f^{\mu\nu} = k_2(r) \begin{bmatrix} c_s^2 g^{tt} + (1 - c_s^2)(v_0^t)^2 & v_0^r v_0^t (1 - c_s^2) \\ v_0^r v_0^t (1 - c_s^2) & -c_s^2 g^{rr} + (1 - c_s^2)(v_0^r)^2 \end{bmatrix}, \quad (3.58)$$

where $k_2(r) = -(\sqrt{-g}) / (c_s^2 \rho^{c_s^2 - 1})$.

3.3.1.3 Perturbation of the mass accretion rate

We follow the similar procedure to find out the $f^{\mu\nu}$ matrix by perturbing the mass accretion rate. We define the quantity $\Psi(t, r) = \sqrt{-\tilde{g}} v^r(t, r) \rho(t, r)$ which has the stationary part equal to the stationary mass accretion rate Ψ_0 defined in Eq. (3.24). Using the perturbation Eq. (3.49), we can write $\Psi(t, r) = \Psi_0 + \Psi_1(t, r)$ where Ψ_1 is obtained to be given by

$$\Psi_1(r, t) = \sqrt{-\tilde{g}}(v_0^r \rho_1 + \rho_0 v_1^r). \quad (3.59)$$

Also, using Eq. (3.49) in the continuity equation, i.e., Eq. (3.23) provides

$$\partial_t [v_0^t \rho_1 + \frac{g_{rr} v_0^r}{g_{tt} v_0^t} \rho_0 v_1^r] + \frac{1}{\sqrt{-\tilde{g}}} \partial_r \Psi_1 = 0. \quad (3.60)$$

Using Eq. (3.59) and Eq. (3.60) we express $\partial_t v_1^r$ and $\partial_t \rho_1$ solely in terms of $\partial_t \Psi_1$ and $\partial_r \Psi_1$,

$$\partial_t v_1^r = \frac{g_{tt} v_0^t}{\rho_0 \sqrt{-\tilde{g}}} [v_0^t \partial_t \Psi_1 + v_0^r \partial_r \Psi_1], \quad (3.61)$$

$$\partial_t \rho_1 = -\frac{1}{\sqrt{-\tilde{g}}} [g_{rr} v_0^r \partial_t \Psi_1 + g_{tt} v_0^t \partial_r \Psi_1]. \quad (3.62)$$

Now, we use Eq. (3.52) to substitute ξ_1 in Eq. (3.51) which provides

$$\frac{\alpha}{v_0^r} \partial_t v_1^r + \frac{c_s^2}{\rho_0} \alpha \partial_t \rho_1 + \partial_r \left(\frac{\alpha}{v_0^t} v_1^r + \frac{c_s^2}{\rho_0} \rho_1 \right) = 0. \quad (3.63)$$

Taking time derivative of the above equation and substituting $\partial_t v_1^r$ and $\partial_t \rho_1$ using Eq. (3.61) and Eq. (3.62), respectively, gives the perturbation equation in terms of Ψ_1 ,

$$\begin{aligned} & \partial_t [k_3(r) \{c_s^2 g^{tt} + (1 - c_s^2)(v_0^t)^2\} \partial_t \Psi_1] + \partial_t [k_3(r) v_0^r v_0^t (1 - c_s^2) \partial_r \Psi_1] \\ & + \partial_r [k_3(r) v_0^r v_0^t (1 - c_s^2) \partial_t \Psi_1] + \partial_r [k_3(r) \{-c_s^2 g^{rr} + (1 - c_s^2)(v_0^r)^2\} \partial_r \Psi_1] = 0 \end{aligned} \quad (3.64)$$

Similar to the previous section, the above perturbation equation is of the form $\partial_\mu (f^{\mu\nu} \partial_\nu \Psi_1) = 0$. Therefore, we obtain $f^{\mu\nu}$ to be given by

$$f^{\mu\nu} = k_3(r) \begin{bmatrix} c_s^2 g^{tt} + (1 - c_s^2)(v_0^t)^2 & v_0^r v_0^t (1 - c_s^2) \\ v_0^r v_0^t (1 - c_s^2) & -c_s^2 g^{rr} + (1 - c_s^2)(v_0^r)^2 \end{bmatrix}, \quad (3.65)$$

where $k_3(r) = -(g_{rr} v_0^r)/(v_0^t)$.

3.3.2 Linear perturbation of axially symmetric flow

In this section, we consider an accretion flow where the accreting matter forms an axially symmetric disc around the accretor. we consider three different geometric configuration for accretion disc, namely, the constant height flow (CH), the conical flow (CF) and the disc under hydrostatic equilibrium along the vertical direction (VE). We have discussed these flow geometries in Sec. 2.1 and Sec. 3.2.3. We shall work with these three models of accretion disc in a unified way.

The normalization condition $v_\mu v^\mu = -1$ gives

$$g_{tt}(v_t)^2 = 1 + g_{rr}(v^r)^2 + g_{\phi\phi}(v^\phi)^2. \quad (3.66)$$

From irrotationality condition, given by Eq. (3.15), with $\mu = t$ and $\nu = \phi$ and with axial symmetry we have

$$\partial_t (v_\phi \rho^{c_s^2}) = 0, \quad (3.67)$$

and with $\mu = r$ and $\nu = \phi$ we have

$$\partial_r (v_\phi \rho^{c_s^2}) = 0. \quad (3.68)$$

Eq. (3.67) and Eq. (3.68) implies that $v_\phi \rho^{c_s^2}$ is a constant of motion for axially symmetric irrotational flow. Similar to the previous sections we express the accretion variables in terms of time-dependent linear perturbations about their background stationary values,

$$\begin{aligned}
 v^t(t, r) &= v_0^t(r) + v_1^t(t, r), \\
 v^r(t, r) &= v_0^r(r) + v_1^r(t, r), \\
 v^\phi(t, r) &= v_0^\phi(r) + v_1^\phi(t, r), \\
 \rho(t, r) &= \rho_0(r) + \rho_1(t, r),
 \end{aligned} \tag{3.69}$$

where the subscript ‘0’ stands for stationary part and ‘1’ stands for the linear perturbations. Using Eq. (3.69) in the expression $v_\phi \rho^{c_s^2} = \text{constant}$, we find the relation between v_1^ϕ and ρ_1 to be

$$v_1^\phi = -\frac{c_s^2 v_0^\phi}{\rho_0} \rho_1. \tag{3.70}$$

Similarly, using Eq. (3.69) in Eq. (3.66) and substituting v_1^ϕ using Eq. (3.70) we get

$$v_1^t = \alpha_1 v_1^r + \alpha_2 \rho_1, \tag{3.71}$$

where

$$\alpha_1 = \frac{g_{rr} v_0^r}{g_{tt} v_0^t}, \quad \alpha_2 = -\frac{g_{\phi\phi} (v_0^\phi)^2 c_s^2}{g_{tt} v_0^t \rho_0}. \tag{3.72}$$

For accretion flow governed by isothermal equation of state, the pressure–density relation is given by $p \propto \rho$. For flow in hydrostatic equilibrium along the vertical direction, i.e., for VE model of accretion disc, the disc height is given by the relation provided in Eq. (3.31). Linear perturbation of Eq. (3.31) using Eq. (3.69) gives

$$\frac{(H_\theta)_1}{(H_\theta)_0} = c_s^2 \frac{\rho_1}{\rho_0}, \tag{3.73}$$

where we have used Eq. (3.70) to substitute v_1^ϕ . Eq. (3.73) gives the expression of the linear perturbation of the disc height for VE model. For other two models, i.e., CH and CF, the expression for the disc height does not contain any accretion variables and there the disc heights for these two models are not affected by the

perturbation in the accretion flow. Therefore, we can combine the three cases and express the linear perturbation of the disc height as

$$\frac{(H_\theta)_1}{(H_\theta)_0} = \beta \frac{\rho_1}{\rho_0}, \quad \beta = \begin{cases} 0 & \text{CH, CF} \\ c_s^2 & \text{VE.} \end{cases} \quad (3.74)$$

Using Eq. (3.69) in the continuity equation given by Eq. (3.27) gives

$$\begin{aligned} & \partial_t \left[\sqrt{-\tilde{g}} \{ v_0^t (H_\theta)_0 \rho_1 + \rho_0 (H_\theta)_0 v_1^t + \rho_0 v_0^t (H_\theta)_1 \} \right] \\ & + \partial_r \left[\sqrt{-\tilde{g}} \{ v_0^r (H_\theta)_0 \rho_1 + \rho_0 (H_\theta)_0 v_1^r + \rho_0 v_0^r (H_\theta)_1 \} \right] = 0 \end{aligned} \quad (3.75)$$

3.3.2.1 Perturbation of velocity potential

From irrotationality condition it was found that $v_\phi \rho^{c_s^2}$ is a constant of motion. Velocity potential is defined as $v_\mu \rho^{c_s^2} = \partial_\mu \psi$ which gives $\partial_\phi \psi_1 = 0$. Therefore, Eq. (3.38) for axially symmetric flow gives

$$\rho_1 = \frac{1}{\rho_0^{c_s^2-1} c_s^2} [v_0^t \partial_t \psi_1 + v_0^r \partial_r \psi_1], \quad (3.76)$$

and Eq. (3.39) gives

$$v_1^t = \frac{1}{\rho_0^{c_s^2}} [(g^{tt} - (v_0^t)^2) \partial_t \psi_1 - v_0^r v_0^t \partial_r \psi_1] \quad (3.77)$$

$$v_1^r = \frac{1}{\rho_0^{c_s^2}} [(-g^{rr} - (v_0^r)^2) \partial_r \psi_1 - v_0^r v_0^t \partial_t \psi_1] \quad (3.78)$$

Now we substitute ρ_1, v_1^t, v_1^r and $(H_\theta)_1$ in Eq. (3.75) using Eq. (3.76), (3.77), (3.78) and Eq. (3.74), respectively, to obtain the perturbation equation,

$$\begin{aligned} & \partial_t \left[\tilde{k}_1(r) \left\{ -g^{tt} + \left(1 - \frac{1+\beta}{c_s^2} \right) (v_0^t)^2 \right\} \partial_t \psi_1 \right] \\ & + \partial_t \left[\tilde{k}_1(r) \left(1 - \frac{1+\beta}{c_s^2} \right) v_0^r v_0^t \partial_r \psi_1 \right] \\ & + \partial_r \left[\tilde{k}_1(r) \left(1 - \frac{1+\beta}{c_s^2} \right) v_0^r v_0^t \partial_t \psi_1 \right] \\ & + \partial_t \left[\tilde{k}_1(r) \left\{ g^{rr} + \left(1 - \frac{1+\beta}{c_s^2} \right) (v_0^r)^2 \right\} \partial_t \psi_1 \right] \\ & = 0, \end{aligned} \quad (3.79)$$

where $\tilde{k}_1(r) = \sqrt{-\tilde{g}}/(\rho_0^{c_s^2-1})$. As earlier, we compare the above equation to the wave equation of the form $\partial_\mu(f^{\mu\nu}\partial_\nu\psi_1) = 0$ and obtain the $f^{\mu\nu}$ matrix as

$$f^{\mu\nu} = \tilde{k}_1 \begin{bmatrix} -g^{tt} + \left(1 - \frac{1+\beta}{c_s^2}\right) (v_0^t)^2 & \left(1 - \frac{1+\beta}{c_s^2}\right) v_0^r v_0^t \\ \left(1 - \frac{1+\beta}{c_s^2}\right) v_0^r v_0^t & g^{rr} + \left(1 - \frac{1+\beta}{c_s^2}\right) (v_0^r)^2 \end{bmatrix} \quad (3.80)$$

3.3.2.2 Perturbation of relativistic Bernoulli's constant

As earlier, we introduce the time-dependent variable $\xi(t, r) = -v_t(t, r)\rho^{c_s^2}(t, r)$ which has the stationary part equal to the relativistic Bernoulli's constant ξ_0 and may be expressed as $\xi(t, r) = \xi_0 + \xi_1(t, r)$ under linear perturbation. Using the perturbation equations given by Eq. (3.69) in Eq. (3.20) we get

$$-\frac{\alpha_1 \xi_0}{v_0^r} \partial_t v_1^r - \frac{c_s^2}{\rho_0} \alpha_1 \xi_0 \partial_t \rho_1 = \partial_r \xi_1, \quad (3.81)$$

whereas using the Eq. (3.69) in the expression for ξ , one obtains

$$\xi_1 = \frac{\xi_0}{v_0^t} v_1^t + \frac{\xi_0 c_s^2}{\rho_0} \rho_1. \quad (3.82)$$

We differentiate the above equation with respect to t and substitute v_1^t using Eq. (3.71) to obtain

$$\partial_t \xi_1 = \frac{\alpha_1 \xi_0}{v_0^t} \partial_t v_1^r + \left(\frac{\xi_0 c_s^2}{\rho_0} + \frac{\xi_0}{v_0^t} \alpha_2\right) \partial_t \rho_1. \quad (3.83)$$

Now, we use Eq. (3.81) and Eq. (3.83) to express $\partial_t v_1^r$ and $\partial_t \rho_1$ solely in terms of derivatives of ξ_1 ,

$$\partial_t v_1^r = \frac{1}{\delta} \left[\left(\frac{\xi_0 c_s^2}{\rho_0} + \frac{\xi_0}{v_0^t} \alpha_2\right) \partial_r \xi_1 + \frac{\xi_0 \alpha_1 c_s^2}{\rho_0} \partial_t \xi_1 \right], \quad (3.84)$$

$$\partial_t \rho_1 = -\frac{\xi_0 \alpha_1}{\delta} \left[\frac{1}{v_0^t} \partial_r \xi_1 + \frac{1}{v_0^r} \partial_t \xi_1 \right], \quad (3.85)$$

where $\delta = (\xi_0^2 c_s^2 \alpha_1)/(v_0^r \rho_0 g_{tt} (v_0^t)^2)$. Differentiating the Eq. (3.75) with respect to t and rearranging gives

$$\begin{aligned} & \partial_t \left[\sqrt{-\tilde{g}}(H_\theta)_0 \{v_0^t(1+\beta) + \alpha_2 \rho_0\} \partial_t \rho_1 + \sqrt{-\tilde{g}}(H_\theta)_0 \rho_0 \alpha_1 \partial_t v_1^r \right] \\ & + \partial_r \left[\sqrt{-\tilde{g}}(H_\theta)_0 \{v_0^r(1+\beta) \partial_t \rho_1 + \rho_0 \partial_t v_1^r\} \right] = 0. \end{aligned} \quad (3.86)$$

Substitution of $\partial_t v_1^r$ and $\partial_t \rho_1$ in the above equation using Eq. (3.84) and (3.85), respectively, gives the perturbation equation in terms of ξ_1

$$\begin{aligned}
 & \partial_t \left[\tilde{k}_2(r) \left\{ -g^{tt} + \left(1 - \frac{1+\beta}{c_s^2} \right) (v_0^t)^2 \right\} \partial_t \xi_1 \right] \\
 & + \partial_t \left[\tilde{k}_2(r) \left(1 - \frac{1+\beta}{c_s^2} \right) v_0^r v_0^t \partial_r \xi_1 \right] \\
 & + \partial_r \left[\tilde{k}_2(r) \left(1 - \frac{1+\beta}{c_s^2} \right) v_0^r v_0^t \partial_t \xi_1 \right] \\
 & + \partial_t \left[\tilde{k}_2(r) \left\{ g^{rr} + \left(1 - \frac{1+\beta}{c_s^2} \right) (v_0^r)^2 \right\} \partial_t \xi_1 \right] \\
 & = 0,
 \end{aligned} \tag{3.87}$$

where $\tilde{k}_2(r) = (\sqrt{-\tilde{g}}(H_\theta)_0)/(\rho_0^{c_s^2-1})$. The above equation, when compared to the equation $\partial_\mu \{ f^{\mu\nu} \partial_\nu \xi_1 \} = 0$, gives the $f^{\mu\nu}$ matrix as

$$f^{\mu\nu} = \tilde{k}_2 \begin{bmatrix} -g^{tt} + \left(1 - \frac{1+\beta}{c_s^2} \right) (v_0^t)^2 & \left(1 - \frac{1+\beta}{c_s^2} \right) v_0^r v_0^t \\ \left(1 - \frac{1+\beta}{c_s^2} \right) v_0^r v_0^t & g^{rr} + \left(1 - \frac{1+\beta}{c_s^2} \right) (v_0^r)^2 \end{bmatrix} \tag{3.88}$$

3.3.2.3 Perturbation of the mass accretion rate

Now, let us find out the $f^{\mu\nu}$ matrix by perturbing the mass accretion rate. We define the variable $\Psi(t, r) = \sqrt{-\tilde{g}}\rho(t, r)v^r(t, r)(H_\theta)$ which has the stationary part equal to the stationary mass accretion rate Ψ_0 given by Eq. (3.30), i.e., $\Psi(t, r) = \Psi_0 + \Psi_1(t, r)$. Thus, using the perturbation equations given by Eq. (3.69), we get the perturbation of the mass accretion rate $\Psi_1(t, r)$ to be given by

$$\Psi_1(r, t) = \sqrt{-\tilde{g}}\{\rho_0 v_0^r (H_\theta)_1 + \rho_1 v_0^r (H_\theta)_0 + \rho_0 v_1^r (H_\theta)_0\}. \tag{3.89}$$

Taking time derivative of the above equation and substituting $(H_\theta)_1$ using Eq. (3.74) gives

$$\frac{\partial_t \Psi_1}{\Psi_0} = (1 + \beta) \frac{\partial_t \rho_1}{\rho_0} + \frac{\partial_t v_1^r}{v_0^r}. \tag{3.90}$$

Also, substituting velocity components and density in the continuity Eq. (3.27) using Eq. (3.69) provides

$$\frac{\partial_r \Psi_1}{\Psi_0} = -\left[\left\{ \frac{v_0^t}{v_0^r \rho_0} (1 + \beta) + \frac{\alpha_2}{v_0^r} \right\} \partial_t \rho_1 + \frac{\alpha_1}{v_0^r} \partial_t v_1^r \right]. \tag{3.91}$$

Eq. (3.90) and (3.91) can be used to write $\partial_t v_1^r$ and $\partial_t \rho_1$ in terms of the derivatives of Ψ_1 ,

$$\frac{\partial_t v_1^r}{v_0^r} = \frac{1}{\Lambda} [\{g_{tt}(v_0^t)^2(1+\beta) - g_{\phi\phi}(v_0^\phi)^2 c_s^2\} \frac{\partial_t \Psi_1}{\Psi_0} + (1+\beta) g_{tt} v_0^r v_0^t \frac{\partial_r \Psi_1}{\Psi_0}], \quad (3.92)$$

$$\frac{\partial_t \rho_1}{\rho_0} = -\frac{1}{\Lambda} [g_{rr}(v_0^r)^2 \frac{\partial_t \Psi_1}{\Psi_0} + g_{tt} v_0^r v_0^t \frac{\partial_r \Psi_1}{\Psi_0}], \quad (3.93)$$

where $\Lambda = (1+\beta) + (1+\beta - c_s^2) g_{\phi\phi} (v_0^\phi)^2$.

Substituting ξ_1 in Eq. (3.81) using Eq. (3.82) provides

$$\frac{\alpha_1}{v_0^r} \partial_t v_1^r + \frac{c_s^2}{\rho_0} \alpha_1 \partial_t \rho_1 + \partial_r \left(\frac{v_1^t}{v_0^t} + \frac{c_s^2}{\rho_0} \rho_1 \right) = 0, \quad (3.94)$$

where v_1^t is given by Eq. (3.77). Differentiating the above equation with respect to t gives

$$\partial_t \left(\frac{\alpha_1}{v_0^r} \partial_t v_1^r \right) + \partial_t \left(\frac{\alpha_1 c_s^2}{\rho_0} \partial_t \rho_1 \right) + \partial_r \left(\frac{\alpha_1}{v_0^t} \partial_t v_1^r \right) + \partial_r \left\{ \left(\frac{\alpha_2}{v_0^t} + \frac{c_s^2}{\rho_0} \right) \partial_t \rho_1 \right\} = 0. \quad (3.95)$$

A substitution of $\partial_t v_1^r$ and $\partial_t \rho_1$ in the above equation using Eq. (3.92) and Eq. (3.93), respectively, provides the perturbation equation in terms of Ψ_1 ,

$$\begin{aligned} & \partial_t \left[\tilde{k}_3(r) \left\{ -g^{tt} + \left(1 - \frac{1+\beta}{c_s^2} \right) (v_0^t)^2 \right\} \partial_t \Psi_1 \right] \\ & + \partial_t \left[\tilde{k}_3(r) \left(1 - \frac{1+\beta}{c_s^2} \right) v_0^r v_0^t \partial_r \Psi_1 \right] \\ & + \partial_r \left[\tilde{k}_3(r) \left(1 - \frac{1+\beta}{c_s^2} \right) v_0^r v_0^t \partial_t \Psi_1 \right] \\ & + \partial_t \left[\tilde{k}_3(r) \left\{ g^{rr} + \left(1 - \frac{1+\beta}{c_s^2} \right) (v_0^r)^2 \right\} \partial_t \Psi_1 \right] \\ & = 0, \end{aligned} \quad (3.96)$$

where $\tilde{k}_3(r) = (g_{rr} v_0 c_s^2) / (v_0^t \Lambda)$. The above equation is of the form $\partial_\mu \{ f^{\mu\nu} \partial_\nu \Psi_1 \} = 0$ which helps us to identify the $f^{\mu\nu}$ as

$$f^{\mu\nu} = \tilde{k}_2 \begin{bmatrix} -g^{tt} + \left(1 - \frac{1+\beta}{c_s^2} \right) (v_0^t)^2 & \left(1 - \frac{1+\beta}{c_s^2} \right) v_0^r v_0^t \\ \left(1 - \frac{1+\beta}{c_s^2} \right) v_0^r v_0^t & g^{rr} + \left(1 - \frac{1+\beta}{c_s^2} \right) (v_0^r)^2 \end{bmatrix} \quad (3.97)$$

3.3.3 Acoustic metric

In the previous section, we performed a linear perturbation analysis to find out the perturbation equation in terms of three different quantities—the velocity potential

ψ_1 , the relativistic Bernoulli's constant ξ_1 and the mass accretion rate Ψ_1 . This was done for two different accretion flow—the spherically symmetric Michel flow and the axially symmetric disc-like flow. For disc like axially symmetric flow, we considered three different kinds of geometric configurations of the disc and derived the perturbation equations in a unified way introducing the variable β defined in Eq. (3.74). As stated earlier, the acoustic spacetime metric is obtained from the perturbation equation of the form $\partial_\mu(f^{\mu\nu}\partial_\nu x_1) = 0$, where x_1 is the linear perturbation of the accretion variable x . The acoustic spacetime metric $G^{\mu\nu}$ is obtained from the relation given by Eq. (3.34) which is obtained by comparing the perturbation equation and the wave equation of a massless scalar field in curved spacetime as given by Eq. (3.33). Thus, the acoustic metric $G^{\mu\nu}$ is related to $f^{\mu\nu}$ as

$$G^{\mu\nu} = \frac{1}{\sqrt{-G}} f^{\mu\nu}, \quad (3.98)$$

which implies that the acoustic metric is conformally the same to $f^{\mu\nu}$. The conformal factor is known if we know the determinant G of the acoustic metric. This, in general, is simply done by taking determinant of the both sides of the Eq. (3.98). For a 1+3 dimensional problem, this gives $G = \det(f^{\mu\nu})$ and for a general 1+($n-1$) dimensional problem we have

$$-G = \{-\det(f^{\mu\nu})\}^{\frac{2}{n-2}}. \quad (3.99)$$

It is evident from the above expression that for 1+1 dimensional system, the above expression encounters a problem and it is not possible to define G and hence the metric $G^{\mu\nu}$ from $f^{\mu\nu}$. However, this is a problem of concern only when the system is intrinsically two dimensional. But in our problem, the system is 1+3 dimensional and the $f^{\mu\nu}$ is 2×2 only due to the symmetries of the problem. Therefore, the problem is rather formal and not fundamental. One can always augment the 1+1 dimensional spacetime with two extra flat dimensions to make the problem go away [8, 9]

Due to the fact that G contributes only as a conformal factor, we, in principle, do not need to find out G exactly to study the conformally invariant features of the acoustic spacetime. The location of the acoustic horizon, the causal structure

of the acoustic spacetime or the acoustic surface gravity are conformally invariant. Therefore, we study these conformally invariant features of the acoustic spacetime without considering the conformal factor in the acoustic spacetime metric. Thus, in the following, we work with the expression for acoustic metric without the overall conformal factors.

3.3.3.1 Acoustic metric for Michel flow

In Sec. 3.3.1, we derived the perturbation equation for spherically symmetric Michel flow. It could be noticed that $f^{\mu\nu}$ matrix obtained by perturbing the three different quantities (given by Eq. (3.48), (3.58) and (3.65) for velocity potential, relativistic Bernoulli's constant and the mass accretion rate, respectively) are the same apart from an over all multiplicative factor $k_i(r)$ ($i = 1, 2, 3$ represents the case of velocity potential, relativistic Bernoulli's constant and the mass accretion rate, respectively) and it is given by

$$f^{\mu\nu} = k_i(r) \begin{bmatrix} c_s^2 g^{tt} + (1 - c_s^2)(v_0^t)^2 & (1 - c_s^2)v_0^r v_0^t \\ (1 - c_s^2)v_0^r v_0^t & -c_s^2 g^{rr} + (1 - c_s^2)(v_0^r)^2 \end{bmatrix} \quad (3.100)$$

where

$$k_1 = k_2 = -(\sqrt{-g})/(\rho^{c_s^2-1} c_s^2), \quad k_3 = -(g_{rr} v_0^r)/(v_0^t). \quad (3.101)$$

Therefore, the acoustic metric $G^{\mu\nu}$, neglecting the conformal factor which contains k_i and G , is given by

$$G^{\mu\nu} = - \begin{bmatrix} c_s^2 g^{tt} + (1 - c_s^2)(v_0^t)^2 & (1 - c_s^2)v_0^r v_0^t \\ (1 - c_s^2)v_0^r v_0^t & -c_s^2 g^{rr} + (1 - c_s^2)(v_0^r)^2 \end{bmatrix} \quad (3.102)$$

and therefore, $G_{\mu\nu}$ (where we again neglect any overall factor arising in the process of taking the inverse of $G^{\mu\nu}$) is given by

$$G_{\mu\nu} = \begin{bmatrix} -c_s^2 g^{rr} + (1 - c_s^2)(v_0^r)^2 & -(1 - c_s^2)v_0^r v_0^t \\ -(1 - c_s^2)v_0^r v_0^t & c_s^2 g^{tt} + (1 - c_s^2)(v_0^t)^2 \end{bmatrix} \quad (3.103)$$

3.3.3.2 Acoustic metric for Axially symmetric flow

For axially symmetric flow in Sec. 3.3.2, we also consider different flow configurations. We worked with different disc models by introducing the variable β and we notice that the $f^{\mu\nu}$ matrix contains the β term. Therefore, the final acoustic metric is dependent on the model of the accretion disc. As in the case of the Michel flow, for axially symmetric flow also, we notice that the $f^{\mu\nu}$ matrix is the same (apart from an overall multiplicative factor) for all the three quantities we perturb and may be given as

$$f^{\mu\nu} = \tilde{k}_i(r) \begin{bmatrix} -g^{tt} + (1 - \frac{1+\beta}{c_s^2})(v_0^t)^2 & (1 - \frac{1+\beta}{c_s^2})v_0^r v_0^t \\ (1 - \frac{1+\beta}{c_s^2})v_0^r v_0^t & g^{rr} + (1 - \frac{1+\beta}{c_s^2})(v_0^r)^2 \end{bmatrix} \quad (3.104)$$

where $i = 1, 2, 3$ for the linear perturbation of velocity potential, relativistic Bernoulli's constant and the mass accretion rate, respectively and

$$\tilde{k}_1 = \sqrt{-\tilde{g}}/(\rho_0^{c_s^2-1}), \quad \tilde{k}_2 = (\sqrt{-\tilde{g}}(H_\theta)_0)/(\rho_0^{c_s^2-1}), \quad \tilde{k}_3 = (g_{rr}v_0^r c_s^2)/(v_0^t \Lambda), \quad (3.105)$$

where Λ is defined below Eq. (3.93). We notice that the factors \tilde{k}_i in $f^{\mu\nu}$ obtained by perturbing the velocity potential and the relativistic Bernoulli's constant are the same (apart from the H_θ which comes due to vertical averaging), whereas the \tilde{k}_i obtained by perturbing the mass accretion rate is different from that of the other two cases. This can be explained in the following way: The relativistic Bernoulli's constant is obtained by integrating the temporal component of the relativistic Euler equation and the velocity potential is defined via the irrotationality condition. However, we have used the irrotationality condition in order to find the temporal component of the Euler equation and to define the relativistic Bernoulli's constant. One can easily see that these two quantities are related by a time derivative. Thus, it is expected that the linear perturbation of these two quantities gives the same acoustic metric with the same conformal factors. The mass accretion rate is, on the other hand, derived from the continuity equation where the irrotationality condition plays no part. Thus the conformal factor of the acoustic metric obtained by perturbing the mass accretion rate is different from the other two cases.

As in the case of Michel flow, we neglect the overall conformal factors and use the expressions for the acoustic metric given below

$$G^{\mu\nu} = \begin{bmatrix} -g^{tt} + \left(1 - \frac{1+\beta}{c_s^2}\right) (v_0^t)^2 & v_0^r v_0^t \left(1 - \frac{1+\beta}{c_s^2}\right) \\ v_0^r v_0^t \left(1 - \frac{1+\beta}{c_s^2}\right) & g^{rr} + \left(1 - \frac{1+\beta}{c_s^2}\right) (v_0^r)^2 \end{bmatrix} \quad (3.106)$$

and

$$G_{\mu\nu} = - \begin{bmatrix} g^{rr} + \left(1 - \frac{1+\beta}{c_s^2}\right) (v_0^r)^2 & -v_0^r v_0^t \left(1 - \frac{1+\beta}{c_s^2}\right) \\ -v_0^r v_0^t \left(1 - \frac{1+\beta}{c_s^2}\right) & -g^{tt} + \left(1 - \frac{1+\beta}{c_s^2}\right) (v_0^t)^2 \end{bmatrix} \quad (3.107)$$

We will use the expressions of the acoustic metric given by Eq. (3.102), (3.103), (3.106) and (3.107) in the next section to study the location of the acoustic horizon and the causal structure of the acoustic spacetime.

3.4 Location of the acoustic horizon

The acoustic spacetime metric $G_{\mu\nu}$ given by Eq. (3.103) and (3.107) for Michel flow and Axially symmetric flow, respectively, are time-independent and hence the acoustic spacetime is stationary. The spacetime metric is also spherically symmetric. In the asymptotic limit $r \rightarrow \infty$ (with the fact that at $r \rightarrow \infty$, the velocity components $v^\mu \rightarrow 0$), the acoustic metric is the same as the flat Minkowski metric. In other words, the acoustic metric is stationary spherically symmetric and asymptotically flat. For such a spacetime, in analogy to the general relativity, we can define the acoustic horizon as time-like hypersurface $r = \text{constant}$ whose normal $n_\mu = \delta_\mu^r$ is null with respect to the acoustic metric [7, 12]

$$G^{\mu\nu} n_\mu n_\nu = 0. \quad (3.108)$$

Thus the acoustic horizon is found by solving the equation

$$G^{\mu\nu} \delta_\mu^r \delta_\nu^r = G^{rr} = 0. \quad (3.109)$$

3.4.1 Michel flow

For Michel flow, the acoustic horizon, given by $G^{rr} = 0$, satisfies

$$-c_s^2 + g_{rr} (v_0^r)^2 (1 - c_s^2) = 0 \quad (3.110)$$

or

$$c_s^2 = \frac{g_{rr}(v_0^r)^2}{1 + g_{rr}(v_0^r)^2} \quad (3.111)$$

It is convenient to express the above equation in terms of the ‘advective velocity’ u which is defined, for Michel flow, as the radial speed of the accreting matter as measured by a stationary observer. A stationary observer is an observer with fixed spatial coordinates. The four-velocity components of the accreting matter can be expressed in terms of its radial speed u_0 (the stationary value of u) with respect to the stationary observer as

$$v_0^t = \frac{1}{\sqrt{g_{tt}}} \frac{1}{\sqrt{1 - u_0^2}}, \quad (3.112)$$

$$v_0^r = \frac{u_0}{\sqrt{g_{rr}}} \frac{1}{\sqrt{1 - u_0^2}}. \quad (3.113)$$

Using the above two equations, we can rewrite Eq. (3.111) in terms of u_0 as

$$c_s^2|_h = u_0^2|_h. \quad (3.114)$$

Hereafter, the suffix ‘h’ would imply that the equation is to be evaluated at the acoustic horizon. Thus, we find that the acoustic horizon is located at a radial distance where the local sound speed and the advective speed becomes equal. In other words, the acoustic horizon and the transonic surface (defined as the surface where the Mach number $\mathcal{M} \equiv u_0/c_s$ becomes 1) coincide.

3.4.2 Axially symmetric flow

For axially symmetric flow, the condition $G^{rr} = 0$ for acoustic horizon gives

$$c_s^2 = \frac{(1 + \beta)g_{rr}(v_0^r)^2}{1 + g_{rr}(v_0^r)^2}. \quad (3.115)$$

The ‘advective velocity’ u for axially symmetric flow, is defined as the radial speed of the accreting matter as measured in a frame co-rotating (CF) with the accreting matter. The accretion in the CF is described by two variables— u and the specific angular momentum $\lambda = -v_\phi/v_t$. In terms of u_0 and λ_0 (stationary value of λ), the

velocity components v_0^μ can be expressed as

$$v_0^t = \sqrt{\frac{g_{\phi\phi}}{g_{tt}(g_{\phi\phi} - \lambda_0^2 g_{tt})}} \sqrt{\frac{1}{1 - u_0^2}}, \quad (3.116)$$

$$v_0^r = \frac{u_0}{\sqrt{g_{rr}(1 - u_0^2)}}, \quad (3.117)$$

$$v_0^\phi = \lambda_0 \sqrt{\frac{g_{tt}}{g_{\phi\phi}(g_{\phi\phi} - \lambda_0^2 g_{tt})}} \sqrt{\frac{1}{1 - u_0^2}}. \quad (3.118)$$

Using the above three equations, we express the horizon condition given by Eq. (3.115) in terms of u_0 and λ_0 as

$$u_0^2|_h = \frac{c_s^2}{1 + \beta}|_h. \quad (3.119)$$

For constant height flow and conical flow, $\beta = 0$ and therefore for these two models, the acoustic horizon coincide with the transonic surface. For, flow in hydrostatic equilibrium along the vertical direction, $\beta \neq 0$ and the effective sound speed in the VE model is therefore observed to be $c_{\text{eff}} = c_s/(1 + \beta)$. c_{eff} is the actual speed of propagation of linear perturbation inside the transonic fluid. This effective sound speed will be discussed in great details in Chap. 7.

3.5 Causal structure

In this section, we will study the causal structure of the acoustic spacetime at and around the acoustic horizon to illustrate the behavior of the phonon null geodesics. The causal structure of the acoustic spacetime is independent of the conformal factor. The null geodesic corresponding to the radially traveling phonons is given by $ds^2|_{\theta=\text{const}, \phi=\text{const}} = 0$. This provides

$$\left(\frac{dr}{dt}\right)_\pm \equiv b_\pm = \frac{-G_{rt} \pm \sqrt{G_{rt}^2 - G_{rr}G_{tt}}}{G_{rr}}. \quad (3.120)$$

So $t(r)$ is obtained as

$$t(r)_\pm = t_0 + \int_{r_0}^r \frac{1}{b_\pm} dr. \quad (3.121)$$

3.5.1 Causal structure for Michel flow

The acoustic metric elements for the Michel flow is given by Eq. (3.103). The metric elements can be expressed in terms of u_0 using Eq. (3.112) and Eq. (3.113),

$$G_{tt} = g_{tt} \left(\frac{u_0^2 - c_s^2}{1 - u_0^2} \right), \quad (3.122)$$

$$G_{tr} = - \left(\frac{1 - c_s^2}{1 - u_0^2} \right) u_0, \quad (3.123)$$

$$G_{rr} = g_{rr} \left(\frac{1 - u_0^2 c_s^2}{1 - u_0^2} \right). \quad (3.124)$$

Thus, b_{\pm} becomes

$$b_{\pm} = g_{tt} \left(\frac{u_0 \pm c_s}{1 - u_0 c_s} \right). \quad (3.125)$$

For accretion flow, $u_0 < 0$ which implies the in fall of matter. Near the acoustic horizon which coincide with the transonic surface, u_0 can be approximated as

$$u_0 = -c_s + \left. \frac{du_0}{dr} \right|_h (r - r_h) + \mathcal{O}(r - r_h)^2 + .. \quad (3.126)$$

Therefore, it is noticed that at the acoustic horizon, i.e., at $r = r_h$, $b_+ \rightarrow 0$ which makes the coordinate t_+ diverge as $\ln |r - r_h|$ at the acoustic horizon. However, b_- remains non-zero at the acoustic horizon and hence t_- remains finite.

In order to draw the causal structure, we need to perform the integration in Eq. (3.121). The expression for b_{\pm} contains u_0 which could be found by numerically solving the accretion flow equations. Below we discuss briefly how to solve for the stationary solutions using the continuity and Euler equation.

In order to solve for the stationary solutions for spherically symmetric accretion, we use two expressions—first one is the mass accretion rate, $\Psi_0 = \sqrt{-\tilde{g}} \rho_0 v_0^r$, which is obtained by integrating the continuity equation and the relativistic Bernoulli's constant given by Eq. (3.19) which obtained by integrating the temporal component of the Euler equation. In terms of u_0 , these are given by

$$\Psi_0 = \frac{1}{\sqrt{g_{rr}}} \frac{\rho_0 u_0 r^2}{\sqrt{1 - u_0^2}}, \quad (3.127)$$

$$\xi_0 = \sqrt{g_{tt}} \frac{1}{\sqrt{1 - u_0^2}} \rho_0^{c_s^2}, \quad (3.128)$$

where we have used $v_{t0} = -g_{tt}v_0^t$. Logarithmic differentiation of the above two equations provides, respectively,

$$u'_0 = -u_0(1 - u_0^2) \left[\frac{\rho'_0}{\rho_0} + \frac{2}{r} + \frac{g'_{tt}}{2g_{tt}} \right], \quad (3.129)$$

$$\frac{\rho'_0}{\rho_0} = -\frac{1}{c_s^2} \left[\frac{u_0 u'_0}{(1 - u_0^2)} + \frac{g'_{tt}}{2g_{tt}} \right], \quad (3.130)$$

where, the ‘prime’ stands for differentiation with respect to the radial coordinate r . Substituting Eq. (3.130) in Eq. (3.129) provides the gradient of the radial velocity as [75]

$$u'_0 = \frac{u_0(1 - u_0^2)}{u_0^2 - c_s^2} \left[\frac{2c_s^2}{r} - \frac{g'_{tt}}{2g_{tt}}(1 - c_s^2) \right]. \quad (3.131)$$

The above equation can be solved for $u_0(r)$, numerically for given value of the sound speed which is a constant for isothermal flow. The isothermal sound speed may be expressed in terms of the bulk ion temperature, T , through the Clapeyron-Mendeleev equation [78, 79],

$$c_s = \sqrt{\frac{k_B T}{\mu m_H}}, \quad (3.132)$$

where k_B is the Boltzmann constant, m_H is the mass of the hydrogen atom ($m_H \approx m_p$ for one temperature fluid) and μ is the mean molecular weight. Thus, we solve Eq. (3.131) for u_0 for given temperature T of the background flow. It is to be noticed that the denominator in the expression for u'_0 in Eq. (3.131) vanishes at $u_0^2 = c_s^2$ and thus introduces a singularity in the differential equation. However, there is no physical singularity in the background flow at any radial distance outside the event horizon of the black hole. Therefore, in order that u'_0 is non-singular at the transonic surface, the numerator also must vanish at that same location. This condition provides us with the location of the transonic surface and hence the location of the acoustic event horizon. Equating the numerator and denominator of Eq. (3.131) to zero, simultaneously, gives

$$u_0^2|_h = c_s^2|_h = \frac{1}{(2r - 3)} \Big|_h. \quad (3.133)$$

The above condition, obtained by equating denominator and numerator simultaneously to zero, is generally called the critical point condition in accretion literature

and the radial points satisfying this condition are called critical points of the flow and are denoted as r_c . We also notice that the critical point and the acoustic horizon are the same and we will use them interchangeably.

At the critical points, the gradient of the radial velocity has $\frac{0}{0}$ form. Therefore, the value of the gradient of the radial velocity at the critical points is evaluated by taking limit $r \rightarrow r_c$ (and consequently $u_0^2 \rightarrow c_s^2$) of the right-hand side of Eq. (3.131) using L'Hospital method. Thus, we have

$$u'_0|_h = \pm \sqrt{\frac{c_s^2(1 - c_s^2)}{2} \left[\frac{(1 - c_s^2)}{2c_s^2} \left\{ \frac{g_{tt}'}{g_{tt}^2} - \frac{g_{tt}''}{g_{tt}} \right\} - \frac{2}{r^2} \right]_h}, \quad (3.134)$$

where ‘double prime’ stands for double derivative with respect to r . It is to be noted that $u_0 < 0$ for accretion flow and $u_0 > 0$ for wind solution, so we have to pick the ‘sign’ accordingly for accretion or wind solution. For accretion solutions, the flow becomes supersonic from subsonic at the horizon. In other words, the magnitude $|u_0|$ increases with decreasing r . Therefore, the slope $d|u_0|/dr$ at the horizon would be negative and $u'_0 = -d|u_0|/dr$ would correspond to the positive sign in Eq. (3.134). For a given temperature of the background flow, using Eq. (3.131) and Eq. (3.134) we can solve for u_0 and find out the Mach number, which is the ratio of $|u_0|$ and the sound speed c_s , as a function of the radial distance and we can also perform the integration in Eq. (3.121), numerically, to find $t_{\pm}(r)$ and thus draw the causal structure of the acoustic spacetime.

In Fig. 3.1, the plot at the top shows the variation of the Mach number \mathcal{M} as a function of the radial distance r for a given temperature $T = 10^{10}\text{K}$. The acoustic horizon is located at $r_h = 274.08$. The plot at the bottom shows the corresponding causal structure of the acoustic spacetime. As can be seen in causal structure, the t_+ lines (solid lines) diverge at the acoustic horizon whereas the t_- lines (dotted lines) are non-singular at the horizon. Outside the horizon, i.e., for $r > r_h$, the radial coordinate increases along t_+ and decreases along t_- . Thus, the phonons can move outward as well as inward. However, inside the horizon, i.e., $r < r_h$, radial coordinate decreases along both t_+ and t_- implying the fact that the phonons are allowed to move only inward. Thus, it is clear from the causal structure that the acoustic horizon behaves like a one-way membrane in the same way as the event

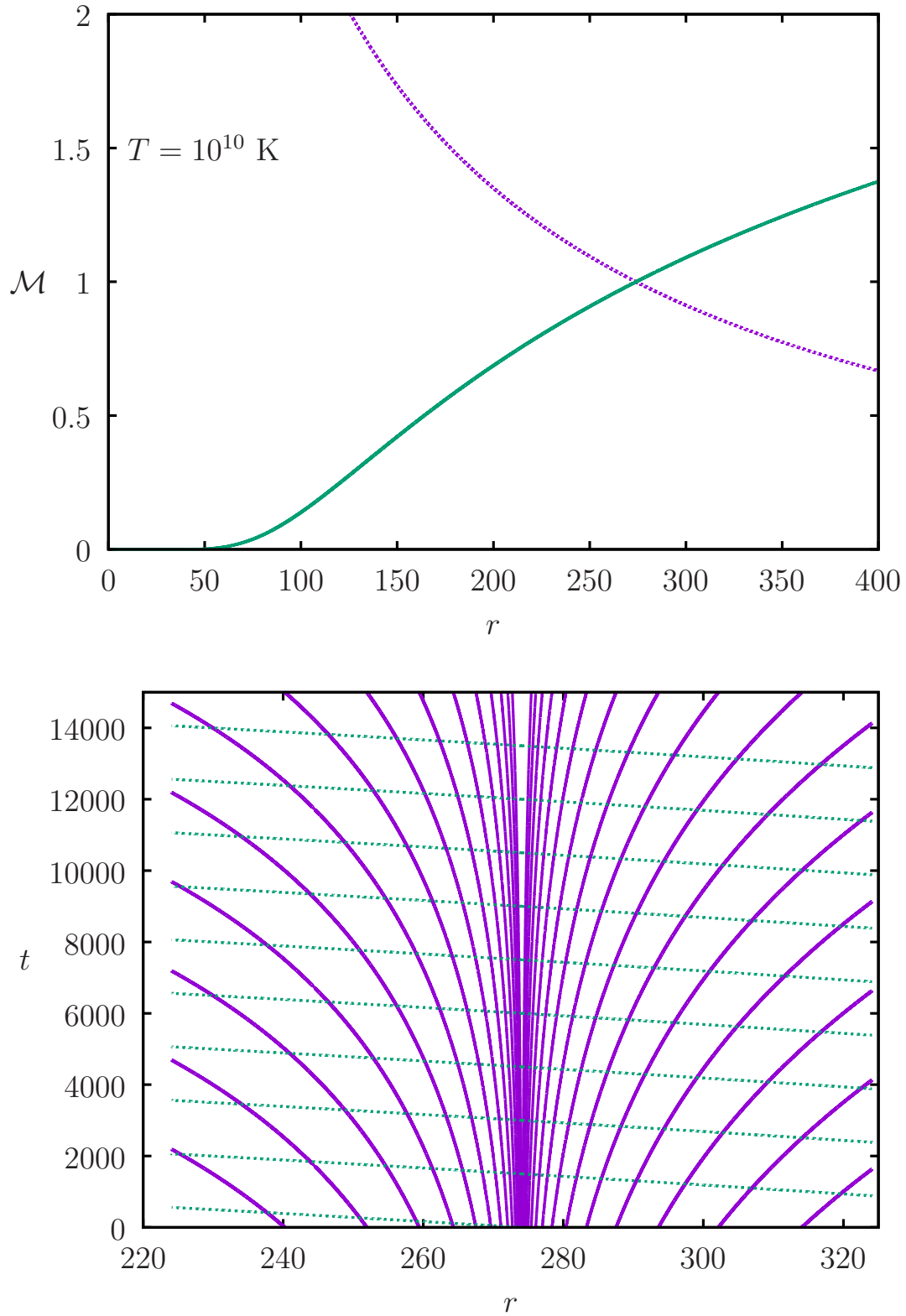


Figure 3.1: Top: Mach number vs radius plot of Michel flow. Bottom: Causal structure of the acoustic spacetime corresponding to the transonic flow (dashed line in the left figure). The dotted line is the $t(r)_-$ vs r and the solid line is $t(r)_+$ vs r . where $t(r)_\pm$ is given by Eq. (3.121).

horizon of a general relativistic black hole. In case of a black hole, nothing can come out of the event horizon whereas, in case of acoustic spacetime time, acoustic phonons are trapped inside the acoustic horizon and cannot escape from it.

3.5.2 Causal structure for axially symmetric flow

For axially symmetric flow, the stationary flow configuration depends on the specific angular momentum also. Thus, the Mach number versus radial distance plot depends on the set of parameters $[T, \lambda_0]$. A different set of values of these parameters would result in different Mach number versus radial distance plots. Unlike the Michel flow, axially symmetric flow can allow more than one critical points in the flow. One can construct a parameter space of $[T, \lambda_0]$ which allows multiple critical points. Such construction of parameter space will be demonstrated in the next chapter. For our current purpose, we have chosen particular set values of the parameters $[T, \lambda_0]$ which allows multiple critical points and the accretion flow passes through the outer critical point. We will talk more about the critical points and possible transonic flow with shock formation in the next chapter.

The metric elements for axially symmetric flow is given by Eq. (3.107) which can be expressed in terms of u_0 and λ_0 as

$$G_{tt} = \frac{(1 + \beta)u_0^2 - c_s^2}{c_s^2(1 - u_0^2)(1 - 2/r)^{-1}}, \quad (3.135)$$

$$G_{tr} = G_{rt} = \frac{-u_0(1 + \beta - c_s^2)\sqrt{\frac{r^2}{r^2 - \lambda^2(1 - 2/r)}}}{c_s^2(1 - u_0^2)}, \quad (3.136)$$

$$G_{rr} = \frac{c_s^2(1 - u_0^2) + (1 + \beta - c_s^2)\frac{r^2}{r^2 - \lambda^2(1 - 2/r)}}{c_s^2(1 - u_0^2)(1 - 2/r)}. \quad (3.137)$$

The acoustic horizon is located at $u_0^2 = c_s^{\text{eff}2}$, where $c_s^{\text{eff}} = c_s/\sqrt{1 + \beta}$. Thus near the acoustic horizon, u_0 may be expanded as

$$u_0 = -c_s^{\text{eff}} + \left. \frac{du_0}{dr} \right|_h (r - r_h) + \mathcal{O}(r - r_h)^2 + \dots, \quad (3.138)$$

which again implies that $b_+ \propto (r - r_h)$ near the acoustic horizon and therefore, $t_+ \propto \ln|r - r_h|$ near the horizon. Thus t_+ diverges at the acoustic horizon while t_- remains finite. In order to find t_{\pm} as function of r we have to solve for u_0 for

given values of $[T, \lambda_0]$. The procedure to find the solution is similar to the case of Michel flow. We start with the two integrals of motion—the mass accretion rate and the relativistic Bernoulli's constant. The mass accretion rate is given by Eq. (3.30) which in terms of u_0 becomes

$$\Psi_0 = \rho_0 u_0 H_0 \sqrt{\frac{\Delta}{1 - u_0^2}}, \quad (3.139)$$

where $\Delta = r(r - 2)$ (such that $g_{rr} = g_{tt}^{-1} = r^2/\Delta$) and $H_0(r) = (H_\theta)_{0r}$ is the local disk thickness. The relativistic Bernoulli's constant is given in terms of u_0 and λ_0 as

$$\xi_0 = \rho_0^{c_s^2} \sqrt{\frac{\Delta}{B(1 - u_0^2)}}, \quad (3.140)$$

where $B = g_{\phi\phi} - \lambda_0^2 g_{tt}$. Taking logarithmic derivative of the Eq. (3.140) provides

$$\frac{\rho'_0}{\rho_0} = -\frac{1}{c_s^2} \left[\frac{u_0 u'_0}{1 - u_0^2} + \frac{1}{2} \left(\frac{\Delta'}{\Delta} - \frac{B'}{B} \right) \right]. \quad (3.141)$$

The expression of the mass accretion rate given by Eq. (3.139) contains the term H_0 and therefore explicitly depends on the model of the accretion disc. Taking logarithmic derivative of Eq. (3.139) gives

$$\frac{\rho'_0}{\rho_0} + \frac{u'_0}{u_0} \frac{1}{1 - u_0^2} + \frac{\Delta'}{2\Delta} + \frac{H'_0}{H_0} = 0. \quad (3.142)$$

Below we provide the equations necessary to solve for u_0 for different models of accretion disc.

3.5.2.1 Constant height flow (CF)

For constant height flow, the thickness of the accretion disc is the same at all radial distances. Therefore, $H_0 = \text{constant}$. Eq. (3.142) for constant height flow becomes

$$\frac{\rho'_0}{\rho_0} + \frac{u'_0}{u_0} \frac{1}{1 - u_0^2} + \frac{\Delta'}{2\Delta} = 0. \quad (3.143)$$

Using the above equation, we substitute ρ'_0/ρ_0 in Eq. (3.141) which gives the differential equation for u_0 as

$$u'_0 = \frac{u_0(1 - u_0^2)}{u_0^2 - c_s^2} \left[\frac{B'}{2B} - (1 - c_s^2) \frac{\Delta'}{2\Delta} \right] \equiv \frac{N^{\text{CH}}}{D^{\text{CH}}}. \quad (3.144)$$

The critical points of the flow is obtained by setting $N^{\text{CH}} = D^{\text{CH}} = 0$. $D^{\text{CH}} = 0$ shows that the critical points are located at $u_0^2 = c_s^2$ which also gives the location of the acoustic horizon.

$$u_0^2|_c = c_s^2|_c = \left. \frac{\frac{\Delta'}{\Delta} - \frac{B'}{B}}{\frac{\Delta'}{\Delta}} \right|_c. \quad (3.145)$$

Using the L'Hospital method we find u'_0 at the critical point as

$$u'_0|_c = \pm \sqrt{\frac{1 - c_s^2}{4} \left[(1 - c_s^2) \left(\frac{\Delta'^2}{\Delta^2} - \frac{\Delta''}{\Delta} \right) - \left(\frac{B'^2}{B^2} - \frac{B''}{B} \right) \right]}. \quad (3.146)$$

In Fig. 3.2, the top panel shows the Mach number versus r plot on the left and the corresponding causal structure of the acoustic spacetime on the right for the values of the parameters $[T = 10^{10} \text{ K}, \lambda_0 = 3.75]$.

3.5.2.2 Conical Flow (CF)

H_0 for conical flow is given as $H_0 \propto r$. Therefore, for CF, Eq. (3.142) becomes

$$\frac{\rho'_0}{\rho_0} + \frac{u'_0}{u_0} \frac{1}{1 - u_0^2} + \frac{\Delta'}{2\Delta} + \frac{1}{r} = 0. \quad (3.147)$$

Using Eq. (3.141) and Eq. (3.147) we get

$$u'_0 = \frac{u_0(1 - u_0^2)}{u_0^2 - c_s^2} \left[\frac{B'}{2B} - (1 - c_s^2) \frac{\Delta'}{2\Delta} + \frac{c_s^2}{r} \right] \equiv \frac{N^{\text{CF}}}{D^{\text{CF}}}. \quad (3.148)$$

The critical points and the acoustic horizon are located at $u_0^2 = c_s^2$ and are given by

$$u_0^2|_c = c_s^2|_c = \left. \frac{\frac{\Delta'}{\Delta} - \frac{B'}{B}}{\frac{\Delta'}{\Delta} + \frac{2}{r}} \right|_c. \quad (3.149)$$

The gradient of the advective velocity at the critical points is obtained to be given by

$$u'_0|_c = \pm \sqrt{\frac{1 - c_s^2}{4} \left[(1 - c_s^2) \left(\frac{\Delta'^2}{\Delta^2} - \frac{\Delta''}{\Delta} \right) - \left(\frac{B'^2}{B^2} - \frac{B''}{B} \right) - \frac{2c_s^2}{r^2} \right]}. \quad (3.150)$$

In Fig. 3.2, the middle panel shows the Mach number versus r plot for conical flow on the left and the corresponding causal structure on the right side for the values of the parameters $[T = 10^{10} \text{ K}, \lambda_0 = 3.75]$.

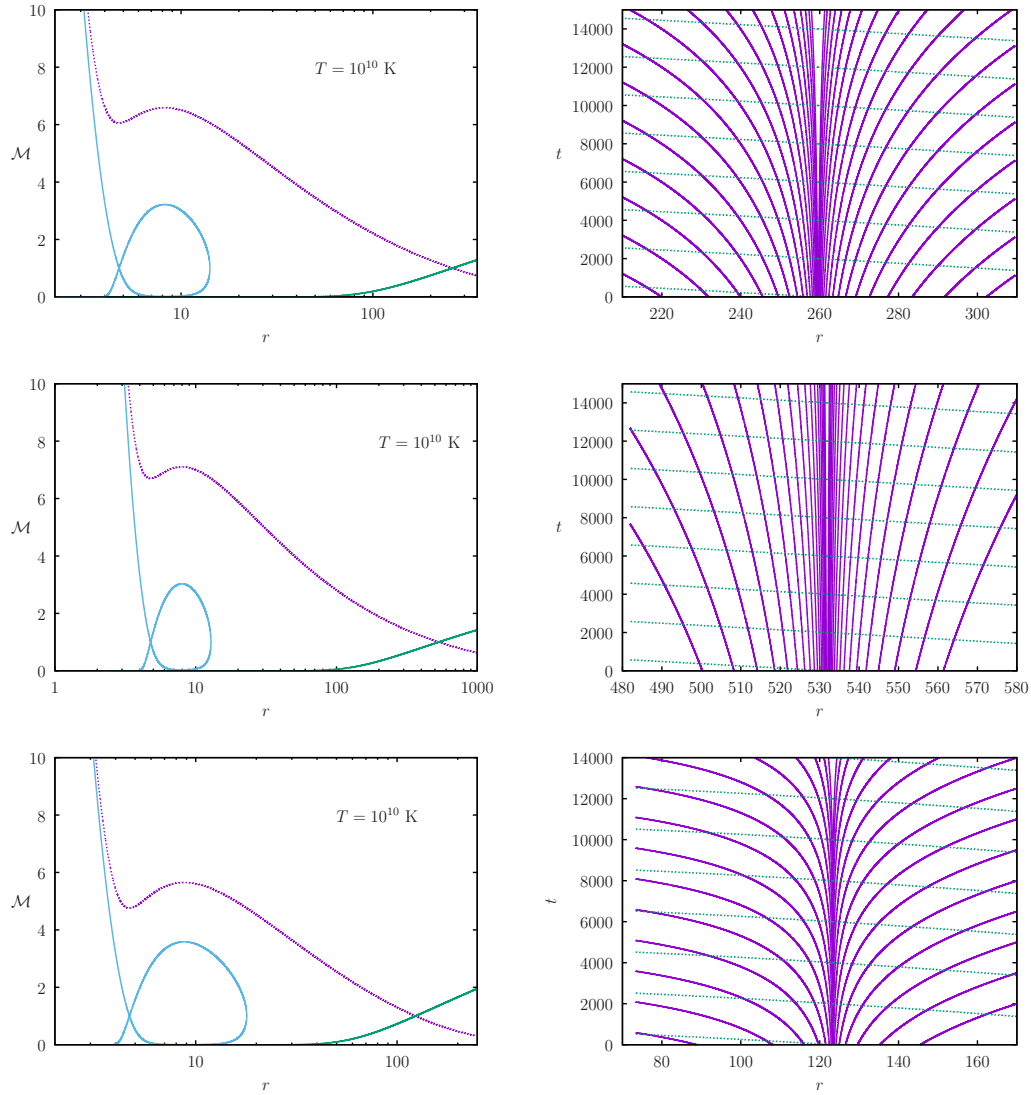


Figure 3.2: We demonstrate the Mach number (\mathcal{M}) Vs. radial distance (r) structure (phase portrait) for multi-transonic axisymmetric accretion and its corresponding causal structures (at and around the sonic point(s)) for three different flow geometries, namely, constant height flow (top panel), conical flow (middle panel) and flow in the hydrostatic equilibrium along the vertical direction (lower panel). The isothermal accretion has been characterized by $\lambda = 3.75$ and $T = 10^{10} K$. The panels show how the location of acoustic horizon and the curvature at and around the horizon varies for different flow geometries. On the right the dashed line is the $t(r)_-$ vs r and the solid line is $t(r)_+$ vs r . where $t(r)_\pm$ is given by Eq. (3.121).

3.5.2.3 Flow under vertical hydrostatic equilibrium (VE)

Unlike the CH and CF models of the accretion disc, the disc height for accretion flow with hydrostatic equilibrium along the vertical direction depends on the accretion variables such as density, pressure and the velocity. The expression of the disc height as given by Abramowicz *et al.* [72] in the Schwarzschild limit becomes

$$H_0 = \sqrt{\frac{2P_0}{\rho_0} \frac{r^2}{|v_{\phi 0}|}} = \sqrt{\frac{2P_0}{\rho_0} \frac{r^2}{\lambda_0 |v_{t0}|}} = \sqrt{\frac{2P_0}{\rho_0} \frac{r^2}{\lambda_0}} \sqrt{\frac{B}{\Delta}} \sqrt{1 - u_0^2}. \quad (3.151)$$

Using Eq. (3.151), (3.142) and (3.141) gives

$$u'_0 = \frac{u_0(1 - u_0^2)}{(1 + c_s^2) \left(u_0^2 - \frac{c_s^2}{1 + c_s^2}\right)} \left[(1 + c_s^2) \frac{B'}{2B} - \frac{\Delta'}{2\Delta} + \frac{2c_s^2}{r} \right] \equiv \frac{N^{\text{VE}}}{D^{\text{VE}}}. \quad (3.152)$$

The critical points are obtained at $u_0^2 = c_s^2/(1 + c_s^2) = c_s^{\text{eff}2}$. Thus critical point or the acoustic horizon location is given by

$$c_s^2|_c = \frac{\frac{\Delta'}{\Delta} - \frac{B'}{B}}{\frac{B'}{B} + \frac{4}{r}} \Big|_c. \quad (3.153)$$

Using L'Hospital method at $r \rightarrow r_c$ we obtain u'_0 at the critical point as

$$u'_0|_c = \pm \sqrt{\frac{1 - c_s^2}{4(1 + c_s^2)} \left[\left(\frac{\Delta'^2}{\Delta^2} - \frac{\Delta''}{\Delta} \right) - (1 + c_s^2) \left(\frac{B'^2}{B^2} - \frac{B''}{B} \right) - \frac{4c_s^2}{r^2} \right]}. \quad (3.154)$$

In Fig. 3.2, the bottom panel shows the Mach number versus r plot on the left side and the corresponding causal structure for accretion flow on the right side for the values of the parameters [$T = 10^{10}$ K, $\lambda_0 = 3.75$].

In our current analysis, we have not considered the formation of shock in the accretion flow. Presence of shock formation alters the nature of the accretion flow by allowing the flow to be multi-transonic. In such a case, the flow passes through more than one or specifically two critical points-outer and inner critical points. At the location of the shock formation, the accretion variables such as velocity and density become discontinuous and the flow makes a discontinuous jump from supersonic to subsonic state. It has been shown that the presence of shock formation also gives rise to an acoustic white hole at the location of the shock formation [52, 73, 77]. We shall consider shocked accretion flow and discuss the corresponding effects on the acoustic spacetime in the next chapters.

3.6 Acoustic surface gravity

In theoretical physics, one of the main objectives to study the analogue gravity phenomenon is to understand the Hawking-like effects – the emission of phonons from the close vicinity of the acoustic horizon which is considered to be analogous to the usual Hawking radiation emanating out from the standard gravitational black holes. In fact, the main goal of Unruh’s work [1] was to show that a transonic fluid system shows Hawking-like effect and the quantized phonons emitted from the acoustic horizon has a thermal spectrum with an analogue Hawking temperature T_{AH} . The Hawking temperature (as measured at infinity) of a black hole is given in terms of the surface gravity κ_g ³ as $T_H = \frac{\hbar\kappa_g}{2\pi k_B}$ (in the units we are working with)[3, 80]. The analogue Hawking temperature could be given by a similar formula with the acoustic surface gravity κ and hence the acoustic surface gravity provides a way to evaluate the corresponding analogue Hawking temperature T_{AH} .

The acoustic spacetime metric $G_{\mu\nu}$ is the same up to a conformal factor for the three quantities that we perturb linearly. The acoustic surface gravity is a conformally invariant quantity. Therefore, we get the same acoustic geometry irrespective of the quantity we perturb for a particular flow geometry.

3.6.1 Acoustic surface gravity for Michel flow

The acoustic metric elements given by Eq. (3.103) is independent of the time coordinate. Therefore, the spacetime possesses the stationary Killing vector $\chi^\mu = \delta_t^\mu$. The norm of the Killing vector at the horizon is given by

$$\chi_\mu \chi^\mu|_h = G_{tt}|_h = 0. \quad (3.155)$$

Thus, the Killing vector is null at the acoustic horizon and therefore, the Killing horizon and the acoustic horizon coincide. For such a spacetime, the acoustic surface gravity could be given in terms of the Killing vector by the following relation to be

³The subscript g is used to denote black hole surface gravity as we have already denoted the acoustic surface gravity by κ .

evaluated at the horizon [11]

$$\nabla_\alpha(-\chi_\mu\chi^\mu) = 2\kappa\chi_\alpha, \quad (3.156)$$

where κ is the surface gravity. $\alpha = r$ component of the above equation gives the surface gravity as

$$\kappa = - \left. \frac{G'_{tt}}{2G_{tr}} \right|_h. \quad (3.157)$$

In terms of the background metric elements and velocity, κ becomes

$$\kappa = \left. \frac{\sqrt{g_{tt}/g_{rr}} u'_0}{1 - c_s^2} \right|_h. \quad (3.158)$$

3.6.2 Acoustic surface gravity for axially symmetric flow

Similar to the acoustic geometry in Michel flow, the acoustic metric, as given by Eq. (3.107), also possesses the stationary Killing vector $\chi^\mu = \delta_t^\mu$ which is null at the acoustic horizon $u_0^2 = c_s^2/(1 + c_s^2)$. Therefore, the surface gravity is given by the formula

$$\kappa = - \left. \frac{G'_{tt}}{2G_{tr}} \right|_h = \left. \frac{1 + \beta}{1 + \beta - c_s^2} \sqrt{\frac{g_{tt}(g_{\phi\phi} - \lambda_0^2 g_{tt})}{g_{rr}g_{\phi\phi}}} u'_0 \right|_h. \quad (3.159)$$

Using the expressions for the background metric elements, the surface gravity for the axially symmetric flow becomes

$$\kappa = \left. \frac{1 + \beta}{1 + \beta - c_s^2} \frac{r - 2}{r^2} \sqrt{r^2 - \lambda_0^2 \left(1 - \frac{2}{r}\right)} u'_0 \right|_h. \quad (3.160)$$

It is to be clarified that the surface gravity has been calculated on the equatorial plane since the radial Euler equation has been solved to obtain the stationary integral solutions for the height averaged expressions for the thermodynamic quantities. For time-dependent stability analysis, only the radial Euler equation has been perturbed as well, under similar physical conditions. The acoustic horizon is thus a circular ring located on the equatorial plane and the surface gravity corresponding to that geometric structure has been computed in this work.

3.7 Critical points and the transonic points in VE model

In Sec. 3.5, it was how the location of the acoustic horizon may be determined. In order to obtain the location of the acoustic horizon, first, we had to find out the differential equation for the advective velocity u_0 by taking special derivatives of the two constant integrals of motion—the relativistic Bernoulli’s constant and the mass accretion rate. From the equation of u'_0 , we identified the critical points of the flow which we noticed that coincide with the location of the acoustic horizon. The critical points are also identical to the transonic points for Michel flow as well as for CH and CF. However, the critical points and the transonic points are not the same in case of flow under vertical equilibrium. In case of VE, the critical points are located at $u_0^2 = c_s^{\text{eff}2}$ instead of at $u_0^2 = c_s^2$ which hints to the fact that in VE flow, the effective speed with the acoustic perturbation propagate is c_s^{eff} . In Chap. 7, this apparent non-isomorphism of the critical points and the transonic points has been discussed in details.

In the work presented in this chapter, one of the most important findings is the following: The salient features of the acoustic geometry do not depend on the physical quantity we perturb to obtain the same metric. Linear perturbation of the velocity potential, the relativistic Bernoulli’s constant and the mass accretion rate give rise to the same acoustic metric, apart from a conformal factor. The conformal factor does not contribute to the acoustic horizon as well as the acoustic surface gravity. The acoustic geometry is thus an intrinsic property of the accreting black hole system. At the same time, we also find that for the same set of initial boundary conditions used to describe the accretion flow, the location of the acoustic horizon, as well as the value of the acoustic surface gravity, depends, quite sensitively, on the geometric configuration of matter—different disc models provide different values of r_h and κ for the same set of values $[T, \lambda_0]$. Hence, the properties of the acoustic metric do not depend on the physical quantity we perturb to obtain the metric, rather such properties get influenced by the matter geometry in connection to the

axially symmetric accretion.

We have studied the acoustic geometry embedded in accretion flow onto a Schwarzschild black hole. However, the astronomers believe that most of the astrophysical black holes possess a non-zero spin angular momentum. Thus, it is important to know how the features of the acoustic metric that we studied depend on the spin of the black hole. In the next chapter, we investigate the features of the acoustic spacetime for isothermal accretion flow onto a Kerr black hole.

4

Relativistic sonic geometry for isothermal accretion in the Kerr metric¹

In the previous chapter, we studied the acoustic spacetime metric embedded in an isothermal accretion flow onto a non-rotating Schwarzschild black hole. In this chapter, we investigate the emergence of the analogue gravity phenomenon by linearly perturbing an isothermal accretion flow onto a rotating Kerr black hole. Similar to the Schwarzschild case, we find that the acoustic metric obtained by perturbing the three different physical quantity—the velocity potential, the relativistic Bernoulli’s constant and the mass accretion rate—give rise to the same acoustic metric apart from a conformal factor. We show how the salient features of the acoustic spacetime get influenced by spin of the black hole. The causal structure of the acoustic spacetime is constructed with as well as without shock formation. We explicitly show the dependence of the acoustic horizon and the acoustic surface gravity on the black hole spin. We also show how the perturbation equation may be used to perform a linearly stability analysis of the stationary accretion flow.

¹This chapter is based on the work titled “*Relativistic sonic geometry for isothermal accretion in the Kerr metric*” by M. A. Shaikh [73].

4.1 Basic set up

The accretion flow is governed by a few number of basic equations which include the mass conservation equation (continuity equation), the energy-momentum conservation equation (the relativistic Euler equation) and the irrotationality condition. We consider the accreting fluid to be perfect and to be governed by isothermal equation of state. Below we provide these basic equations as well as set the necessary background to study the acoustic spacetime embedded in the accretion system and perform linear stability analysis of the stationary accretion solutions.

We consider the following metric for a stationary rotating spacetime

$$ds^2 = -g_{tt}dt^2 + g_{rr}dr^2 + g_{\theta\theta}d\theta^2 + 2g_{\phi t}d\phi dt + g_{\phi\phi}d\phi^2, \quad (4.1)$$

where the metric elements are functions of r and θ . The metric elements in Boyer-Lindquist (BL) coordinates are given by [81]

$$\begin{aligned} g_{tt} &= \left(1 - \frac{2}{\mu r}\right), \\ g_{rr} &= \frac{\mu r^2}{\Delta}, \\ g_{\theta\theta} &= \mu r^2, \\ g_{t\phi} = g_{\phi t} &= -\frac{2a \sin^2 \theta}{\mu r}, \\ g_{\phi\phi} &= \frac{\Sigma}{\mu r^2} \sin^2 \theta, \end{aligned} \quad (4.2)$$

where a is the spin of the black hole and

$$\begin{aligned} \mu &= 1 + \frac{a^2}{r^2} \cos^2 \theta, \\ \Delta &= r^2 - 2r + a^2, \\ \Sigma &= (r^2 + a^2)^2 - a^2 \Delta \sin^2 \theta. \end{aligned} \quad (4.3)$$

The event horizon of the Kerr black hole is located at $g^{rr} = 0$ which, in the units we are working with ($G = c = M_{\text{BH}} = 1$), is located at $r_+ = 1 + \sqrt{1 - a^2}$. r_+ is the outer solution of $g^{rr} = 0$.

The continuity equation in Eq. (3.4), relativistic Euler equation in Eq. (3.10) and the irrotationality condition in Eq. (3.15) were provided in the previous chapter

for a general background metric $g_{\mu\nu}$ and therefore are applicable for accretion flow onto a Kerr black hole also.

The accretion flow is described by the four-velocity $(v^t, v^r, v^\theta, v^\phi)$. We assume the flow to be axially symmetric and also to be symmetric about the equatorial plane and the velocity along the vertical direction to be negligible compared to the radial velocity, i.e., $v^\theta \ll v^r$. Due to the axial symmetry, any term with derivative with respect to the azimuthal coordinate ϕ would vanish. We perform a vertical averaging of the continuity equation using the approximation provided by Eq. (3.26)

$$\partial_t(\sqrt{-\tilde{g}}\rho v^t H_\theta) + \partial_r(\sqrt{-\tilde{g}}\rho v^r H_\theta) = 0. \quad (4.4)$$

The value of the determinant of the Kerr metric is $g = -\mu^2 r^4 \sin^2 \theta$ and its value on the equatorial plane is $\tilde{g} = -r^4$. H_θ is the local angular scale of the flow and is related to the local disc thickness $H(r)$ as $H_\theta = H/r$. For the present work, we consider the flow to be a wedge-shaped conical flow such that $H(r) \propto r$ and $H_\theta = \text{constant}$. H_θ (and therefore $H(r)$) does not depend on any accretion variable such as the velocity components or the density. Thus, linear perturbation of the accretion flow variables will not affect H_θ . The vertical averaging allows us to work fully on the equatorial plane by containing the information about the vertical structure inside H_θ . From now on all the equations will be derived by assuming the flow to be vertically averaged and the variables have values equal to that on the equatorial plane.

Apart from the Boyer-Lindquist coordinate frame (BLF), we shall use a second reference frame which is called the corrotating frame (CRF)[69]. This frame is obtained by an azimuthal Lorentz boost from the locally nonrotating frame (LNRF) into a tetrad basis that corotates with the fluid. LNRF is an orthonormal tetrad basis who lives at $\theta = \text{constant}, r = \text{constant}, \phi = \omega t + \text{constant}$, where $\omega = \frac{2a}{r^3 + a^2(r+2)}$ on the equatorial plane (originally calculated by Bardeen *et al.* [82]). Let u be the radial velocity (referred as the ‘advective velocity’) of the fluid as measured in the CRF and $\lambda = -\frac{v_\phi}{v_t}$ be the specific angular momentum of the fluid. Then the

four-velocity components in BLF is related to u and λ in the following way [69]

$$v^r = \frac{u}{\sqrt{g_{rr}(1-u^2)}}, \quad (4.5)$$

$$v^t = \sqrt{\frac{(g_{\phi\phi} + \lambda g_{\phi t})^2}{(g_{\phi\phi} + 2\lambda g_{\phi t} - \lambda^2 g_{tt})(g_{\phi\phi} g_{tt} + g_{\phi t}^2)(1-u^2)}}, \quad (4.6)$$

$$v_t = -\sqrt{\frac{g_{tt} g_{\phi\phi} + g_{\phi t}^2}{(g_{\phi\phi} + 2\lambda g_{\phi t} - \lambda^2 g_{tt})(1-u^2)}}. \quad (4.7)$$

u and λ are the two velocity variables needed to describe the flow in the equatorial plane.

4.2 Linear perturbation of velocity potential, mass accretion rate and the relativistic Bernoulli's constant

In this section, we will linearly perturb the accretion flow equations to obtain the perturbation equation in terms of the velocity potential, relativistic Bernoulli's constant and the mass accretion rate. The procedure to obtain the perturbations equation is the same as provided in the previous chapter for accretion onto Schwarzschild black hole. From the perturbation equation, we identify the $f^{\mu\nu}$ matrix to obtain the acoustic spacetime metric. Before going to the details of the derivation of the acoustic metric by perturbing the three different quantities, we first write down some useful equations which will be essential later in the section.

The normalization condition is given by $v_\mu v^\mu = -1$ which gives

$$g_{tt}(v^t)^2 = 1 + g_{rr}(v^r)^2 + g_{\phi\phi}(v^\phi)^2 + 2g_{\phi t}v^\phi v^t. \quad (4.8)$$

From the irrotationality condition given by Eq. (3.15) with $\mu = t$ and $\nu = \phi$ and using the axial symmetry, we have $\partial_t(v_\phi \rho^{c_s^2}) = 0$ and with $\mu = r$ and $\nu = \phi$ we have $\partial_r(v_\phi \rho^{c_s^2}) = 0$. Therefore, $v_\phi \rho^{c_s^2}$ is a constant of motion for irrotational isothermal accretion flow. $\partial_t(v_\phi \rho^{c_s^2}) = 0$ can be expanded to give

$$\partial_t v_\phi = -\frac{v_\phi c_s^2}{\rho} \partial_t \rho. \quad (4.9)$$

Substitution of $v_\phi = g_{\phi\phi}v^\phi + g_{\phi t}v^t$ in the above equation provides

$$\partial_t v^\phi = -\frac{g_{\phi t}}{g_{\phi\phi}}\partial_t v^t - \frac{v_\phi c_s^2}{g_{\phi\phi}\rho}\partial_t \rho. \quad (4.10)$$

Differentiation of both sides of Eq. (4.8) with respect to t gives

$$\partial_t v^t = \alpha_1 \partial_t v^r + \alpha_2 \partial_t v^\phi, \quad (4.11)$$

where $\alpha_1 = -(g_{rr}v^r)/v^t$ and $\alpha_2 = -v^\phi/v^t$. We substitute $\partial_t v^\phi$ in Eq. (4.11) using Eq. (4.10) to get

$$\partial_t v^t = \left(\frac{-\alpha_2 v_\phi c_s^2 / (\rho g_{\phi\phi})}{1 + \alpha_2 g_{\phi t} / g_{\phi\phi}} \right) \partial_t \rho + \left(\frac{\alpha_1}{1 + \alpha_2 g_{\phi t} / g_{\phi\phi}} \right) \partial_t v^r \quad (4.12)$$

We perturb the velocity and density about their stationary background values as following

$$v^\mu(t, r) = v_0^\mu(r) + v_1^\mu(t, r), \quad (4.13)$$

$$\rho(t, r) = \rho_0(r) + \rho_1(t, r), \quad (4.14)$$

where, as usual, the subscript '0' stands for the stationary part and '1' stands for the linear time-dependent perturbation. Using Eq. (4.13) and (4.14) in Eq. (4.12) and keeping only the terms that are first order in perturbed quantities give

$$\partial_t v_1^t = \eta_1 \partial_t \rho_1 + \eta_2 \partial_t v_1^r, \quad (4.15)$$

where

$$\eta_1 = -\frac{c_s^2}{\Lambda v_0^t \rho_0} [\Lambda (v_0^t)^2 - 1 - g_{rr} (v_0^r)^2], \quad \eta_2 = \frac{g_{rr} v_0^r}{\Lambda v_0^t} \quad \text{and} \quad \Lambda = g_{tt} + \frac{g_{\phi t}^2}{g_{\phi\phi}}. \quad (4.16)$$

4.2.1 Linear perturbation of velocity potential

We introduce the velocity potential field ψ using the irrotationality condition given by Eq. (3.15) in the following way

$$-\partial_\mu \psi = v_\mu \rho c_s^2. \quad (4.17)$$

We showed that $v_\phi \rho c_s^2$ is a constant of motion and hence $\partial_\phi \psi$ is a constant of motion. The velocity potential is perturbed in the following way $\psi = \psi_0 + \psi_1$. Therefore,

$\partial_\phi \psi = \text{constant}$, gives $\delta(\partial_\phi \psi) = \partial_\phi \psi_1 = 0$. Contracting both sides of Eq. (4.17) with v^μ and using the normalization condition $v_\mu v^\mu = -1$ gives

$$\rho^{c_s^2} = v^\mu \partial_\mu \psi. \quad (4.18)$$

Linear perturbation of the above equation provides

$$\rho_1 = \frac{1}{c_s^2 \rho_0^{c_s^2 - 1}} [v^r \partial_r \psi_1 + v^t \partial_t \psi_1]. \quad (4.19)$$

Linear perturbation of Eq. (4.17) gives

$$v_1^t = \frac{1}{\rho_0^{c_s^2}} [(g^{tt} - (v_0^t)^2) \partial_t \psi_1 - v_0^t v_0^r \partial_r \psi_1], \quad (4.20)$$

$$v_1^r = \frac{1}{\rho_0^{c_s^2}} [(-g^{rr} - (v_0^r)^2) \partial_r \psi_1 - v_0^r v_0^t \partial_t \psi_1]. \quad (4.21)$$

Linear perturbation of the continuity equation, e.g., Eq. (4.4) gives

$$\partial_t [\sqrt{-\tilde{g}} H_\theta (\rho_0 v_1^t + v_0^t \rho_1)] + \partial_r [\sqrt{-\tilde{g}} H_\theta (\rho_0 v_1^r + v_0^r \rho_1)] = 0. \quad (4.22)$$

Now we substitute v_1^t, v_1^r and ρ_1 in the above equation using Eq. (4.20), (4.21) and (4.19), respectively, to obtain the perturbation equation in terms of ψ_1 as

$$\begin{aligned} & \partial_t \left[k_\psi(r) \left\{ -g^{tt} + (v_0^t)^2 \left(1 - \frac{1}{c_s^2} \right) \right\} \partial_t \psi_1 \right] + \partial_t \left[k_\psi(r) \left\{ v_0^r v_0^t \left(1 - \frac{1}{c_s^2} \right) \right\} \partial_r \psi_1 \right] \\ & + \partial_r \left[k_\psi(r) \left\{ v_0^r v_0^t \left(1 - \frac{1}{c_s^2} \right) \right\} \partial_t \psi_1 \right] + \partial_r \left[k_\psi(r) \left\{ g^{rr} + (v_0^r)^2 \left(1 - \frac{1}{c_s^2} \right) \right\} \partial_r \psi_1 \right] \\ & = 0, \end{aligned} \quad (4.23)$$

where $k_\psi(r) = -(\sqrt{-\tilde{g}} H_\theta) / \rho_0^{c_s^2 - 1}$. The above equation can be written as $\partial_\mu (f_\psi^{\mu\nu} \partial_\nu \psi_1) = 0$, where $f_\psi^{\mu\nu}$ is given as

$$f_\psi^{\mu\nu} = k_\psi(r) \begin{bmatrix} -g^{tt} + (v_0^t)^2 \left(1 - \frac{1}{c_s^2} \right) & v_0^r v_0^t \left(1 - \frac{1}{c_s^2} \right) \\ v_0^r v_0^t \left(1 - \frac{1}{c_s^2} \right) & g^{rr} + (v_0^r)^2 \left(1 - \frac{1}{c_s^2} \right) \end{bmatrix} \quad (4.24)$$

4.2.2 Linear perturbation of mass accretion rate

For stationary accretion flow, partial differentiation with respect to t vanishes. Therefore, the continuity equation, given by Eq. (4.4), for stationary flow becomes

$$\partial_r(\sqrt{-\tilde{g}}\rho_0 v_0^r H_\theta) = 0, \quad (4.25)$$

which under spatial integration provides $\sqrt{-\tilde{g}}\rho_0 v_0^r H_\theta = \text{constant}$. Multiplying this quantity with the azimuthal component of the volume element, i.e., $d\phi$ and integrating gives the mass accretion rate

$$\dot{M} = -\Omega\sqrt{-\tilde{g}}\rho_0 v_0^r H_\theta, \quad (4.26)$$

where Ω arises due to the integration over the ϕ angle and the negative sign implies the infall of matter. Ω being merely a geometrical factor, we redefine the mass accretion rate to be $\Psi_0 \equiv -\dot{M}/\Omega$ without any loss of generality,

$$\Psi_0 = \sqrt{-\tilde{g}}\rho_0 v_0^r H_\theta. \quad (4.27)$$

Ψ_0 is the stationary mass accretion rate of the stationary accretion flow. For, non-stationary, i.e. for time-dependent flow, we define the mass accretion rate as $\Psi(t, r) = \sqrt{-\tilde{g}}\rho(t, r)v^r(t, r)H_\theta$ which has the stationary part equal to Ψ_0 and can be written as

$$\Psi(t, r) = \Psi_0 + \Psi_1(t, r), \quad (4.28)$$

where

$$\Psi_1(t, r) = \sqrt{-\tilde{g}}H_\theta(\rho_0 v_1^r + v_0^r \rho_1). \quad (4.29)$$

Eq. (4.22) can be written as

$$a_1 \partial_t v_1^r + b_1 \partial_t \rho_1 = \partial_r \Psi_1, \quad (4.30)$$

where

$$a_1 = -\sqrt{-\tilde{g}}H_\theta \rho_0 \eta_2, \quad b_1 = -\sqrt{-\tilde{g}}H_\theta(v_0^t + \rho_0 \eta_1). \quad (4.31)$$

Differentiation of Eq. (4.29) with respect to t provides

$$c_1 \partial_t v_1^r + d_1 \partial_t \rho_1 = \partial_t \Psi_1, \quad (4.32)$$

where

$$c_1 = \sqrt{-\tilde{g}H_\theta\rho_0}, \quad d_1 = \sqrt{-\tilde{g}H_\theta v_0^r}. \quad (4.33)$$

With the help of Eq. (4.30) and Eq. (4.32), we write down $\partial_t v_1^r$ and $\partial_t \rho_1$ solely in terms of derivatives of Ψ_1 ,

$$\partial_t v_1^r = \frac{1}{\Delta_1} (b_1 \partial_t \Psi_1 - d_1 \partial_r \Psi_1) \quad (4.34)$$

$$\partial_t \rho_1 = \frac{1}{\Delta_1} (-a_1 \partial_t \Psi_1 + c_1 \partial_r \Psi_1), \quad (4.35)$$

where $\Delta_1 = b_1 c_1 - a_1 d_1 = -\tilde{g}H_\theta^2 \rho_0 \tilde{\Lambda}$ and

$$\tilde{\Lambda} = \frac{g_{rr}(v_0^r)^2}{\Lambda v_0^t} - v_0^t + \frac{c_{s0}^2}{\Lambda v_0^t} [\Lambda (v_0^t)^2 - 1 - g_{rr}(v_0^r)^2]. \quad (4.36)$$

Also, we can write $v_t = v_{t0} + v_{t1}$ and $\partial_t v_{t1}$ as

$$\partial_t v_{t1} = \tilde{\eta}_1 \partial_t \rho_1 + \tilde{\eta}_2 \partial_t v_1^r, \quad (4.37)$$

where

$$\tilde{\eta}_1 = - \left[\Lambda \eta_1 + \frac{g_{\phi t} v_{\phi 0} c_s^2}{g_{\phi\phi} \rho_0} \right], \quad \tilde{\eta}_2 = -\Lambda \eta_2, \quad (4.38)$$

where η_1 and η_2 has been defined in Eq. (4.16). Now, we go back to the irrotationality condition given by Eq. (3.15). We use $\mu = t$ and $\nu = r$ and divide by $v_t \rho^{c_s^2}$ to get

$$\frac{g_{rr}}{v_t} \partial_t v^r + \frac{c_s^2 g_{rr} v^r}{\rho v_t} \partial_t \rho - \partial_r \left(\ln(\rho^{c_s^2} v_t) \right) = 0. \quad (4.39)$$

We linearly perturb the above equation and use Eq. (4.37) to get

$$\partial_t \left[\frac{g_{rr}}{v_{t0}} \partial_t v_1^r \right] + \partial_t \left[\frac{g_{rr} c_s^2 v_0^r}{\rho_0 v_{t0}} \partial_t \rho_1 \right] - \partial_r \left[\frac{\tilde{\eta}_2}{v_{t0}} \partial_t v_1^r \right] - \partial_r \left[\left(\frac{\tilde{\eta}_1}{v_{t0}} + \frac{c_s^2}{\rho_0} \right) \partial_t \rho_1 \right] = 0. \quad (4.40)$$

Finally, substitution of $\partial_t v_1^r$ and $\partial_t \rho_1$ in the above equation using Eq. (4.34) and (4.35), respectively, provides the perturbation equation in terms of Ψ_1 ,

$$\begin{aligned} & \partial_t \left[k_\Psi(r) \left\{ -g^{tt} + (v_0^t)^2 \left(1 - \frac{1}{c_s^2} \right) \right\} \partial_t \Psi_1 \right] + \partial_t \left[k_\Psi(r) \left\{ v_0^r v_0^t \left(1 - \frac{1}{c_s^2} \right) \right\} \partial_r \Psi_1 \right] \\ & + \partial_r \left[k_\Psi(r) \left\{ v_0^r v_0^t \left(1 - \frac{1}{c_s^2} \right) \right\} \partial_t \Psi_1 \right] + \partial_r \left[k_\Psi(r) \left\{ g^{rr} + (v_0^r)^2 \left(1 - \frac{1}{c_s^2} \right) \right\} \partial_r \Psi_1 \right] \\ & = 0, \end{aligned}$$

$$(4.41)$$

where

$$k_{\Psi}(r) = \frac{g_{rr}v_0^r c_s^2}{v_0^t v_{t0} \tilde{\Lambda}} \quad \text{and} \quad g^{tt} = \frac{1}{\tilde{\Lambda}} = \frac{1}{g_{tt} + g_{\phi t}^2 / g_{\phi\phi}}. \quad (4.42)$$

Eq. (4.41) can be written as $\partial_{\mu}(f_{\Psi}^{\mu\nu})\partial_{\nu}\Psi_1 = 0$, where $f_{\Psi}^{\mu\nu}$ is given by the 2×2 symmetric matrix

$$f_{\Psi}^{\mu\nu} = k_{\Psi}(r) \begin{bmatrix} -g^{tt} + (v_0^t)^2 \left(1 - \frac{1}{c_s^2}\right) & v_0^r v_0^t \left(1 - \frac{1}{c_s^2}\right) \\ v_0^r v_0^t \left(1 - \frac{1}{c_s^2}\right) & g^{rr} + (v_0^r)^2 \left(1 - \frac{1}{c_s^2}\right) \end{bmatrix} \quad (4.43)$$

4.2.3 Linear perturbation of relativistic Bernoulli's constant

The energy-momentum conservation equation can be written as $\nabla_{\mu}T_{\nu}^{\mu} = 0$. Using the definition of co-variant derivative $\nabla_{\mu}v_{\nu} = \partial_{\mu}v_{\nu} - \Gamma_{\mu\nu}^{\lambda}v_{\lambda}$, the energy-momentum conservation equation can be written as

$$v^{\mu}\partial_{\mu}v_{\nu} - \Gamma_{\mu\nu}^{\lambda}v_{\lambda}v^{\mu} + \frac{c_s^2}{\rho}(v^{\mu}v_{\nu}\partial_{\mu}\rho + \partial_{\nu}\rho) = 0. \quad (4.44)$$

Therefore, the temporal component $\nu = t$ of the relativistic Euler equation is given by

$$v^t\partial_t v_t + v^r\partial_r v_t - \Gamma_{\mu t}^{\lambda}v_{\lambda}v^{\mu} + \frac{c_s^2}{\rho}(v^t v_t \partial_t \rho + v^r v_t \partial_r \rho + \partial_t \rho) = 0. \quad (4.45)$$

It can be shown that $\Gamma_{\mu t}^{\lambda}v_{\lambda}v^{\mu} = 0$. Therefore, the temporal component of the relativistic Euler equation becomes

$$v^t\partial_t v_t + \frac{c_s^2}{\rho}(v^t v_t + 1)\partial_t \rho + v^r v_t \partial_r \{\ln(v_t \rho^{c_s^2})\} = 0. \quad (4.46)$$

For the stationary accretion flow, where all the time derivatives vanish, the above equation provides the relativistic Bernoulli's constant $\xi_0 = v_{t0}\rho_0^{c_s^2}$ which is a constant of motion for stationary flow. We now define a quantity $\xi(t, r) = v_t \rho^{c_s^2}$ for non-stationary flow such that the stationary part of ξ is equal to ξ_0 , i.e.,

$$\xi(t, r) = \xi_0 + \xi_1(t, r), \quad (4.47)$$

where ξ_1 is given by

$$\xi_1(r, t) = \frac{c_s^2 \xi_0}{\rho_0} \rho_1(r, t) + \frac{\xi_0}{v_{t0}} v_{t1}. \quad (4.48)$$

Differentiating both sides of the above equation and using Eq. (4.37) gives

$$\xi_0 \left[\frac{c_s^2}{\rho_0} + \frac{\tilde{\eta}_1}{v_{t0}} \right] \partial_t \rho_1 + \frac{\xi_0 \tilde{\eta}_2}{v_{t0}} \partial_t v_1^r = \partial_t \xi_1. \quad (4.49)$$

Linear perturbation of Eq. (4.46) provides

$$\frac{\xi_0 g_{rr} v_0^r}{v_{t0}} \frac{c_s^2}{\rho_0} \partial_t \rho_1 + \frac{\xi_0 g_{rr}}{v_{t0}} \partial_t v_1^r = \partial_r \xi_1. \quad (4.50)$$

In deriving the above equation, Eq. (4.37), (4.38) and (4.16) are also used. Eq. (4.49) and Eq. (4.50) can be used to express $\partial_t v_1^r$ and $\partial_t \rho_1$ in terms of derivatives of ξ_1 ,

$$\partial_t v_1^r = \frac{1}{\Delta_2} [b_2 \partial_t \xi_1 - d_2 \partial_r \xi_1], \quad (4.51)$$

$$\partial_t \rho_1 = \frac{1}{\Delta_2} [-a_2 \partial_t \xi_1 + c_2 \partial_r \xi_1], \quad (4.52)$$

where

$$\begin{aligned} a_2 &= \frac{\xi_0 g_{rr}}{v_{t0}}, \\ b_2 &= \frac{\xi_0 g_{rr} v_0^r}{v_{t0}} \frac{c_s^2}{\rho_0}, \\ c_2 &= \frac{\xi_0 \tilde{\eta}_2}{v_{t0}}, \\ d_2 &= \xi_0 \left[\frac{c_s^2}{\rho_0} + \frac{\tilde{\eta}_1}{v_{t0}} \right], \\ \Delta_2 &= b_2 c_2 - a_2 d_2 = \frac{\xi_0^2 g_{rr} c_s^2}{\rho_0 v_{t0}^2 v_0^t}. \end{aligned} \quad (4.53)$$

Differentiating Eq. (4.22) with respect to t and using Eq. (4.15) provides

$$\partial_t [\sqrt{-\tilde{g}} H_0 \{(\rho_0 \eta_2) \partial_t v_1^r + (\rho_0 \eta_1 + v_0^t) \partial_t \rho_1\}] + \partial_r [\sqrt{-\tilde{g}} H_0 (\rho_0 \partial_t v_1^r + v_0^r \partial_t \rho_1)] = 0 \quad (4.54)$$

Substitution of $\partial_t v_1^r$ and $\partial_t \rho_1$ in the above equation, using Eq. (4.51) and (4.52), respectively, gives

$$\begin{aligned} & \partial_t \left[k_\xi(r) \left\{ -g^{tt} + (v_0^t)^2 \left(1 - \frac{1}{c_s^2} \right) \right\} \partial_t \xi_1 \right] + \partial_t \left[k_\xi(r) \left\{ v_0^r v_0^t \left(1 - \frac{1}{c_s^2} \right) \right\} \partial_r \xi_1 \right] \\ & + \partial_r \left[k_\xi(r) \left\{ v_0^r v_0^t \left(1 - \frac{1}{c_s^2} \right) \right\} \partial_t \xi_1 \right] + \partial_r \left[k_\xi(r) \left\{ g^{rr} + (v_0^r)^2 \left(1 - \frac{1}{c_s^2} \right) \right\} \partial_r \xi_1 \right] \\ & = 0, \end{aligned}$$

(4.55)

where $k_\xi = \sqrt{-\tilde{g}}H_0/\rho c_s^2$. Comparing the above equation with $\partial_\mu(f^{\mu\nu}\partial_\nu\xi_1) = 0$, we find out the symmetric 2×2 matrix $f^{\mu\nu}$ as

$$f_\xi^{\mu\nu} = k_\xi(r) \begin{bmatrix} -g^{tt} + (v_0^t)^2 \left(1 - \frac{1}{c_s^2}\right) & v_0^r v_0^t \left(1 - \frac{1}{c_s^2}\right) \\ v_0^r v_0^t \left(1 - \frac{1}{c_s^2}\right) & g^{rr} + (v_0^r)^2 \left(1 - \frac{1}{c_s^2}\right) \end{bmatrix} \quad (4.56)$$

4.3 Acoustic metric

The linear perturbation of the velocity potential, mass accretion rate and the relativistic Bernoulli's constant performed in Sec. 4.2.1, 4.2.2 and 4.2.3, respectively, provides the perturbation equation of the following form

$$\partial_\mu(f_x^{\mu\nu}\partial_\nu x_1) = 0, \quad x = (\psi, \Psi, \xi). \quad (4.57)$$

We compare the above equation with the equation of massless scalar field φ in curved spacetime with metric $g_{\mu\nu}$ which is given by $\partial_\mu(\sqrt{-g}g^{\mu\nu}\partial_\nu\varphi) = 0$. This gives the acoustic spacetime metric $G_x^{\mu\nu}$ in terms of $f_x^{\mu\nu}$ as $\sqrt{-G_x}G_x^{\mu\nu} = f_x^{\mu\nu}$. Thus, the acoustic metric is related to the $f_x^{\mu\nu}$ matrix by just a conformal factor $\sqrt{-G_x}$. Also $f_x^{\mu\nu}$ are also the same for different quantities x apart from an overall multiplicative factor $k_x(r)$. Therefore, similar to what we did in the previous chapter, we neglect these conformal factors $k_x/\sqrt{-G_x}$ and work with an acoustic metric which the same for the all three cases of perturbations. Thus, the acoustic metric that we work with is given by

$$G^{\mu\nu} = \begin{bmatrix} -g^{tt} + (v_0^t)^2 \left(1 - \frac{1}{c_s^2}\right) & v_0^r v_0^t \left(1 - \frac{1}{c_s^2}\right) \\ v_0^r v_0^t \left(1 - \frac{1}{c_s^2}\right) & g^{rr} + (v_0^r)^2 \left(1 - \frac{1}{c_s^2}\right) \end{bmatrix} \quad (4.58)$$

and

$$G_{\mu\nu} = \begin{bmatrix} -g^{rr} - (v_0^r)^2 \left(1 - \frac{1}{c_s^2}\right) & v_0^r v_0^t \left(1 - \frac{1}{c_s^2}\right) \\ v_0^r v_0^t \left(1 - \frac{1}{c_s^2}\right) & g^{tt} - (v_0^t)^2 \left(1 - \frac{1}{c_s^2}\right) \end{bmatrix} \quad (4.59)$$

4.4 Location of the acoustic event horizon

The procedure to locate the acoustic event horizon was discussed in the last chapter in Sec. 3.4, which gives the location of acoustic horizon as the condition $G^{rr} = 0$. Therefore, the location of the acoustic event horizon is obtained by solving the following equation which is to be evaluated at the horizon, i.e., at $r = r_h$

$$c_s^2 = \frac{g_{rr}(v_0^r)^2}{1 + g_{rr}(v_0^r)^2}. \quad (4.60)$$

In the CRF, i.e., in terms of u_0 (the stationary value of u defined in Sec. 4.1), the horizon condition becomes

$$u_0^2 = c_s^2. \quad (4.61)$$

The transonic point of a transonic fluid is defined as the location where the fluid becomes supersonic from subsonic, i.e., where the Mach number \mathcal{M} becomes equal to 1. Therefore, we find that the acoustic horizon and the transonic point are basically the same radial location.

One of the main goals of this chapter is to see how the different properties of the acoustic spacetime get influenced by the spin of the background spacetime. Thus, we would like to study the dependence of the acoustic horizon on the black hole spin a . In order to do that, first we need to solve the stationary accretion flow equations.

It is not possible to solve the accretion flow equations analytically and therefore we solve the equations numerically. The solutions depend on a set of parameters that governs the accretion flow. We can solve the equations for a particular set of values of these parameters. The nature of the solutions would depend critically on the selected values of these parameters. For axially symmetric isothermal accretion on to a Kerr black hole, these parameters are namely, the bulk-ion temperature of flow T , the specific angular momentum of the flow λ_0 and the black hole spin a . Depending the given values of the set of parameters $[T, \lambda_0, a]$, the Eq. (4.61) may have one or more than one solutions. Therefore, we first discuss about the choice of parameters and then we discuss the dependence of acoustic horizon on the black hole spin a for fixed values of other parameters.

4.4.1 Choice of parameters $[T, \lambda_0, a]$

The characteristic features of the axially symmetric isothermal accretion flow onto a rotating Kerr black hole (with the disc model considered here) are determined by the set of three parameters $[T, \lambda_0, a]$. We use the same method as described in Sec. 3.5.2 to set up the equations for the gradient of the advective velocity. We write down the mass accretion rate Ψ_0 and the relativistic Bernoulli's constant obtained in Sec. 4.2.2 and 4.2.3, respectively, in terms of the advective velocity u_0 and the specific angular momentum λ_0 . Then we take logarithmic derivative of the equations $\Psi_0 = \text{constant}$ and $\xi_0 = \text{constant}$. We use these two equations to eliminate the density term ρ'_0/ρ_0 , where the 'dash' represents single derivative with respect to the radial coordinate, as usual. This provides the gradient of the advective velocity as

$$u'_0 = \frac{u_0(1 - u_0^2)}{u_0^2 - c_s^2} \left[\frac{B'}{2B} - (1 - c_s^2) \frac{\Delta'}{2\Delta} + \frac{c_s^2}{r} \right] \equiv \frac{N}{D}, \quad (4.62)$$

where $\Delta = r^2 - 2r + a^2$ as defined in Eq. (4.3) and $B = g_{\phi\phi} + 2\lambda_0 g_{\phi t} - \lambda_0^2 g_{tt}$. The critical points of the flow are defined by the points where $N = D = 0$. Thus, critical points are located at $u_0^2 = c_s^2$ and critical points, transonic points and the acoustic horizon coincide for the particular accretion flow described here and therefore such points may be referred by these names interchangeably. This gives the following condition to be satisfied at the critical points

$$u_c^2 = c_{sc}^2 = \frac{\frac{\Delta'}{\Delta} - \frac{B'}{B}}{\frac{2}{r} + \frac{\Delta'}{\Delta}} \quad (4.63)$$

The roots of the above equation lying outside the event horizon of the Kerr black hole (given by $r_+ = 1 + \sqrt{1 - a^2}$) are the critical points of the flow. Due to the fact that $N = D = 0$ at the critical points ($r = r_c$), the advective velocity gradient $u'_0|_c$ at the critical points is obtained by taking the limit as $r \rightarrow r_c$ (and $u_0^2 \rightarrow c_{s0}^2$) by using L'Hospital rule. This gives the velocity gradient to be

$$u'_0|_c = \pm \sqrt{\frac{1 - c_s^2}{4} \left[(1 - c_s^2) \left(\frac{\Delta'^2}{\Delta^2} - \frac{\Delta''}{\Delta} \right) - \left(\frac{B'^2}{B^2} - \frac{B''}{B} \right) - \frac{2c_s^2}{r^2} \right]}. \quad (4.64)$$

where the double 'dash' stands for the second derivative with respect to the radial coordinate r .

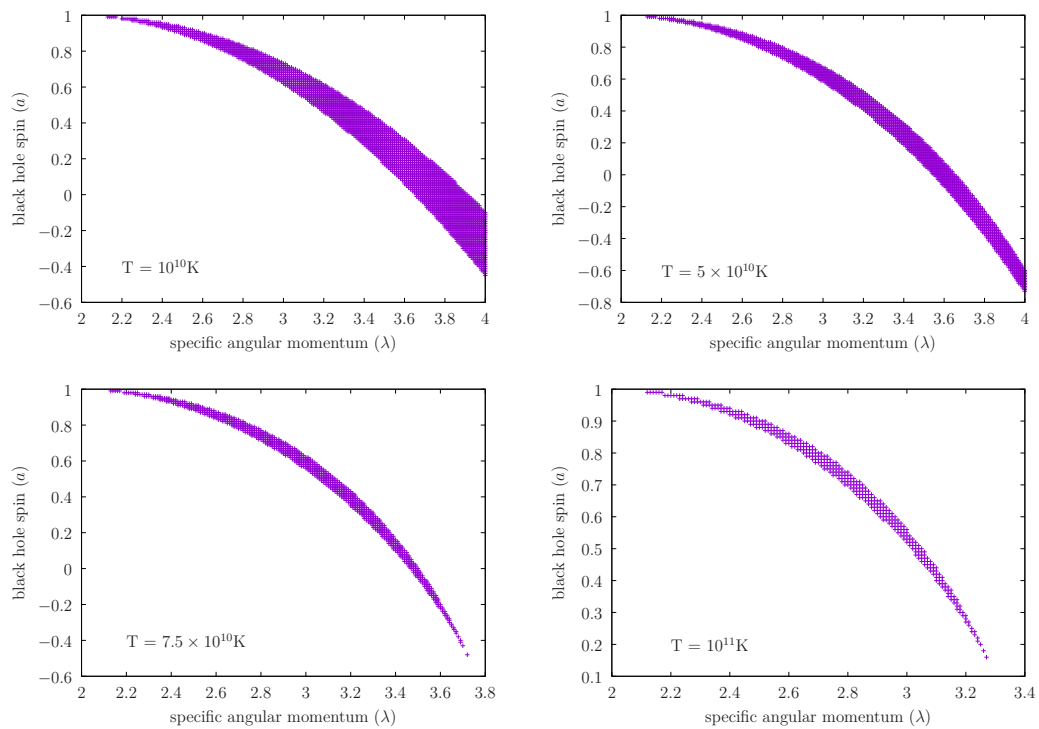


Figure 4.1: Regions of parameter space $[\lambda_0, a]$ allowing multiple critical points for different values of T . For prograde motion higher spin corresponds to lower λ_0 whereas for retrograde motion higher spin corresponds to higher λ_0 for a particular T . For fixed fixed values of $[T, \lambda_0]$ only a finite range of a allow multi-critical accretion.

Depending on the values of the parameters $[T, \lambda_0, a]$, the equation (4.63), and hence the accretion flow, can have one or more than one (or more specifically three) solutions for $r > r_+$. If the flow has only one critical point then the flow passes through this point and the flow is called mono-critical. Such flow is always mono transonic, i.e., the flow makes the transition from subsonic state to supersonic state only once. However, we are more interested in the case where the flow has more than one critical points. The corresponding flow in such case is said to be multi-critical flow as it allows multiple critical points $r_{\text{in}}, r_{\text{mid}}, r_{\text{out}}$ such that $r_{\text{in}} < r_{\text{mid}} < r_{\text{out}}$ (see Fig. 4.4, for example, below). These critical points can be characterized by performing a critical point analysis. Such analysis shows that the inner and outer critical points r_{in} and r_{mid} , respectively, are saddle type, whereas the middle critical point r_{mid} is center type. Thus the accretion flow can pass only through the outer or inner critical points. when the accretion flow passes through both the outer and inner critical points, the accretion flow is called multi-transonic flow. Multi-critical flows are not necessarily multi-transonic flows. This could be understood as the following: suppose the flow starts its journey from large radial distance subsonically. At $r = r_{\text{out}}$, it makes a transition from subsonic state to supersonic state. Thus r_{out} is basically the outer acoustic horizon. After the flow becomes supersonic it may encounter a shock formation which makes the flow subsonic from supersonic discontinuously, i.e., the dynamical variables such as the velocity, sound speed, density and pressure makes discontinuous jump. After it becomes subsonic due the shock formation, it again passes through the inner critical point and becomes supersonic from subsonic. Therefore in presence of shock formation, the flow can pass through both outer and inner critical points and hence the flow is multi-transonic. But all parameters which allow multiple critical points do not allow shock formation. Thus the parameters space which allows shock formation is smaller than the parameter space for multiple critical points.

In Fig. 4.1 we show the region of the parameter space $[a, \lambda_0]$ which allows multi-critical flow, for four fixed values of temperatures. It can be noticed that for multi-critical accretion at a fixed value of T , for prograde motion ($a > 0$), higher spin

corresponds to lower λ whereas for retrograde motion ($a < 0$), higher spin corresponds to higher λ . Here as well as in the following, whenever we talk about the dependence of any quantity on the black hole spin a and explicitly mention whether the motion is prograde or retrograde, we would imply the dependence on the magnitude of the spin a .

4.4.2 Dependence of the acoustic event horizon of $[T, \lambda_0, a]$

For multi-critical accretion, the inner critical point r_{in} generally is found to be very close to the event horizon of the accreting black hole which is located at r_+ . There exist few important circular orbits of test particles very close to the event horizon. These are, namely, the inner most stable circular orbit (ISCO) at r_{ISCO} , the photon sphere at r_{photon} and the inner most unstable bound orbit at r_{bound} . Thus, it would be interesting to compare the location of the inner critical point r_{in} , with the above mentioned radii of circular orbits of test particles [82–84].

The radius of innermost circular orbit, closest to the black hole, (along which the motion is at the speed of light) is given by

$$r_{\text{photon}} = 2 \left(1 + \cos \left(\frac{2}{3} \cos^{-1}(-a) \right) \right) \quad (4.65)$$

and the last bound but unstable circular orbit on which energy of the orbit is equal to the rest mass of the particle is given by

$$r_{\text{bound}} = 2 - a + 2\sqrt{1 - a} \quad (4.66)$$

if a particle in the equatorial plane comes from infinity, with $v_\infty \ll c$, where c is the speed of light, and passes within r_{bound} , then it will be captured by the black hole. Lastly the radius of the inner most circular orbit which is stable is given by

$$r_{\text{ISCO}} = 3 + Z_2 \mp \sqrt{(3 - Z_1)(3 + Z_1 + 2Z_2)} \quad (4.67)$$

where

$$Z_1 = 1 + (1 - a^2)^{\frac{1}{3}} \left[(1 + a)^{\frac{1}{3}} + (1 - a)^{\frac{1}{3}} \right] \quad (4.68)$$

4.4. Location of the acoustic event horizon

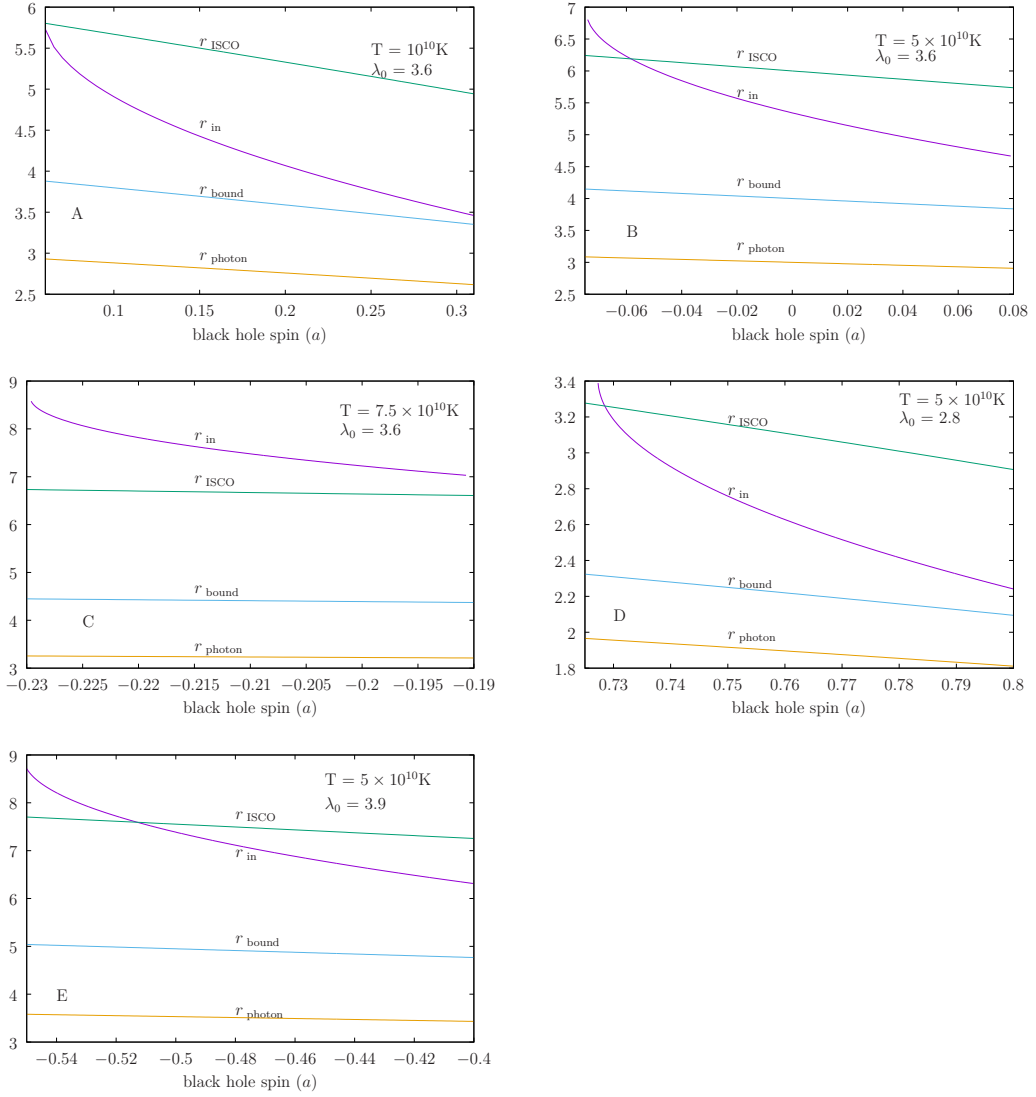


Figure 4.2: Inner acoustic horizon r_{in} (along the vertical axis) vs black hole spin a (along the horizontal axis) plots for different sets of $[T, \lambda_0]$ values. T and λ_0 are the temperature and the specific angular momentum respectively. **A**, **B** and **C** corresponds to a fixed $\lambda_0 = 3.6$ and $T = 10^{10}K, 5 \times 10^{10}K$ and $7.5 \times 10^{10}K$, respectively. **D**, **B** and **E** corresponds to a fixed $T = 5 \times 10^{10}K$ and $\lambda_0 = 2.8, 3.6$ and 3.9 respectively. For all the set of parameters $[T, \lambda_0]$, r_{in} decreases with a for prograde motion whereas it increases with a for retrograde motion. r_{photon} , r_{bound} and r_{ISCO} represent the radius of the circular photon orbit, innermost bound but unstable circular orbit and the innermost stable circular orbit (ISCO), respectively. At least for these values of parameters $[T, \lambda_0]$, inner acoustic horizon r_{in} always remains outside the innermost unstable bound circular orbit r_{bound} . See text for more.

and

$$Z_2 = \sqrt{3a^2 + Z_1^2} \quad (4.69)$$

the upper sign and lower sign in Eq. (4.67) are for prograde and retrograde motion of the particle.

Fig. 4.2, shows the dependence of r_{in} on the black hole spin a for different set of values of temperature and specific angular momentum as well as the variation of the radius of the circular orbits with a for that range. Plots **A**, **B** and **C** shows the variation of r_{in} with a for temperatures $10^{10}K$, $5 \times 10^{10}K$ and $7.5 \times 10^{10}K$, respectively, for a fixed specific angular momentum $\lambda_0 = 3.6$. Whereas plots **D**, **B** and **E** shows the same for specific angular momentum $\lambda_0 = 2.8$, $\lambda_0 = 3.6$ and $\lambda_0 = 3.9$, respectively for a fixed temperature $5 \times 10^{10}K$. For a fixed $[T, \lambda_0]$, the location of the inner critical points, i.e., r_{in} decreases with a for prograde motion whereas it increases with a for retrograde motion. Also by plotting the radius of different circular orbits for the corresponding range of a it is noticed that at least for these values of parameters $[T, \lambda_0]$, inner acoustic horizon r_{in} always remains outside the innermost unstable bound circular orbit r_{bound} . However in order to check whether this is true for all the points of the parameter space $[T, \lambda_0]$ the analysis should be done for all values of $[T, \lambda_0]$ which is beyond the scope of the present work.

Fig. 4.3, shows the dependence of the outer acoustic horizon r_{out} on the black hole spin a for different set of values of temperature and specific angular momentum. Plots **A**, **B** and **C** shows the variation of r_{out} with a for temperatures $10^{10}K$, $5 \times 10^{10}K$ and $7.5 \times 10^{10}K$ respectively, for a fixed specific angular momentum $\lambda_0 = 3.6$. Whereas plots **D**, **B** and **E** shows the same for specific angular momentum $\lambda_0 = 2.8$, $\lambda_0 = 3.6$ and $\lambda_0 = 3.9$ respectively for a fixed temperature $5 \times 10^{10}K$. Here also for a fixed $[T, \lambda_0]$, the location of the outer critical points, i.e., r_{out} decreases as the black hole spin a increases for prograde motion and increases with increasing a for retrograde motion.

From plots **A**, **B** and **C** in Fig. 4.3, i.e, for same λ_0 (here for $\lambda_0 = 3.6$), it is seen that for smaller temperature r_{out} is large compared to that for higher temperature

4.4. Location of the acoustic event horizon

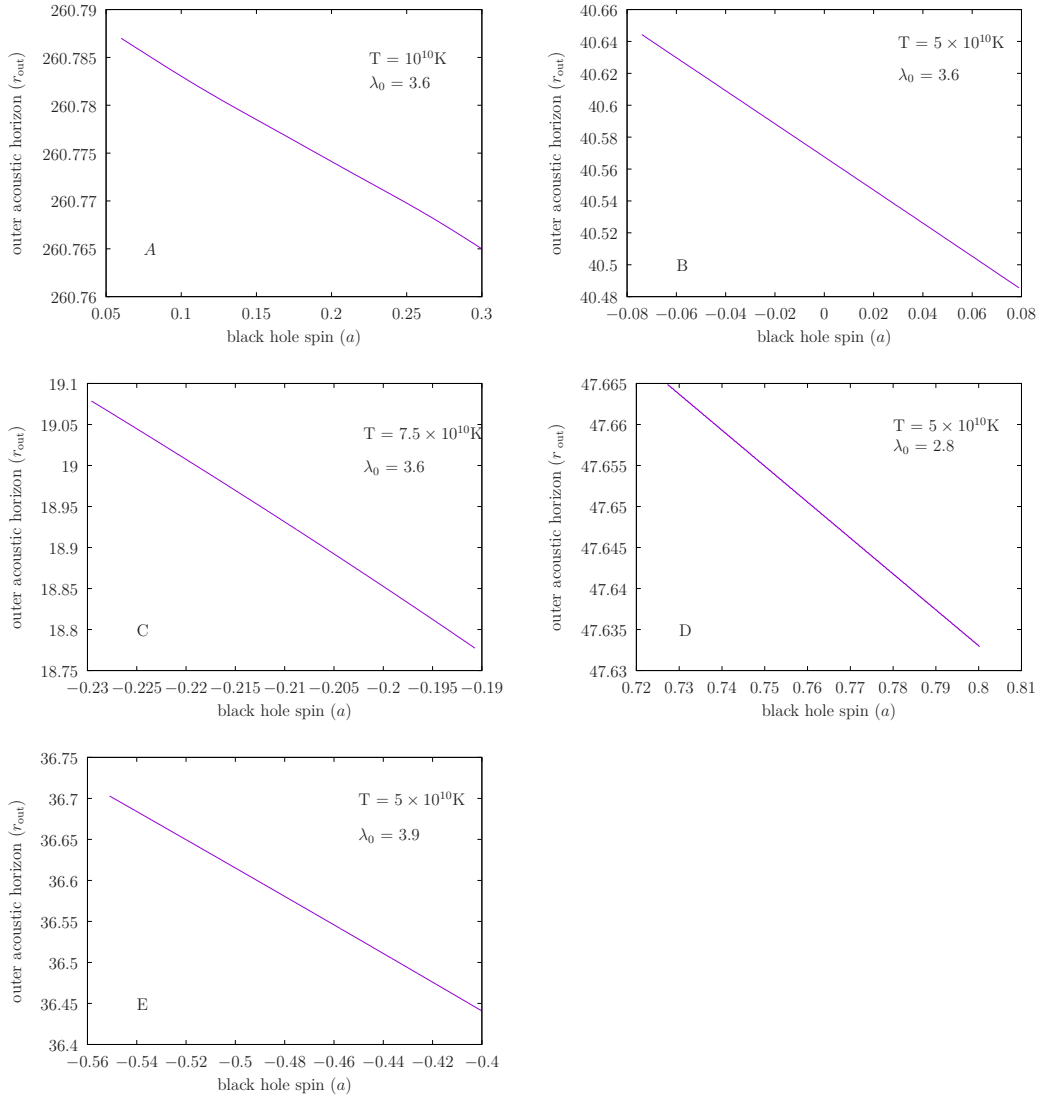


Figure 4.3: Outer acoustic horizon r_{out} vs black hole spin a plot for different set of $[T, \lambda_0]$ values. T and λ_0 are the temperature and the specific angular momentum respectively. **A**, **B** and **C** corresponds to a fixed $\lambda = 3.6$ and $T = 10^{10}K, 5 \times 10^{10}K$ and $7.5 \times 10^{10}K$ respectively. **D**, **B** and **E** corresponds to a fixed $T = 5 \times 10^{10}K$ and $\lambda_0 = 2.8, 3.6$ and 3.9 respectively. For all the set of parameters $[T, \lambda_0]$, r_{out} decreases as the black hole spin a increases for prograde motion and increases with increasing a for retrograde motion.

as argued earlier. Also the change in r_{out} w.r.t a is quite small as compared to the variation of r_{in} with a . This is due to the fact that for large value of r_{out} , the spacetime becomes asymptotically flat, and in such Newtonian gravity limit, the influence of the spin of black hole on the matter flow is less important and that is why change of r_{out} with respect to a is small compared to that of r_{in} .

4.5 Causal structure of the acoustic spacetime

Acoustic null geodesic corresponding to the radially traveling ($d\phi = 0, d\theta = 0$) acoustic phonons is given by $ds^2 = 0$. Thus

$$\left(\frac{dr}{dt}\right)_{\pm} \equiv b_{\pm} = \frac{-G_{rt} \pm \sqrt{G_{rt}^2 - G_{rr}G_{tt}}}{G_{rr}}. \quad (4.70)$$

So $t(r)$ can be obtained as

$$t(r)_{\pm} = t_0 + \int_{r_0}^r \frac{dr}{b_{\pm}}. \quad (4.71)$$

We can introduce two new sets of coordinates as following

$$dz = dt - \frac{1}{b_+} dr, \quad \text{and,} \quad dw = dt - \frac{1}{b_-} dr. \quad (4.72)$$

In terms of these new coordinates the acoustic line element can be written as

$$ds^2|_{\phi=\theta=\text{const}} = \mathcal{D}dzdw, \quad (4.73)$$

where \mathcal{D} is found to be equal to G_{tt} . z and w are called the null coordinates.

The acoustic metric elements $G_{tt}, G_{rt} = G_{tr}, G_{rr}$ given by Eq. (4.59) are expressed in terms of the background metric elements and the velocity variables $u_0(r)$ and λ_0 using Eq. (4.5), (4.6) and (4.7). Thus $b_{\pm}(r)$ is function of the stationary solution $u_0(r)$. Therefore we have to first obtain $u_0(r)$ by solving the relativistic Euler equation for steady state. This is done by numerically integrating Eq. (4.62), which provides the gradient of the advective velocity, i.e, u'_0 , with the initial condition given by Eq. (4.63). Thus for a particular set of $[T, \lambda_0, a]$ we get $u_0(r)$ numerically and hence we get $b_{\pm}(r)$. The integration in Eq. (4.71) is then performed numerically to

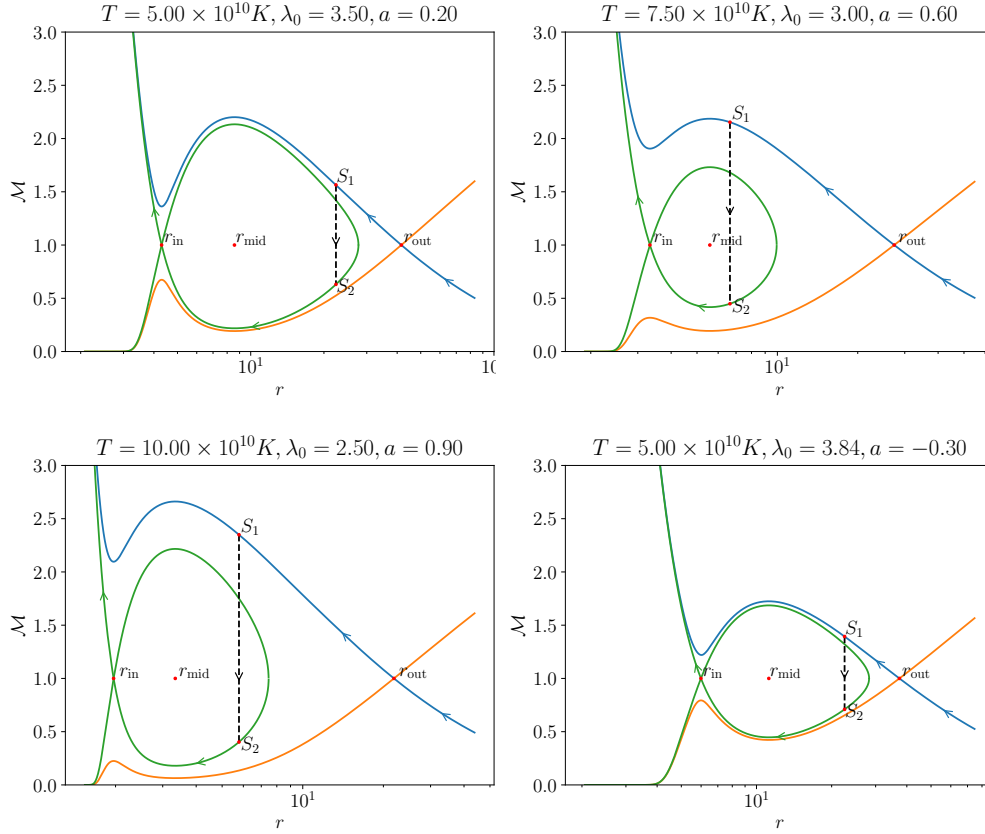


Figure 4.4: Mach number $\mathcal{M} = |u_0|/c_s$ vs radial distance r plots for different values of $[T, \lambda_0, a]$. T, λ_0 and a are the temperature, the specific angular momentum and the black hole spin, respectively. The parameter values for the plots are (row wise) $[T, \lambda_0, a] = [5 \times 10^{10} K, 3.5, 0.2], [7.5 \times 10^{10} K, 3.0, 0.6], [10^{11} K, 2.5, 0.9]$ and $[5 \times 10^{10} K, 3.84, -0.3]$ respectively. The vertical dashed line represents the location of shock formation and the transition from supersonic to subsonic state.

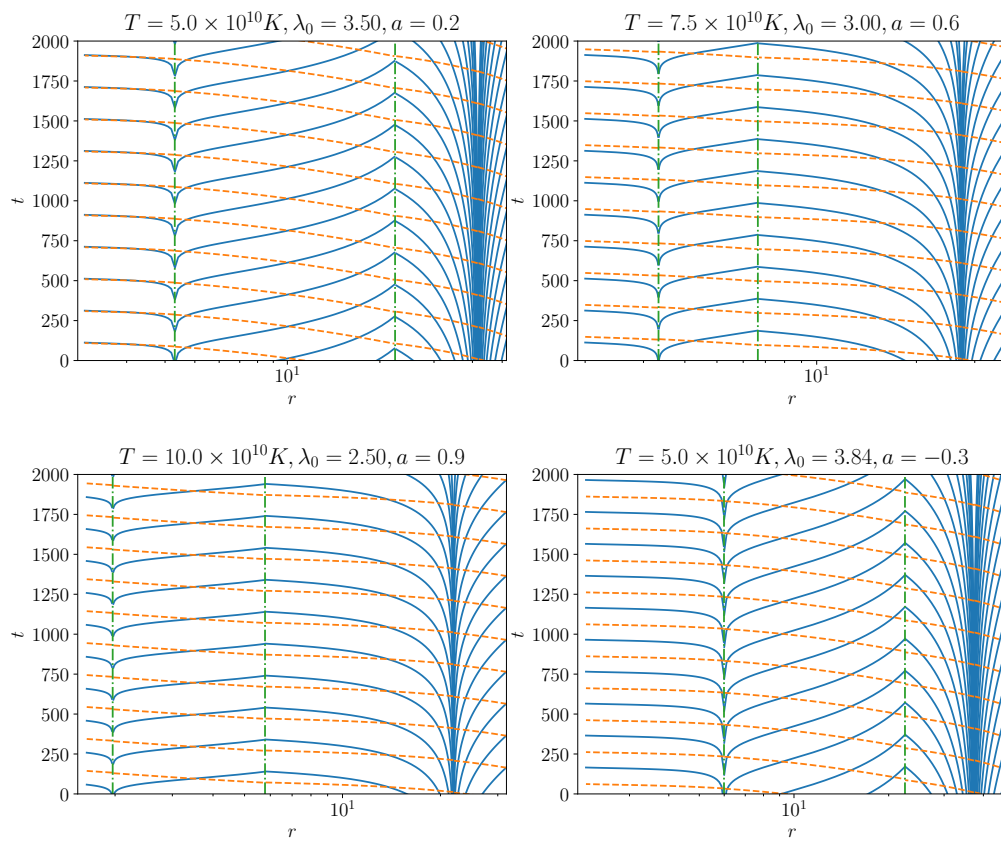


Figure 4.5: The acoustic causal structures for shocked multi-transonic accretion.

The dashed lines denote $t(r)_-$ vs r i.e $w = \text{const}$ and the solid lines denote $t(r)_+$ vs r i.e $z = \text{const}$. The vertical dashed lines indicates the location of inner acoustic horizon (at smaller radii) and that of the shock formation (larger radii). The rows from top to bottom corresponds to $[T, \lambda, a] = [5 \times 10^{10} K, 3.5, 0.2]$, $[7.5 \times 10^{10} K, 3.0, 0.6]$, $[10^{11} K, 2.5, 0.9]$ and $[5 \times 10^{10} K, 3.84, -0.3]$ respectively.

find $t_{\pm}(r)$ as a function of r . Finally we plot $t(r)_{\pm}$ as function of r to see the causal structure of the acoustic spacetime.

If the accretion flow encounters a shock then some quantities are invariant across the shock. The mass flux, i.e., the mass accretion rate is conserved. The momentum flux conservation also requires that the rr component of the energy-momentum tensor is conserved. In addition to these two conditions, there is another condition depending on the radiative efficiency at the shock. In the present case, we consider the temperature of the flow before and after the shock to be the same, i.e., we consider the shock to be temperature preserving. These three conditions are the so called ‘the shock jump conditions’ and could be given by the following set of equations [65]

$$\begin{aligned} [[\rho_0 v_0^r r^2]] &= 0, \\ [[T^{rr}]] &= 0, \\ [[T]] &= 0, \end{aligned} \tag{4.74}$$

where the symbol $[[f]] = f_+ - f_-$, where, f_- and f_+ denote the values of the variable f before and after the shock, respectively. The second condition in the above equation could be reduced to the following condition

$$\left[\left[\rho_0 \left(\frac{(v_0^r)^2}{c_s^2} + g^{rr} \right) \right] \right] = 0. \tag{4.75}$$

From Eq. (4.74) and (4.75), it is easy to obtain a relation between v_{0+}^r and v_{0-}^r which is $v_{0+}^r v_{0-}^r = c_s^2 g^{rr}$. The location of shock formation for an isothermal flow with temperature T and specific angular momentum λ_0 can be obtained numerically. The first condition in Eq. (4.74) is satisfied trivially due to the constancy of mass accretion rate. The third condition is also satisfied trivially because the two braches of accretion flow passing through r_{out} and r_{in} correspond to the same temperature T . Thus in order to obtain the location of the shock formation, we need to ensure that T^{rr} changes continuously at the shock location r_{sh} . This is equivalent to ensuring that the quantity $S_{\text{sh}} \equiv T^{rr}/\Psi_0$ is invariant across the shock. The quantity S_{sh} is called the ‘shock invariant quantity’ and is given by

$$S_{\text{sh}} = \frac{1}{u_0 \sqrt{1 - u_0^2}} (u_0^2 + c_s^2 (1 - u_0^2)). \tag{4.76}$$

The general scheme to find the shock location numerically is the following: Let the numerical value of S_{sh} along the trajectories passing through r_{out} and r_{in} be given by $S_{\text{sh}}^{\text{out}}(r)$ and $S_{\text{sh}}^{\text{in}}(r)$, respectively. Then the location of shock formation r_{sh} is such that $S_{\text{sh}}^{\text{out}}(r_{\text{sh}}) = S_{\text{sh}}^{\text{in}}(r_{\text{sh}})$.

We take few representative values of the parameters as $[T, \lambda_0, a]$ and study the causal structure of the corresponding accretion flow. The phase portraits of the stationary solution for four different sets of $[T, \lambda_0, a]$ are shown in Fig.4.4. The transonic accretion flow passes through the outer critical point r_{out} and becomes supersonic from subsonic state. Then it encounters a shock at r_{sh} and becomes subsonic from supersonic state and after that it crosses r_{in} to become supersonic again. We obtain the causal structure corresponding to this multi-transonic solution. The $[T, \lambda_0]$ are chosen such that the accretion flow allows multiple critical points (See Fig. 4.1) as well as shock formation for the black hole spin $a = 0.2, 0.6, 0.9$ and -0.3 . The parameter values for the plots are (row wise) $[T, \lambda_0, a] = [5 \times 10^{10} K, 3.5, 0.2], [7.5 \times 10^{10} K, 3.0, 0.6], [10^{11} K, 2.5, 0.9]$ and $[5 \times 10^{10} K, 3.84, -0.3]$, respectively. The vertical dashed line represents the location of shock formation and transition from supersonic state to subsonic state. In Fig. 4.5 we plot the causal structures for the multi-transonic accretion flows (plotted in Fig. 4.4). The rows from top to bottom corresponds to $[T, \lambda_0, a] = [5 \times 10^{10} K, 3.5, 0.2], [7.5 \times 10^{10} K, 3.0, 0.6], [10^{11} K, 2.5, 0.9]$ and $[5 \times 10^{10} K, 3.84, -0.3]$ respectively.

As is obvious from the Fig. 4.5, the shock formation in multi-transonic black hole accretion flow can thus be considered as the presence of an acoustic white hole in the corresponding sonic geometry. Where as the inner and outer transonic surfaces act as acoustic black hole horizons.

The aforementioned procedure to construct the relevant causal structures are based on the assumptions that the stationary integral flow solutions are obtained for the steady state (through the integration of the time independent Euler and the continuity equations). Such assumptions, however, are to be justified by showing that the steady states are stable for this case. In subsequent sections, we thus perform the linear stability analysis of the accretion flow to ensure that the steady

states are stable states.

4.6 Acoustic surface gravity

The acoustic metric given by Eq. (4.59) is independent of time t . Therefore we have the stationary Killing vector $\chi^\mu = \delta_t^\mu$. Thus, following the same procedure as described in the previous section, we find that κ can be written as

$$\kappa = \left| \frac{(r^2 - 2r + a^2) \sqrt{(r^3 + a^2r + 2a^2 - 4a\lambda - \lambda^2(r - 2))}}{(1 - c_s^2) \sqrt{r} (r^3 + a^2r + 2a^2 - 2a\lambda)} u'_0 \right|_h \quad (4.77)$$

In the Schwarzschild limit $a = 0$, this reduces to the result derived earlier in [64]. Thus we obtain the acoustic surface gravity as a function of the background metric elements and the stationary values of the accretion variables. The surface gravity depends explicitly on the black hole spin a and the specific angular momentum λ_0 . The acoustic surface gravity is linearly proportional to the gradient of the advective velocity (u'_0) at the acoustic horizon. u'_0 depends on the values of the parameters $[T, \lambda_0, a]$, which could be found from numerical solution of the accretion flow. Thus the dependence of the acoustic surface gravity on the black hole spin a and the specific angular momentum λ_0 could be understood only through numerical analysis of the accretion flow for a given set of values of the parameters $[T, \lambda_0, a]$. In Fig. 4.6, we plot the acoustic surface gravity at the inner acoustic horizon (κ_{in}) as a function of the black hole spin for a given set of values of $[T, \lambda_0]$ and in Fig. 4.7, we do the same for the acoustic surface gravity at the outer acoustic horizon (κ_{out}). It is noticed that κ_{in} increases with increasing a for prograde motion and decreases with increasing a for retrograde motion for a given $[T, \lambda_0]$. Whereas κ_{out} decreases with increasing a for prograde motion and increases with increasing a for retrograde motion for a given $[T, \lambda_0]$. However since the shock forms only for a restricted region of parameter space the nature of the complete dependence of κ on a is difficult to understand explicitly. One can also notice that the value of κ_{out} is up to 10^4 times smaller than that of κ_{in} . One of the reasons for this is that the gradient u'_0 is smaller at the outer acoustic horizon than that at the inner acoustic horizon. Also since the outer acoustic horizon forms at a relatively large distance from the black hole, the

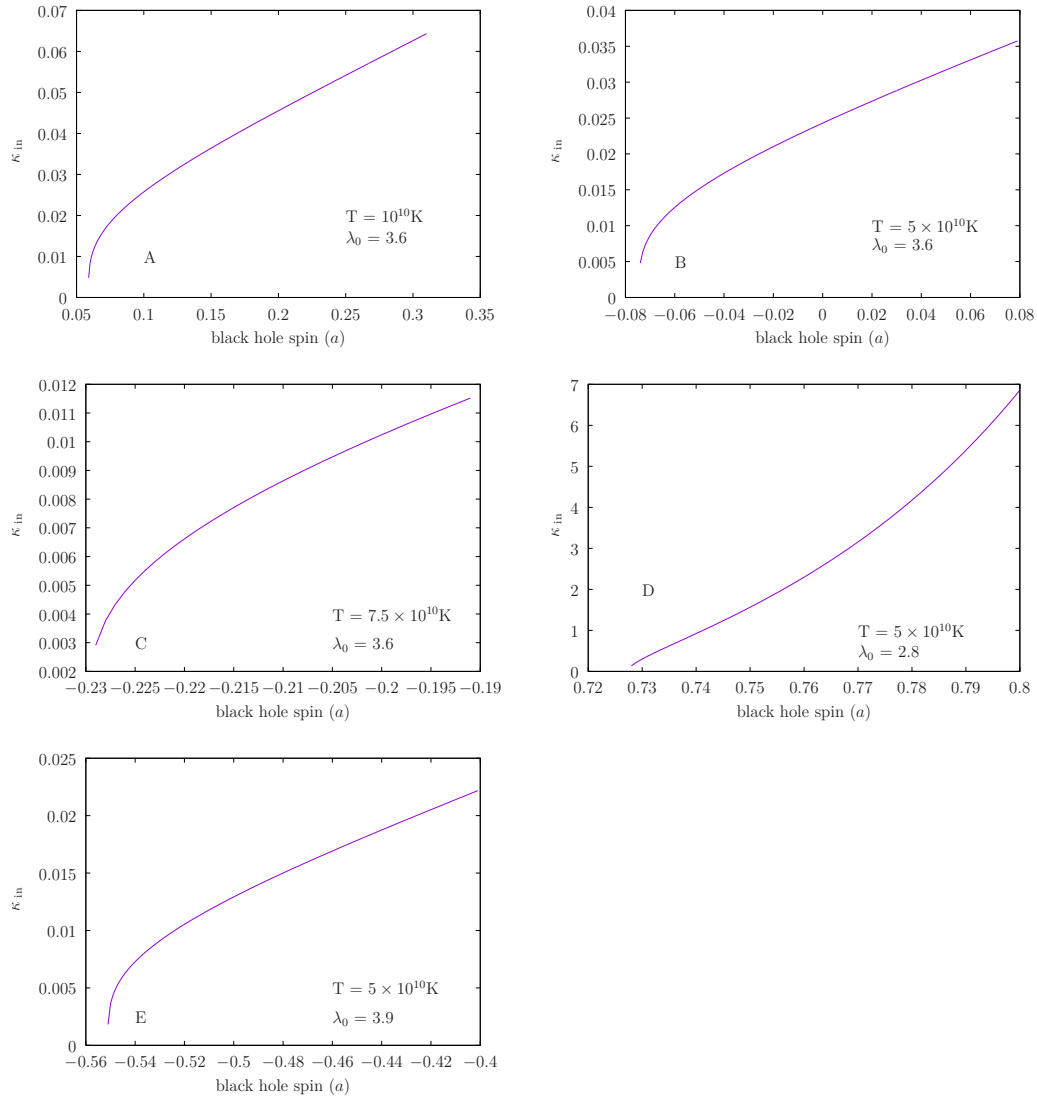


Figure 4.6: Acoustic surface gravity at the inner horizon (κ_{in}) vs black hole spin (a) plot. **A**, **B** and **C** corresponds to a fixed $\lambda_0 = 3.6$ and $T = 10^{10}K$, $5 \times 10^{10}K$ and $7.5 \times 10^{10}K$ respectively. **D**, **B** and **E** corresponds to a fixed $T = 5 \times 10^{10}K$ and $\lambda_0 = 2.8, 3.6$ and 3.9 respectively. For all the set of parameters $[T, \lambda_0]$, κ_{in} increases with increasing a for prograde motion and decreases with increasing a for retrograde motion.

4.6. Acoustic surface gravity

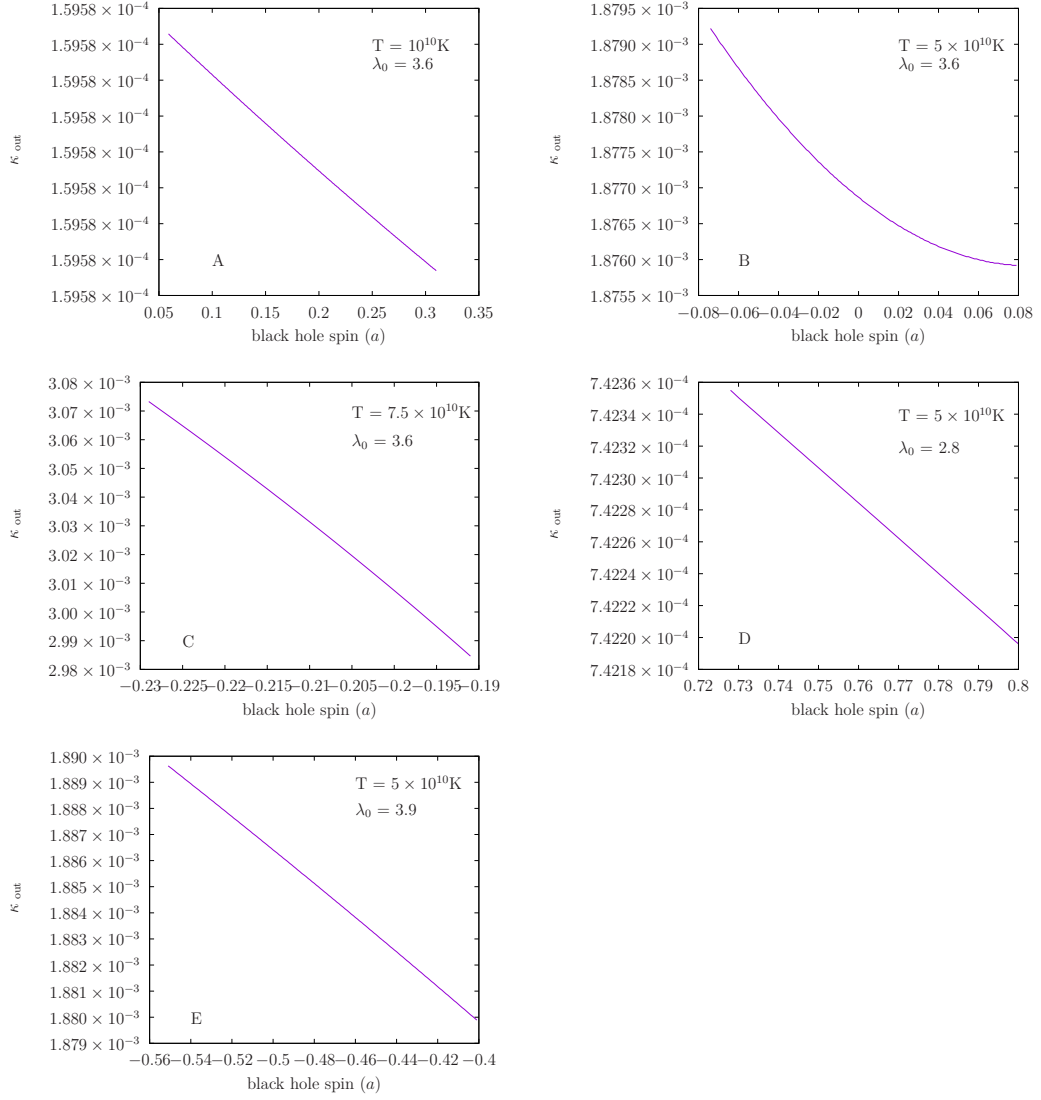


Figure 4.7: Acoustic surface gravity at the outer horizon (κ_{out}) vs black hole spin (a) plot. **A**, **B** and **C** corresponds to a fixed $\lambda_0 = 3.6$ and $T = 10^{10}K$, $5 \times 10^{10}K$ and $7.5 \times 10^{10}K$ respectively. **D**, **B** and **E** corresponds to a fixed $T = 5 \times 10^{10}K$ and $\lambda_0 = 2.8, 3.6$ and 3.9 respectively. For all the set of parameters $[T, \lambda_0]$, κ_{out} decreases with increasing a for prograde motion and increases with increasing a for retrograde motion.

Kerr parameter does not play any significant role to influence the properties of the spacetime close to the outer horizon. Therefore the value of the acoustic surface gravity evaluated at the outer acoustic horizon does not seem to be reasonably sensitive on the black hole spin.

4.7 Effect of the presence of dissipative mechanism

We have considered inviscid accretion of ideal fluid only. Description of non ideal fluid is characterized by various dissipative processes in conjunction with the presence of viscosity. Viscosity, however, breaks the Lorentzian symmetry [5] and acoustic metric cannot be constructed for viscous flow using the formalism we follow in this work. It should also be mentioned that effect of viscosity, as well as magnetic field, may not always be neglected as the dissipative mechanism, through different processes such as comptonisation, bremsstrahlung or synchrotron processes, may become significant. This would influence the overall flow dynamics and therefore turbulent instability may develop. In such cases the linear stability analysis would also become insufficient and non-linear stability analysis would be required to ensure the stability of the system. Such work would require large scale numerical simulation of the flow profile and analysis for such flow is beyond the scope of the present work. Hence the study of the viscous accretion of non ideal fluid as well as analogue system is beyond the scope of this work. We have also assumed that the accretion flow is axially symmetric. Thus for any non-axially asymmetric flow, the present formalism would not be appropriate.

5

Relativistic sonic geometry for adiabatic accretion in the Kerr metric¹

5.1 Introduction

In the previous chapters, we investigated the emergence of acoustic spacetime metric and its properties for accretion on to Schwarzschild and Kerr black hole where the accreting matter is governed by an isothermal equation of state. In isothermal flow, the total energy of the flow is not conserved but the temperature of the flow is constant throughout the flow. However, there also exist another common type of flow where instead of the temperature, the entropy of flow along the fluid trajectory is conserved. Such a flow is governed by an adiabatic equation of state. If the entropy of the flow is constant throughout the fluid, then the flow may be called an isentropic flow.

In isothermal flow, the speed of sound is taken to be a constant. Thus the gradient of the local sound speed is zero throughout the accretion flow. However, it is more

¹This chapter is based on the work titled “*Linear perturbations of low angular momentum accretion flow in the Kerr metric and the corresponding emergent gravity phenomena*” by M. A. Shaikh and T. K. Das [77].

general to consider a flow where the sound speed is also position-dependent and hence the gradient of the sound speed c'_{s0} is non-zero. Adibatic flow, where the sound speed is position-dependent, thus provides a more general description of the accretion flow as well as that of the emergence of analogue gravity spacetime in accretion flow.

In this chapter, we study the acoustic geometry embedded in adiabatic flow accreting on to a Kerr black hole. The basic set up for the accretion system will be mostly the same as provided in the case of an isothermal accretion on to Kerr black hole discussed in the last chapter (Chap. 4). Therefore, in this chapter we will mainly provide the results for adiabatic flow while referring the reader for the basics to the Chap. 3 and 4.

5.2 Basic equations governing the flow

We consider the spacetime metric for a stationary rotating spacetime given by Eq. 4.1. We assume the hydrodynamic fluid accreting onto the Kerr black hole to be perfect, irrotational, and is described by an adiabatic equation of state. The energy momentum tensor for such fluid is given by Eq. 3.3. v^μ is the four-velocity of the fluid which satisfies the normalization condition $v^\mu v_\mu = -1$. The adiabatic equation of state is given by the relation $p = k\rho^\gamma$ where ρ is the rest-mass energy density and $\gamma = c_p/c_v$ is the adiabatic index (c_p and c_v are specific heats at constant pressure and at constant volume, respectively). The total energy density ε is the sum of the rest-mass energy density and the internal energy density (due to the thermal energy), i.e., $\varepsilon = \rho + \varepsilon_{\text{thermal}}$. The continuity equation and energy-momentum conservation equation is given by Eq. (3.4) and (3.5), respectively. The general relativistic Euler equation for barotropic ideal fluid is thus given by

$$(p + \varepsilon)v^\mu \nabla_\mu v^\nu + (g^{\mu\nu} + v^\mu v^\nu) \nabla_\mu p = 0. \quad (5.1)$$

The specific enthalpy of the flow is defined as $h = (p + \varepsilon)/\rho$. We assume the flow to be isentropic, i.e., the specific entropy of the flow s/ρ is constant, where s is the entropy density. Therefore, for an isentropic flow, the following thermodynamical

identity, where T is the temperature of the fluid,

$$dh = Td\left(\frac{s}{\rho}\right) + \frac{1}{\rho}dp \quad (5.2)$$

gives $dp = \rho dh$ which when used in $h = (p + \varepsilon)/\rho$ also gives $d\varepsilon = \rho dh$. Thus the adiabatic sound speed is given by

$$c_s^2 = \left. \frac{\partial p}{\partial \varepsilon} \right|_{\frac{s}{\rho} = \text{constant}} = \frac{\rho}{h} \frac{\partial h}{\partial \rho}. \quad (5.3)$$

The relativistic Euler equation for isentropic flow can thus be written as

$$v^\mu \nabla_\mu v^\nu + \frac{c_s^2}{\rho} (v^\mu v^\nu + g^{\mu\nu}) \partial_\mu \rho = 0. \quad (5.4)$$

For general relativistic irrotational isentropic fluid, the irrotationality condition is given by ([6])

$$\partial_\mu (h v_\nu) - \partial_\nu (h v_\mu) = 0. \quad (5.5)$$

5.3 Accretion flow geometry

We consider an axially symmetric accretion flow in the Kerr background. The flow is assumed to be symmetric about the equatorial plane. The four velocity components are written as $(v^t, v^r, v^\theta, v^\phi)$. We assume that the velocity component along the vertical direction is negligible compared to the radial component v^r , i.e., $v^\theta \ll v^r$. Also due the axial symmetry ∂_ϕ term in the continuity equation would vanish. Thus the continuity equation for such flow can be written as

$$\partial_t (\rho v^t \sqrt{-g}) + \partial_r (\rho v^r \sqrt{-g}) = 0 \quad (5.6)$$

where g is the determinant of the metric $g_{\mu\nu}$. For Kerr metric, $g = -\sin^2 \theta r^4 \mu^2$. The accretion flow variables, i.e., velocity components and the density are in general functions of t, r, θ coordinates. However, assuming that the flow thickness is small compared to the radial size of the accretion disc, we do an averaging of any flow variable $f(t, r, \theta)$ along the θ direction using Eq. (3.26). Thus the continuity

equation for vertically averaged axially symmetric accretion can be written as ([64, 76])

$$\partial_t(\rho v^t \sqrt{-\tilde{g}} H_\theta) + \partial_r(\rho v^r \sqrt{-\tilde{g}} H_\theta) = 0 \quad (5.7)$$

where \tilde{g} is the value of g on the equatorial plane, i.e., $\tilde{g} = -r^4$. The angular scale H_θ of the flow thickness, i.e., the angle made by the flow thickness at the center of the black hole at any radial distances r from the center of the black hole along the equatorial plane is given by $H_\theta = H(r)/r$, assuming the the flow thickness to be small at all r .

In the present work, we consider the conical flow model where the accretion flow is assumed to maintain a wedge-shaped conical geometry. As mentioned earlier, in such flow the local flow thickness is proportional to the radial distance measured along the equatorial plane, i.e., $\frac{H}{r} = \text{constant}$ or H_θ being the characteristic angular scale of local flow is constant for such conical flow geometry. Thus H_θ does not depend on the accretion flow variables like velocity or density. Therefore linear perturbation of these quantities (discussed in the next section) will have no effect on it. For simplicity, therefore, we will write H_θ simply as H_θ . The same is true for the CH model also. However, due to the complicated dependence of $H(r)$ on the flow variables in the VE model, the flow thickness will also be perturbed when the flow variables are perturbed. This will make the analysis too complicated to be presented here. Therefore as mentioned earlier, we do not consider CH and VE models and work only with the CF model. From now on all the equations will be derived by assuming that the flow variables are vertically averaged and their values are computed on the equatorial plane.

5.4 Linear perturbation analysis and the acoustic geometry

The scheme of the linear perturbation analysis would be the the same as provided in Chap. 3 and 4: We shall write the accretion variables, e.g., four velocity com-

ponents and density about their stationary background values upto first order in perturbation. These expressions are then used in the basic governing equations such as the continuity equation, normalization condition and the irrotationality condition. Keeping only the terms that are linear in the perturbed quantities gives equations relating different perturbed quantities upto first order in perturbations. Further manipulations of these equations gives a wave equation which describes the propagation of the perturbation of the mass accretion rate. Perturbation equation in terms of velocity potential or the relativistic Bernoulli's constant could be found easily following the same procedure as discussed in Chap. 4. In this chapter, we perform perturbation analysis for mass accretion rate only.

Below we derive some useful relations using the irrotationality condition (Eq. (5.5)), the normalization condition $v^\mu v_\mu = -1$ and the axial symmetry which will be later used to derive the wave equation for linear perturbation. From irrotationality condition given by Eq. (5.5) with $\mu = t$ and $\nu = \phi$ and with axial symmetry we have

$$\partial_t(hv_\phi) = 0, \quad (5.8)$$

again with $\mu = r$ and $\nu = \phi$ and the axial symmetry the irrotationality condition gives

$$\partial_r(hv_\phi) = 0. \quad (5.9)$$

So we get that hv_ϕ is a constant of the motion. Eq. (5.8) gives

$$\partial_t v_\phi = -\frac{v_\phi c_s^2}{\rho} \partial_t \rho. \quad (5.10)$$

Substituting $v_\phi = g_{\phi\phi}v^\phi + g_{\phi t}v^t$ in the above equation provides

$$\partial_t v^\phi = -\frac{g_{\phi t}}{g_{\phi\phi}} \partial_t v^t - \frac{v_\phi c_s^2}{g_{\phi\phi} \rho} \partial_t \rho. \quad (5.11)$$

The normalization condition $v^\mu v_\mu = -1$ provides

$$g_{tt}(v^t)^2 = 1 + g_{rr}(v^r)^2 + g_{\phi\phi}(v^\phi)^2 + 2g_{\phi t}v^\phi v^t \quad (5.12)$$

which after differentiating with respect to t gives

$$\partial_t v^t = \alpha_1 \partial_t v^r + \alpha_2 \partial_t v^\phi \quad (5.13)$$

where $\alpha_1 = -v_r/v_t$, $\alpha_2 = -v_\phi/v_t$ and $v_t = -g_{tt}v^t + g_{\phi t}v^\phi$. Substituting $\partial_t v^\phi$ in Eq. (5.13) using Eq. (5.11) gives

$$\partial_t v^t = \left(\frac{-\alpha_2 v_\phi c_s^2 / (\rho g_{\phi\phi})}{1 + \alpha_2 g_{\phi t} / g_{\phi\phi}} \right) \partial_t \rho + \left(\frac{\alpha_1}{1 + \alpha_2 g_{\phi t} / g_{\phi\phi}} \right) \partial_t v^r \quad (5.14)$$

We perturb the velocities and density around their steady background values as following

$$v^\mu(r, t) = v_0^\mu(r) + v_1^\mu(r, t) \quad (5.15)$$

$$\rho(r, t) = \rho_0(r) + \rho_1(r, t) \quad (5.16)$$

where $\mu = t, r, \phi$ and the subscript “0” denotes the stationary background part and the subscript “1” denotes the linear perturbations. Using Eq. (5.15)-(5.16) in Eq. (5.14) and retaining only the terms of first order in perturbed quantities we obtain

$$\partial_t v_1^t = \eta_1 \partial_t \rho_1 + \eta_2 \partial_t v_1^r \quad (5.17)$$

where

$$\eta_1 = -\frac{c_{s0}^2}{\Lambda v_0^t \rho_0} [\Lambda (v_0^t)^2 - 1 - g_{rr} (v_0^r)^2], \quad \eta_2 = \frac{g_{rr} v_0^r}{\Lambda v_0^t} \quad (5.18)$$

and $\Lambda = g_{tt} + \frac{g_{\phi t}^2}{g_{\phi\phi}}$

5.4.1 Linear perturbation of mass accretion rate

For stationary background flow the ∂_t part of the equation of continuity, i.e., Eq. (5.7) vanishes and integration over spatial coordinate provides $\sqrt{-\tilde{g}} H_0 \rho_0 v_0^r = \text{constant}$. Multiplying the quantity $\sqrt{-\tilde{g}} H_0 \rho_0 v_0^r$ by the azimuthal component of volume element $d\phi$ and integrating the final expression gives the mass accretion rate, $\Psi_0 = \tilde{\Omega} \sqrt{-\tilde{g}} H_0 \rho_0 v_0^r$. Ψ_0 gives the rate of infall of mass through a particular surface. $\tilde{\Omega}$ arises due to the integral over ϕ and is just a geometrical factor and therefore can we can redefine the mass accretion rate by setting it to unity without any loss of generality. Thus we define

$$\Psi_0 \equiv \sqrt{-\tilde{g}} H_0 \rho_0 v_0^r. \quad (5.19)$$

Now let us define a quantity $\Psi \equiv \sqrt{-\tilde{g}}H\rho(r,t)v^r(r,t)$ which has the stationary value equal to Ψ_0 . Using the perturbed quantities given by Eq. (5.15) and (5.16) we have

$$\Psi(r,t) = \Psi_0 + \Psi_1(r,t), \quad (5.20)$$

where

$$\Psi_1(r,t) = \sqrt{-\tilde{g}}H_0(\rho_0v_1^r + v_0^r\rho_1). \quad (5.21)$$

Using Eq. (5.15)-(5.17) and (5.20) in the continuity Eq. (5.7) and differentiating Eq. (5.21) with respect to t gives, respectively

$$\rho_0\eta_2\partial_tv_1^r + (v_0^t + \rho_0\eta_1)\partial_t\rho_1 = -\frac{1}{\sqrt{-\tilde{g}}H_0}\partial_r\Psi_1, \quad (5.22)$$

and

$$\rho_0\partial_tv_1^r + v_0^r\partial_t\rho_1 = \frac{1}{\sqrt{-\tilde{g}}H_0}\partial_t\Psi_1. \quad (5.23)$$

In deriving Eq. (5.22) we have used Eq. (5.17). With these two equations given by Eq. (5.22) and (5.23) we can write $\partial_tv_1^r$ and $\partial_t\rho_1$ solely in terms of derivatives of Ψ_1 as

$$\begin{aligned} \partial_tv_1^r &= \frac{1}{\sqrt{-\tilde{g}}H_0\rho_0\tilde{\Lambda}}[-(v_0^t + \rho_0\eta_1)\partial_t\Psi_1 - v_0^r\partial_r\Psi_1] \\ \partial_t\rho_1 &= \frac{1}{\sqrt{-\tilde{g}}H_0\rho_0\tilde{\Lambda}}[\rho_0\eta_2\partial_t\Psi_1 + \rho_0\partial_r\Psi_1] \end{aligned} \quad (5.24)$$

where $\tilde{\Lambda}$ is given by

$$\tilde{\Lambda} = \frac{g_{rr}(v_0^r)^2}{\Lambda v_0^t} - v_0^t + \frac{c_{s0}^2}{\Lambda v_0^t}[\Lambda(v_0^t)^2 - 1 - g_{rr}(v_0^r)^2]. \quad (5.25)$$

Now let us go back to the irrotationality condition given by the Eq. (5.5). Using $\mu = t$ and $\nu = r$ gives the following equation

$$\partial_t(hg_{rr}v^r) - \partial_r(hv_t) = 0 \quad (5.26)$$

For stationary flow this provides $\xi_0 = -h_0v_{t0} = \text{constant}$ which is the specific energy of the system. We substitute the density and velocities in Eq. (5.26) using Eq. (5.15), (5.16) and

$$v_t(r,t) = v_{t0}(r) + v_{t1}(r,t). \quad (5.27)$$

Keeping only the terms that are linear in the perturbed quantities and differentiating with respect to time t gives

$$\begin{aligned} \partial_t (h_0 g_{rr} \partial_t v_1^r) + \partial_t \left(\frac{h_0 g_{rr} c_{s0}^2 v_0^r}{\rho_0} \partial_t \rho_1 \right) \\ - \partial_r (h_0 \partial_t v_{t1}) - \partial_r \left(\frac{h_0 v_{t0} c_{s0}^2}{\rho_0} \partial_t \rho_1 \right) = 0 \end{aligned} \quad (5.28)$$

We can also write

$$\partial_t v_{t1} = \tilde{\eta}_1 \partial_t \rho_1 + \tilde{\eta}_2 \partial_t v_1^r \quad (5.29)$$

with

$$\tilde{\eta}_1 = - \left(\Lambda \eta_1 + \frac{g_{\phi t} v_{\phi 0} c_{s0}^2}{g_{\phi\phi} \rho_0} \right), \quad \tilde{\eta}_2 = -\Lambda \eta_2. \quad (5.30)$$

Using Eq. (5.29) in the Eq. (5.28) and dividing the resultant equation by $h_0 v_{t0}$ provides

$$\begin{aligned} \partial_t \left(\frac{g_{rr}}{v_{t0}} \partial_t v_1^r \right) + \partial_t \left(\frac{g_{rr} c_{s0}^2 v_0^r}{\rho_0 v_{t0}} \partial_t \rho_1 \right) \\ - \partial_r \left(\frac{\tilde{\eta}_2}{v_{t0}} \partial_t v_1^r \right) - \partial_r \left(\left(\frac{\tilde{\eta}_1}{v_{t0}} + \frac{c_{s0}^2}{\rho_0} \right) \partial_t \rho_1 \right) = 0 \end{aligned} \quad (5.31)$$

where we have used that $h_0 v_{t0} = \text{constant}$. Finally substituting $\partial_t v_1^r$ and $\partial_t \rho_1$ in Eq. (5.31) using Eq. (5.24) we get

$$\begin{aligned} \partial_t \left[k(r) \left(-g^{tt} + (v_0^t)^2 \left(1 - \frac{1}{c_{s0}^2} \right) \right) \right] + \partial_t \left[k(r) \left(v_0^r v_0^t \left(1 - \frac{1}{c_{s0}^2} \right) \right) \right] \\ + \partial_r \left[k(r) \left(v_0^r v_0^t \left(1 - \frac{1}{c_{s0}^2} \right) \right) \right] + \partial_r \left[k(r) \left(g^{rr} + (v_0^r)^2 \left(1 - \frac{1}{c_{s0}^2} \right) \right) \right] = 0 \end{aligned} \quad (5.32)$$

where

$$k(r) = \frac{g_{rr} v_0^r c_{s0}^2}{v_0^t v_{t0} \tilde{\Lambda}} \quad \text{and} \quad g^{tt} = \frac{1}{\Lambda} = \frac{1}{g_{tt} + g_{\phi t}^2 / g_{\phi\phi}} \quad (5.33)$$

Eq. (5.32) can be written as $\partial_\mu (f^{\mu\nu} \partial_\nu \Psi_1) = 0$ where $f^{\mu\nu}$ is given by the symmetric matrix

$$f^{\mu\nu} = \frac{g_{rr} v_0^r c_{s0}^2}{v_0^t v_{t0} \tilde{\Lambda}} \begin{bmatrix} -g^{tt} + (v_0^t)^2 \left(1 - \frac{1}{c_{s0}^2} \right) & v_0^r v_0^t \left(1 - \frac{1}{c_{s0}^2} \right) \\ v_0^r v_0^t \left(1 - \frac{1}{c_{s0}^2} \right) & g^{rr} + (v_0^r)^2 \left(1 - \frac{1}{c_{s0}^2} \right) \end{bmatrix} \quad (5.34)$$

This is the main result of this section and will be used in the next section to obtain the acoustic metric. In the Schwarzschild limit ($a = 0$) we have $v_{t0} \tilde{\Lambda} = 1 + (1 - c_{s0}^2) g_{\phi\phi} (v_0^\phi)^2$. Thus the $f^{\mu\nu}$ in Eq. (5.34) matches the result obtained by [76] in the Schwarzschild limit.

5.4.2 The acoustic metric

The linear perturbation analysis performed in the previous section provides the equation describing the propagation of the linear perturbation of the mass accretion rate $\Psi_1(r, t)$ and is given by the following equation

$$\partial_\mu(f^{\mu\nu}\partial_\nu\Psi_1) = 0 \quad (5.35)$$

where μ, ν each runs over r, t . This equation is compared to the wave equation of a massless scalar field φ propagating in a curved spacetime given by Eq. (3.33). Comparing these two equations one obtains the acoustic metric $G^{\mu\nu}$ which is related to $f^{\mu\nu}$ as given by Eq. (3.98). $f^{\mu\nu}$ could be written as $f^{\mu\nu} = k(r)\tilde{f}^{\mu\nu}$, where $k(r)$ is the overall multiplicative factor and $\tilde{f}^{\mu\nu}$ is the matrix part as given in Eq. 5.34. Thus $G^{\mu\nu} = (k(r)/\sqrt{-G})\tilde{f}^{\mu\nu}$ and therefore, $G^{\mu\nu}$ is related to $\tilde{f}^{\mu\nu}$ by a conformal factor given by $k(r)/\sqrt{-G}$. One of our main goals of the present work is to show that the acoustic horizon are the transonic surface of the accretion flow and to demonstrate that by studying the causal structure of the acoustic spacetime. However, the location of the event horizon or the causal structure of the spacetime do not depend on the conformal factor of the spacetime metric. Thus in order to investigate these properties of the acoustic spacetime we can take $G^{\mu\nu}$ to be the same as $\tilde{f}^{\mu\nu}$ by ignoring the conformal factor. Thus the acoustic metric $G^{\mu\nu}$ and $G_{\mu\nu}$, apart from the conformal factor, are given by

$$G^{\mu\nu} = \begin{bmatrix} -g^{tt} + (v_0^t)^2(1 - \frac{1}{c_{s0}^2}) & v_0^r v_0^t(1 - \frac{1}{c_{s0}^2}) \\ v_0^r v_0^t(1 - \frac{1}{c_{s0}^2}) & g^{rr} + (v_0^r)^2(1 - \frac{1}{c_{s0}^2}) \end{bmatrix} \quad (5.36)$$

and

$$G_{\mu\nu} = \begin{bmatrix} -g^{rr} - (v_0^r)^2(1 - \frac{1}{c_{s0}^2}) & v_0^r v_0^t(1 - \frac{1}{c_{s0}^2}) \\ v_0^r v_0^t(1 - \frac{1}{c_{s0}^2}) & g^{tt} - (v_0^t)^2(1 - \frac{1}{c_{s0}^2}) \end{bmatrix} \quad (5.37)$$

5.5 Location of the acoustic event horizon

The metric corresponding to the acoustic spacetime is given by Eq. (5.37). The metric elements of $G_{\mu\nu}$ are independent of time and thus the metric is stationary.

In Chap. 3 and 4, we showed that the location of the acoustic horizon is obtained from the condition given by $G^{rr} = 0$. Therefore on the event horizon we have the following condition

$$c_{s0}^2 = \frac{g_{rr}(v_0^r)^2}{1 + g_{rr}(v_0^r)^2}. \quad (5.38)$$

Now we move to the co-rotating frame as defined in [69] where u is the radial velocity of the fluid in the co-rotating frame which is referred as the ‘advective velocity’ and $\lambda = -v_\phi/v_t$ is the the specific angular momentum. For stationary flow, the advective velocity and the specific angular momentum will be denoted with a subscript “0” as earlier. In this co-rotating frame, v^r, v^t and v_t are given in terms of u, λ by Eq. (4.5), (4.6) and (4.7), respectively. In co-rotating frame the Eq. (5.38) becomes

$$u_0^2|_h = c_{s0}^2|_h. \quad (5.39)$$

where the subscript “h” implies that the quantity is to be evaluated at the horizon and would imply the same hereafter. Thus we see that the acoustic horizon is located at a radius where the adevcetive velocity u_0 becomes equal to the speed of sound c_{s0} which is exactly the surface known as the transonic surface. Thus the transonic surface of the accretion flow and the acoustic horizon coincide.

5.6 Causal structure of the acoustic spacetime

Acoustic null geodesic corresponding to the radially traveling ($d\phi = 0, d\theta = 0$) acoustic phonons is given by $ds^2 = 0$. Thus

$$\left(\frac{dr}{dt}\right)_\pm \equiv b_\pm = \frac{-G_{rt} \pm \sqrt{G_{rt}^2 - G_{rr}G_{tt}}}{G_{rr}} \quad (5.40)$$

where the acoustic metric elements $G_{tt}, G_{rt} = G_{tr}, G_{rr}$ are given by Eq. (5.37). These are expressed in terms of the background metric elements, the sound speed

and the velocity variables $u_0(r)$ and $\lambda_0 = -v_{\phi 0}/v_{t0}$ using Eq. (4.5) and (4.6)

$$\begin{aligned}
 G_{tt} &= -\frac{1}{g_{rr}(1-u_0^2)} \left(1 - \frac{u_0^2}{c_{s0}^2}\right) \\
 G_{tr} = G_{rt} &= \frac{u_0}{(1-u_0^2)} \left(1 - \frac{1}{c_{s0}^2}\right) \sqrt{\frac{(g_{\phi\phi} + \lambda_0 g_{\phi t})^2}{g_{rr}(g_{\phi\phi} + 2\lambda_0 g_{\phi t} - \lambda_0^2 g_{tt})(g_{\phi\phi} g_{tt} + g_{\phi t}^2)}} \\
 G_{rr} &= \frac{1}{g_{tt}g_{\phi\phi} + g_{\phi t}^2} \left(g_{\phi\phi} - \frac{(g_{\phi\phi} + \lambda_0 g_{\phi t})^2}{(g_{\phi\phi} + 2\lambda_0 g_{\phi t} - \lambda_0^2 g_{tt})} \frac{(1 - \frac{1}{c_{s0}^2})}{(1 - u_0^2)} \right).
 \end{aligned} \tag{5.41}$$

$t(r)$ can be obtained as

$$t(r)_{\pm} = t_0 + \int_{r_0}^r \frac{dr}{b_{\pm}}. \tag{5.42}$$

We can introduce a new set of coordinates as following

$$dz = dt - \frac{1}{b_+} dr, \quad \text{and,} \quad dw = dt - \frac{1}{b_-} dr \tag{5.43}$$

In terms of these new coordinates the acoustic line element can be written as

$$ds^2|_{\phi=\theta=\text{const}} = \mathcal{D} dz dw \tag{5.44}$$

Where \mathcal{D} is found to be equal to G_{tt} .

$b_{\pm}(r)$ is function of the stationary solution $u_0(r)$ and the sound speed $c_{s0}(r)$. Therefore we have to first obtain $u_0(r)$ and $c_{s0}(r)$ for stationary accretion flow. This is done by simultaneously numerically integrating the equations describing the gradient of the advective velocity u'_0 and the gradient of the sound speed c'_{s0} which are derived below. The ‘dash’ represents single derivative with respect to the radial coordinate r . The solutions are characterized by the parameters $[\xi_0, \gamma, \lambda_0, a]$. Remember that $\xi_0 = -h_0 v_{t0}$ is the specific energy of the flow which is a conserved quantity for the flow under consideration. Thus given a particular set of $[\xi_0, \gamma, \lambda_0, a]$ we get $u_0(r)$ and $c_{s0}(r)$ by numerically solving the Eq. (5.52) and (5.51) simultaneously and then using these solutions of $u_0(r)$ and $c_{s0}(r)$ we get $b_{\pm}(r)$. The integration in Eq. (5.42) is then performed by applying Euler method. Finally we plot $t(r)_{\pm}$ as function of r to see the causal structure of the acoustic spacetime.

5.6.1 Equations for u'_0 and c'_{s0}

To derive the expression for the gradient of advective velocity u'_0 and the gradient of the sound speed c'_{s0} we use the expressions for the two conserved quantities of

the flow. The mass accretion rate Ψ_0 in terms of u_0 is given by

$$\Psi_0 = 4\pi H_0 r^2 \rho_0 \frac{u_0}{\sqrt{g_{rr}(1-u_0^2)}} \quad (5.45)$$

and the relativistic Bernoulli's constant is given by

$$\xi_0 = h_0 \sqrt{\frac{g_{tt}g_{\phi\phi} + g_{\phi t}^2}{(g_{\phi\phi} + 2\lambda_0 g_{\phi t} - \lambda_0^2 g_{tt})(1-u^2)}}. \quad (5.46)$$

For adiabatic flow with conserved specific entropy, in other words an isentropic flow, the enthalpy is given by $dh = dp/\rho$ which when used in the definition of enthalpy given $h = (p+\varepsilon)/\rho$ gives $h = d\varepsilon/d\rho$. The energy density ε includes rest-mass energy ρ and an internal energy equal to $p/(\gamma-1)$. Thus $\varepsilon = \rho + p/(\gamma-1)$. For polytropic equation of state $p = k\rho^\gamma$, the enthalpy is therefore given by

$$h_0 = \frac{\gamma-1}{\gamma-(1+c_{s0}^2)} \quad (5.47)$$

To obtain an equation for the gradient of the sound speed one defines a new quantity $\dot{\Xi}$ via the following transformation

$$\dot{\Xi} = \Psi_0 (\gamma k)^{\frac{1}{\gamma-1}} \quad (5.48)$$

k is a measure of the specific entropy of the accreting matter as the entropy per particle σ is related to k as

$$\sigma = \frac{1}{\gamma-1} \log k + \frac{\gamma}{\gamma-1} + \text{constant}. \quad (5.49)$$

Thus $\dot{\Xi}$ represents the total inward entropy flux and could be labelled as the stationary entropy accretion rate. Expressing ρ in terms of k, γ, h, c_{s0}^2 , the entropy accretion rate could be written as

$$\dot{\Xi} = 4\pi H_0 \frac{u_0}{\sqrt{g_{rr}(1-u_0^2)}} r^2 \left(\frac{(\gamma-1)c_{s0}^2}{\gamma-(1+c_{s0}^2)} \right)^{\frac{1}{\gamma-1}} \quad (5.50)$$

Taking the logarithmic derivative of the above equation with respect to r , the gradient of the sound speed could be written as

$$c'_{s0} = -\frac{c_{s0}(\gamma-(1+c_{s0}^2))}{2} \left[\frac{1}{u_0(1-u_0^2)} \frac{du_0}{dr} + \frac{1}{r} + \frac{1}{2} \frac{\Delta'}{\Delta} \right] \quad (5.51)$$

where $\Delta = r^2 - 2r + a^2$ as given by Eq. (4.3) and the Δ' denotes the first derivative of Δ with respect to r . The gradient of the advective velocity could be found by taking logarithmic derivative of eq. (5.45) and eq. (5.46) (substituting $dh/h_0 = c_{s0}^2 d\rho/\rho_0$) and eliminating $d\rho/\rho_0$, which gives

$$u'_0 = \frac{u_0(1 - u_0^2) \left[c_{s0}^2 \left(\frac{2}{r} + \frac{\Delta'}{\Delta} \right) - \frac{\Delta'}{\Delta} + \frac{B'}{B} \right]}{2(u_0^2 - c_{s0}^2)} = \frac{N}{D} \quad (5.52)$$

where $B = (g_{\phi\phi} + 2\lambda_0 g_{\phi t} - \lambda_0^2 g_{tt})$ and B' is the first derivative of B with respect to r . The critical points of the flow are obtained by equating $D = N = 0$. $D = 0$ gives the location of critical points to at $u_0^2|_{r=r_{\text{crit}}} = c_{s0}^2|_{r=r_{\text{crit}}}$. and $N = 0$ gives

$$u_0^2|_{r=r_{\text{crit}}} = c_{s0}^2|_{r=r_{\text{crit}}} = \left. \frac{\frac{\Delta'}{\Delta} - \frac{B'}{B}}{\frac{2}{r} + \frac{\Delta'}{\Delta}} \right|_{r=r_{\text{crit}}} \quad (5.53)$$

Using the above condition we can substitute u_0^2 and c_{s0}^2 in eq. (5.46) at the critical points which provides

$$\xi_0 = \left. \frac{1}{1 - \frac{1}{\gamma-1} \frac{\frac{\Delta'}{\Delta} - \frac{B'}{B}}{\frac{2}{r} + \frac{\Delta'}{\Delta}}} \sqrt{\frac{2\Delta + r\Delta'}{2B + rB'}} \right|_{r=r_{\text{crit}}} \quad (5.54)$$

Thus, for a given value of ξ_0 which is a constant along the flow and that of γ, λ_0 and a , the above equation could be solved for r_{crit} numerically and the critical points could be found. To find the value of the gradient of the advective velocity at the critical points, we use L'Hospital rule which gives

$$u'_0|_{\text{crit}} = \frac{-\beta \pm \sqrt{\beta^2 - 4\alpha\Gamma}}{2\alpha} \quad (5.55)$$

where

$$\begin{aligned} \alpha &= 1 + \gamma - 3c_{s0}^2|_{r=r_{\text{crit}}} \\ \beta &= 2c_{s0}(1 - c_{s0}^2)(\gamma - (1 + c_{s0}^2)) \left(\frac{1}{r} + \frac{\Delta'}{2\Delta} \right) \Big|_{r=r_{\text{crit}}} \\ \Gamma &= c_{s0}^2(1 - c_{s0}^2)^2 \left[(\gamma - (1 + c_{s0}^2)) \left(\frac{1}{r} + \frac{\Delta'}{2\Delta} \right)^2 - \Gamma^1 \right] \Big|_{r=r_{\text{crit}}} \\ \Gamma^1 &= \frac{1 - c_{s0}^2}{2c_{s0}^2} \left(\frac{\Delta'^2}{\Delta^2} - \frac{\Delta''}{\Delta} \right) - \frac{1}{2c_{s0}^2} \left(\frac{B'^2}{B^2} - \frac{B''}{B} \right) - \frac{1}{r^2} \end{aligned} \quad (5.56)$$

Δ'' and B'' are the second derivatives of Δ and B with respect to r , respectively. For a given set of parameters $[\xi_0, \gamma, \lambda_0, a]$, we can now solve eq. (5.52) and (5.51)

simultaneously to obtain the Mach number as a function of the radial coordinate r . Depending on the values of the parameters $[\xi_0, \gamma, \lambda_0, a]$, the phase portrait may contain one or more critical points.

5.6.2 Mono-transonic case

Let us first consider the case where the accretion flow is mono-transonic. For such accretion flow there exist only one transonic surface. In other words, the flow starts its journey from large radial distance subsonically, i.e., $|u_0| < |c_{s0}|$ or $\mathcal{M} = |u_0|/|c_{s0}| < 1$, where \mathcal{M} is the Mach number of the flow and at some certain radial distance r , the advective velocity becomes equal to the speed of sound or $\mathcal{M} = 1$. The radius r at which \mathcal{M} becomes equal to 1 is called the transonic point. For the flow under consideration, the transonic points are the critical points of the flow where the denominator in the expression of u'_0 becomes 0. Thus the transonic points are given by $r = r_{\text{crit}}$ which in turn are obtained by solving the Eq. (5.54) for given values of the parameters $[\xi_0, \gamma, \lambda_0, a]$. For $r < r_{\text{crit}}$ the flow is supersonic, i.e., $\mathcal{M} > 1$ and remains supersonic all the way upto the event horizon r_+ .

We would like to choose the parameters $[\xi_0, \gamma, \lambda_0]$ in a way such that the Eq. (5.54) has exactly one solution outside the event horizon (i.e., for $r > r_+$) for all values of a and see how the radius of the transonic surface or equivalently r_{crit} varies with the black hole spin a . Then with the same $[\xi_0, \gamma, \lambda_0]$ we pick a few values of the black hole spin a and draw the causal structure of the acoustic space time and show that the location of the acoustic horizon matches r_{crit} for that value of a . In Fig. 5.1, we plot the critical points r_{crit} of mono-transonic flow as a function of the black hole spin.

In Fig. 5.2, we show the causal structure of the acoustic spacetime for mono-transonic accretion flow. The parameters $[\xi_0, \gamma, \lambda_0] = [1.1, 1.4, 2.1]$ are same for all the plots while the black hole spins are $a = -0.9, -0.5, 0, 0.5, 0.9$ row-wise from top to bottom. Solid lines represent $t_+(r)$ vs r , i.e., $z = \text{constant}$ lines and the dotted lines represent the $t_-(r)$ vs r , i.e., $w = \text{constant}$ lines. It is illustrated from the causal structures that the radius of the acoustic horizon, where $t_+(r)$ diverges, are

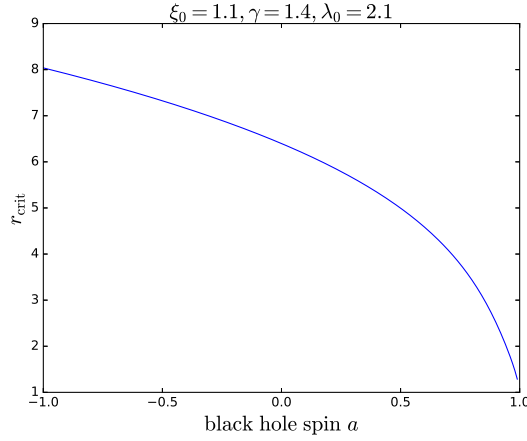


Figure 5.1: The critical points r_{crit} (which are transonic points of the mono-transonic accretion flow) is plotted as function of the black hole spin a for the set of values $[\xi_0, \gamma, \lambda_0] = [1.1, 1.4, 2.1]$.

same as the critical points r_{crit} for the given value of $[\xi_0, \gamma, \lambda_0, a]$.

5.6.3 Multi-transonic case

For a given set of values of the parameters $[\xi_0, \gamma, \lambda_0, a]$, the Eq. (5.54) can have more than one or more specifically three solutions for $r > r_+$. In presence of shock formation, the flow can pass through both outer and inner critical points and hence the flow can be multi-transonic as discussed in Sec. 4.4.1. However, all the set parameters $[\xi_0, \gamma, \lambda_0, a]$ which allow multiple critical points do not allow shock formation. In other words only a subset of the parameters allowing multiple critical points allow shock formation. This is best shown by plotting the parameter space [56].

We have assumed a non-dissipative inviscid accretion flow. Therefore the flow has conserved specific energy and mass accretion rate. Thus the shock produced in such flow is assumed to be energy preserving Rankine Hugoniot type which satisfies the general relativistic Rankine Hugoniot conditions [52, 56, 85–90]

$$\begin{aligned}
 [[\rho v^\mu \eta_\mu]] &= [[\rho v^r]] = 0 \\
 [[T_{t\mu} \eta^\mu]] &= [(p + \varepsilon) v_t v^r] = 0 \\
 [[T_{\mu\nu} \eta^\mu \eta^\nu]] &= [(p + \varepsilon)(v^r)^2 + p g^{rr}] = 0
 \end{aligned} \tag{5.57}$$

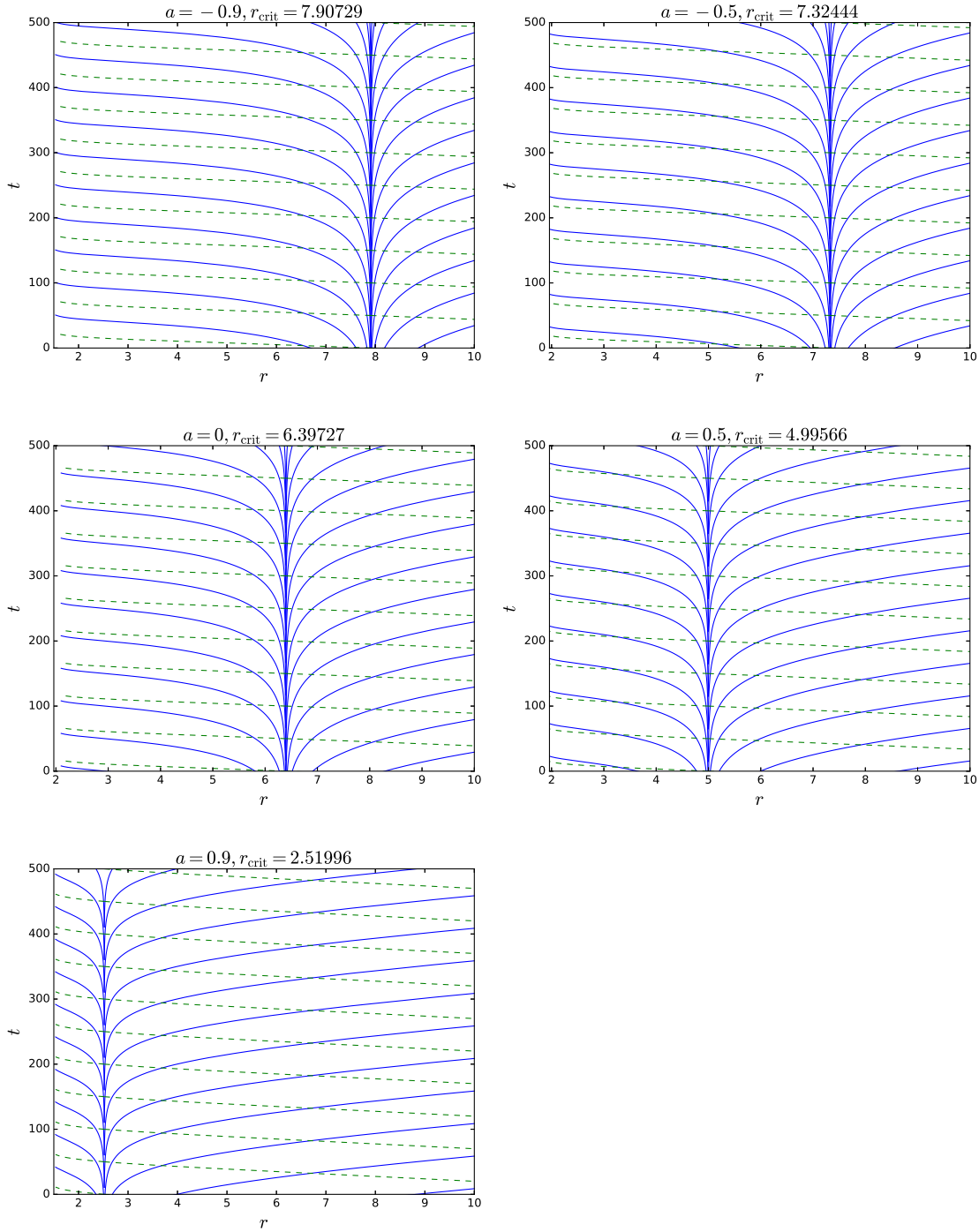


Figure 5.2: Causal structure of the acoustic spacetime for mono-transonic accretion.

$t_+(r)$ vs r , i.e., $z = \text{constant}$ lines are represented by the solid lines and $t_-(r)$ vs r , i.e., $w = \text{constant}$ lines are represented by the dashed lines. $t_{\pm}(r)$ are given by Eq.(5.42). The causal structures are plotted with $[\xi_0, \gamma, \lambda_0] = [1.1, 1.4, 2.1]$ for $a = -0.9, -0.5, 0, 0.5, 0.9$, row-wise from top to bottom. It could be noticed that the acoustic horizon where the $t_+(r)$ lines diverges, coincides with the critical point r_{crit} . See text for more.

Where $\eta_\mu = \delta_\mu^r$ is the normal to the surface of shock formation. $[[f]]$ is defined as $[[f]] = f_+ - f_-$, where f_+ and f_- are values of f after and before the shock, respectively. First condition comes from the conservation of mass accretion rate and the last two conditions come from the energy-momentum conservation. These conditions are to be satisfied at the location of shock formation. In order to find out the location of shock formation, it is convenient to construct a shock invariant quantity, which depends only on u_0, c_{s0} and γ , using the conditions above. The first and second conditions are trivially satisfied owing to the constancy of the mass accretion rate and the specific energy. The first condition is basically $(\Psi_0)_+ = (\Psi_0)_-$ and third condition is $(T^{rr})_+ = (T^{rr})_-$. Thus we can define a shock invariant quantity $S_{\text{sh}} = T^{rr}/\Psi_0$ which also satisfies $[[S_{\text{sh}}]] = 0$. The enthalpy h_0 is given by equation Eq. (5.47) and the sound speed is given as $c_{s0}^2 = (1/h_0)dp/d\rho = (1/h_0)k\gamma\rho^{\gamma-1}$, which gives ρ_0 (and hence also p and ε) in terms of k, γ and c_{s0} . Thus

$$\begin{aligned}\rho &= k^{-\frac{1}{\gamma-1}} \left[\frac{(\gamma-1)c_{s0}^2}{\gamma(\gamma-1-c_{s0}^2)} \right]^{\frac{1}{\gamma-1}} \\ p &= k^{-\frac{1}{\gamma-1}} \left[\frac{(\gamma-1)c_{s0}^2}{\gamma(\gamma-1-c_{s0}^2)} \right]^{\frac{\gamma}{\gamma-1}} \\ \varepsilon &= k^{-\frac{1}{\gamma-1}} \left[\frac{(\gamma-1)c_{s0}^2}{\gamma(\gamma-1-c_{s0}^2)} \right]^{\frac{1}{\gamma-1}} \left(1 + \frac{c_{s0}^2}{\gamma(\gamma-1-c_{s0}^2)} \right)\end{aligned}\tag{5.58}$$

Now $\Psi_0 = \text{constant} \times r^2 \rho v_0^r$ and $T^{rr} = (p+\varepsilon)(v_0^r)^2 + pg^{rr}$, where $v_0^r = u_0/\sqrt{g_{rr}(1-u_0^2)}$. Therefore the shock-invariant quantity $S_{\text{sh}} = T^{rr}/\Psi_0$ becomes

$$S_{\text{sh}} = \frac{(u_0^2(\gamma - c_{s0}^2) + c_{s0}^2)}{u_0 \sqrt{1 - u_0^2(\gamma - 1 - c_{s0}^2)}}\tag{5.59}$$

where we have remove any over all factor of r as shock invariant quantity is to be evaluated at constant $r = r_{\text{sh}}$.

The procedure to find the location of shock formation is the following. Let us denote the values of S_{sh} along the flow passing through outer critical point as $S_{\text{sh}}^{\text{out}}$ and the same for the flow passing through inner critical point as $S_{\text{sh}}^{\text{in}}$. At the location of shock formation r_{sh} , we have $S_{\text{sh}}^{\text{out}} = S_{\text{sh}}^{\text{in}}$. Thus evaluating the $S_{\text{sh}}^{\text{out}}$ and $S_{\text{sh}}^{\text{in}}$ we find out r_{sh} by noting the value of r for which $S_{\text{sh}}^{\text{out}} = S_{\text{sh}}^{\text{in}}$. In general there are two such values of r_{sh} such that one is between inner and middle critical

points $r_{\text{in}} < r_{\text{sh1}} < r_{\text{mid}}$ and the other one is between middle and outer critical points $r_{\text{mid}} < r_{\text{sh2}} < r_{\text{out}}$. However, it has been shown in the literature that the shock formation at r_{sh1} is unstable and that at r_{sh2} is stable. In this context, it is to be mentioned that the stability analysis of the shock does not involve full time dependent calculations, for further details see [44]. Therefore only r_{sh2} is the allowed location of shock formation and hence we shall refer to only this location as the location of shock formation, hereafter.

In the left column of Fig. 5.3, we show the phase portraits of the flow, i.e., the Mach number vs radial distance plots for three different values of the Kerr parameter $a = 0.5, 0.55, 0.6$, keeping $[\xi_0, \gamma, \lambda_0]$ to be the same as $[\xi_0 = 1.002, \gamma = 1.35, \lambda_0 = 3.05]$. These chosen values of the parameters $[\xi_0, \gamma, \lambda_0, a]$ allow the flow to be multi-critical as well as multi-transonic by allowing shock formation. The shock transition of the flow has been denoted by a vertical dashed line in the phase portrait which implies that the shock formation at that location makes the flow to jump from supersonic state in the branch passing through the outer critical point to the subsonic state in the branch passing through the inner critical point.

In the right column of the Fig. 5.3, we show the causal structure corresponding the flow shown by the phase portrait in the left column in the particular row. In the causal structure plots, the vertical dashed line in the left is the location of the inner critical point and the vertical dashed line in the right is the location of shock formation. The outer critical point is located at the white line separating densely populated diverging $t_+(r)$ lines. It is obvious from the causal structure that the inner and outer critical points are the inner and outer acoustic horizon of the acoustic spacetime. Also it could be noticed that for an observer in the region $r_{\text{in}} < r < r_{\text{sh2}}$, the surface of shock formation would resemble a white hole horizon. Thus the shock formation can be regraded as the presence of an acoustic white hole.

5.6. Causal structure of the acoustic spacetime

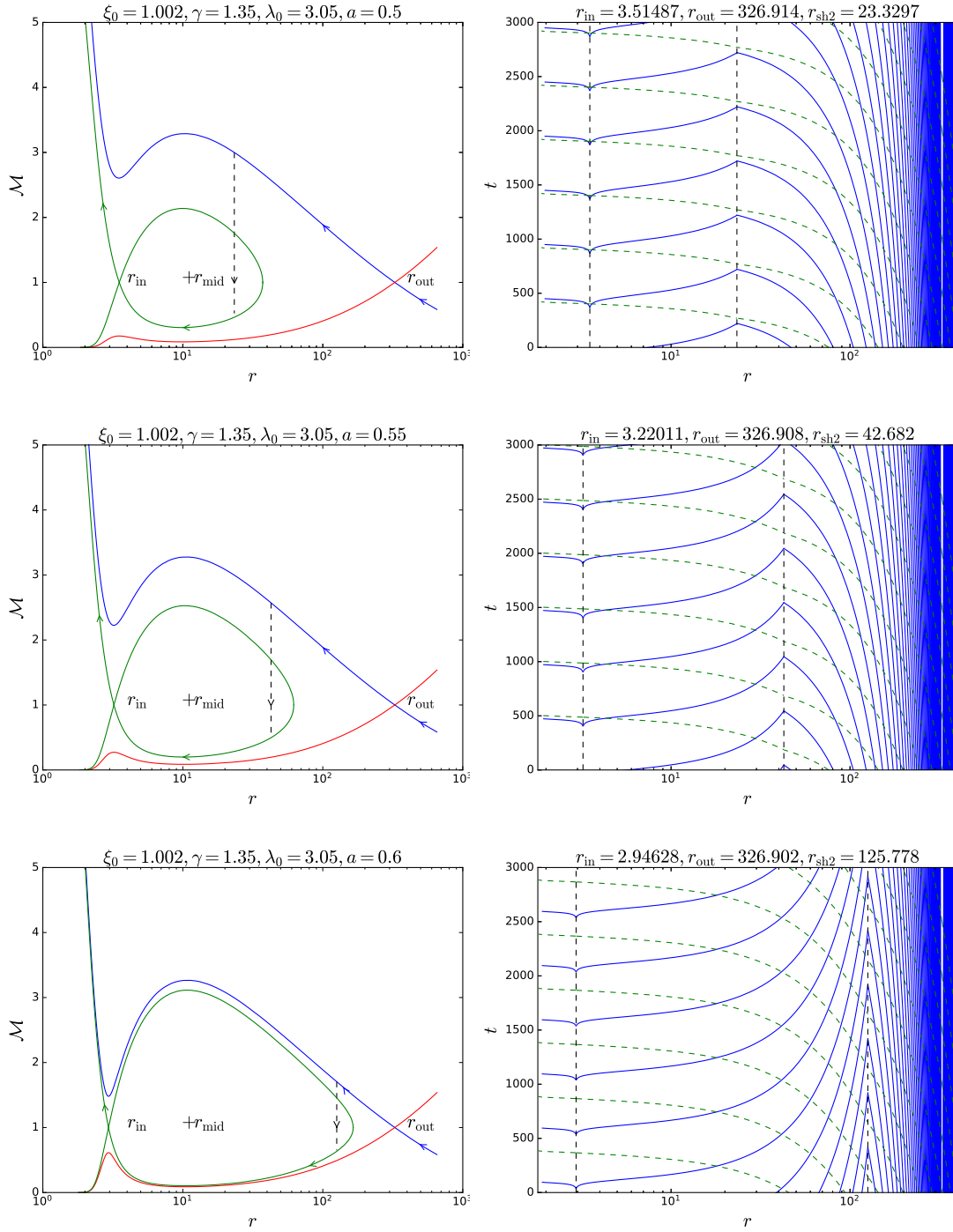


Figure 5.3: Mach number \mathcal{M} vs r plot (on the left) and the corresponding causal structure (on the right). The parameters [$\xi_0 = 1.002, \gamma = 1.35, \lambda_0 = 3.05$] are same where as the black hole spin is $a = 0.5$ (top panel), $a = 0.55$ (middle panel) and $a = 0.6$ (bottom panel). The solid lines represents $t_+(r)$ vs r lines and the dashed lines represents the $t_-(r)$ vs r lines.

5.7 Acoustic surface gravity

The acoustic metric given by Eq. (5.37) is independent of time t . Therefore we have the stationary Killing vector $\chi^\mu = \delta_t^\mu$ which is null on the horizon, i.e., $G_{\mu\nu}\chi^\mu\chi^\nu|_h = G_{tt}|_h = 0$. Thus, following the discussion on acoustic surface gravity in the previous chapters, the acoustic surface gravity is obtained to be given by

$$\kappa = \left| \kappa_0 \left(\frac{du_0}{dr} - \frac{dc_{s0}}{dr} \right) \right|_h \quad (5.60)$$

where

$$\kappa_0 = \frac{\sqrt{(g_{tt}g_{\phi\phi} + g_{\phi t}^2)(g_{\phi\phi} + 2\lambda_0 g_{\phi t} - \lambda_0^2 g_{tt})}}{(1 - c_{s0}^2)(g_{\phi\phi} + \lambda_0 g_{\phi t})\sqrt{g_{rr}}} \quad (5.61)$$

and the subscript ‘‘h’’, as mentioned earlier, denotes that the quantities have been evaluated at the acoustic horizon. On the equatorial plane ($\theta = \frac{\pi}{2}$) the metric elements are given by

$$g_{tt} = 1 - \frac{2}{r}, \quad g_{\phi t} = -\frac{2a}{r}, \quad g_{\phi\phi} = \frac{r^3 + a^2r + 2a^2}{r} \quad (5.62)$$

Thus κ_0 can be further written as

$$\kappa_0 = \frac{r\sqrt{(r^2 - 2r + a^2)(g_{\phi\phi} + 2\lambda_0 g_{\phi t} - \lambda_0^2 g_{tt})}}{(1 - c_{s0}^2)(r^3 + a^2r + 2a^2 - 2a\lambda_0)\sqrt{g_{rr}}} \quad (5.63)$$

The acoustic surface gravity is thus obtained as a function of the background metric elements and the stationary values of the accretion variables. The surface gravity depends explicitly on the black hole spin a .

5.8 Higher order perturbations and non-stationary flow

Up to now, we demonstrated that the emergence of acoustic spacetime as an analogue system is a natural outcome of the linear stability analysis of the relativistic black hole accretion. It is interesting to investigate whether, in general, the emergence of gravity like phenomena is a consequence of linear perturbation analysis

only, or any complex nonlinear perturbation (of any order) of fluid may lead to the emergent gravity phenomena. In other words, it is important to know how universal the analogue gravity phenomena is – whether black hole like spacetime can be generated by only one means (linear perturbation) or any kind of perturbation of general nature would lead to the construction of an analogue system. We have briefly discussed some recent works on this topic in the concluding chapter.

We have explicitly performed the perturbation analysis to make correspondence between the analogue gravity and the accretion astrophysics around black holes. Various properties of the corresponding analogue spacetime, however, can be studied by examining the stationary solutions as well, both for matter flow in spherically symmetric as well as for axially symmetric accretion ([13, 22, 52, 53, 74, 91–93]). It is to be noted that the correspondence between the analogue system and the accretion astrophysics can be established through the process of linear stability analysis of stationary integral accretion solutions. That means, only the steady state accretion has been considered. The body of literature in accretion astrophysics is huge and diverse, and hence there are several excellent works that exist in literature where complete time-dependent numerical simulation has been performed to study non-steady flow of hydrodynamic fluid including various kind of time variabilities ([58, 59, 94–123]).

6

Linear stability analysis of stationary accretion flow in the Kerr metric¹

For large scale astrophysical fluid flows, transient phenomena are not quite uncommon to take place. For accreting black hole systems, any conclusion drawn based on the results obtained using the integral stationary transonic solutions are thus reliable only if the accretion flow under considerations happens to be steady. One thus needs to ensure whether such steady flow is stable, at least within a reasonable astrophysical time scale. Such cross verification can be accomplished by perturbing the corresponding spacetime dependent governing equations (the Euler and the continuity equations for the present case) governing the flow and by investigating whether such perturbation converges (or, at least does not diverge) to ensure the stability of such transonic accretion. In Chap. 4 and Chap. 5, we performed linear perturbation of the accretion flow in the Kerr spacetime for isothermal and adiabatic equation of state, respectively. There, it was shown that the perturbation equation of the mass accretion rate (or that of the velocity potential or the relativistic Bernoulli's constant) has the form $\partial_\mu(f^{\mu\nu}\partial_\nu x_1) = 0$, where x_1 is the time-dependent fluctuation of Linear order around background value x_0 of the quantity x . $f^{\mu\nu}$ is a

¹This chapter is based on the works titled “*Relativistic sonic geometry for isothermal accretion in the Kerr metric*” by M. A. Shaikh [73] and “*Linear perturbations of low angular momentum accretion flow in the Kerr metric and the corresponding emergent gravity phenomena*” by M. A. Shaikh and T. K. Das [77].

2×2 symmetric matrix. In order to show that the stationary solutions are stable, one has to show that the amplitude of the fluctuation $x_1(t, r)$ does not diverge. Below, we seek to perform an analysis of the perturbation equation to understand the behaviour of the fluctuation and hence to check the stability of the stationary solutions.

First, we take the case of an isothermal accretion flow discussed in Chap. 4. We have derived the wave equation describing the propagation of the linear perturbation of velocity potential, mass accretion rate and the relativistic Bernoulli's constant in Eq. (4.23), (4.41) and (4.55), respectively. These equations can be further studied to understand the stability of the stationary accretion solutions. As the wave equations have similar forms, let us study one case, say for the velocity potential, and use the results accordingly for other cases.

Let us take the trial solution as

$$\psi_1(r, t) = P_\omega(r)e^{i\omega t}, \quad (6.1)$$

using this trial solution in the wave equation $\partial_\mu(f^{\mu\nu}\partial_\nu\psi_1) = 0$, where $f^{\mu\nu}$ is equal to $f_\psi^{\mu\nu}$ given by Eq. (4.24), provides

$$-\omega^2 f^{tt}P_\omega + i\omega[f^{tr}\partial_r P_\omega + \partial_r(f^{rt}P_\omega)] + \partial_r(f^{rr}\partial_r P_\omega) = 0. \quad (6.2)$$

6.1 Standing wave analysis

For standing wave to form there must be two nodes, one at some inner point r_1 and another at some outer point r_2 , such that at these two points we have $P_\omega(r_1) = 0 = P_\omega(r_2)$. In other words the perturbation must vanish for all times at two different radii. Multiplying the Eq. (6.2) by $P_\omega(r)$ and integrating the resulting equation between r_1 and r_2 gives

$$\omega^2 \int_{r_1}^{r_2} P_\omega^2 f^{tt} dr - i\omega \int_{r_1}^{r_2} \partial_r [f^{tr} P_\omega^2] dr - \int_{r_1}^{r_2} [P_\omega \partial_r (f^{rr} \partial_r P_\omega)] dr = 0. \quad (6.3)$$

The middle term in the above equation does not contribute as at the boundary r_1 and r_2 , P_ω vanishes. Integrating the last term by parts, the Eq. (6.3) can be written

as

$$\omega^2 \int_{r_1}^{r_2} P_\omega^2 f^{tt} dr + \int_{r_1}^{r_2} f^{rr} (\partial_r P_\omega)^2 dr = 0, \quad (6.4)$$

and thus we get

$$\omega^2 = - \frac{\int_{r_1}^{r_2} f^{rr} (\partial_r P_\omega)^2 dr}{\int_{r_1}^{r_2} f^{tt} P_\omega^2 dr}. \quad (6.5)$$

One thing to be noticed is that the inner boundary condition $P_\omega(r_1) = 0$ may be satisfied only if the accretor has a physical surface. In that case, the outer boundary could be located at the source from which the accreting material is coming and the inner boundary could be located at the surface of the accretor which is accreting the material (see Petterson [62]). Also, the flow should be continuous in the whole range in between these two boundary points. If the accretor is a neutron star then the surface (where the inner boundary with vanishing perturbation is to be located) should be separated from a possible supersonic region by a shock formation. This would imply that the solution, in that case, would not be continuous in the range between the outer boundary point and the surface of the neutron star and therefore standing wave analysis could not be performed. Also in the black hole accretion, the flow enters the horizon supersonically ([30, 60]) and there is no mechanism to make the perturbation vanish and therefore the above-mentioned requirements are not expected to be fulfilled and hence standing wave may not be formed in the context of black hole accretion. Also, the flow has to be subsonic for the whole range as transonic flow would contain a horizon from which the reflected wave cannot come out and superpose with the wave in the outer region. Therefore the standing wave analysis, which relies on the continuity of the solution, is restricted to only subsonic flows. However, provided that the flow is subsonic in a particular astrophysical system (e.g., in case of accretion onto a Newtonian star, depending on the location of the surface of the star, the accretion flow may be subsonic for all radial distance and hit the surface of the star subsonically [42]) we can study Eq. (6.5) to understand the nature of ω . The stability analysis for accretion onto a compact object in flat spacetime was done by Petterson *et al* [62] where the flow was considered to be subsonic.

From Eq. (4.24), f^{tt} for velocity potential is given by

$$f^{tt} = -\frac{\sqrt{-\tilde{g}}H_0}{\rho_0^{c_s^2-1}} \left[-g^{tt} + (v_0^t)^2 \left(1 - \frac{1}{c_s^2} \right) \right]. \quad (6.6)$$

as $g^{tt} > 0$ and $c_s^2 < 1$ we find that $f^{tt} > 0$. Now f^{rr} is given by

$$f^{rr} = -\frac{\sqrt{-\tilde{g}}H_0}{\rho_0^{c_s^2-1}} \left[g^{rr} + (v_0^r)^2 \left(1 - \frac{1}{c_s^2} \right) \right]. \quad (6.7)$$

Using Eq. (4.5), the terms inside the square bracket can be written as

$$g^{rr} + \frac{u_0^2}{g_{rr}(1-u_0^2)} \left(1 - \frac{1}{c_s^2} \right) \quad (6.8)$$

$$= \frac{(1-u_0^2) + u_0^2 \left(1 - \frac{1}{c_s^2} \right)}{g_{rr}(1-u_0^2)} \quad (6.9)$$

$$= \frac{\left(1 - \frac{u_0^2}{c_s^2} \right)}{g_{rr}(1-u_0^2)} \quad (6.10)$$

$$> 0. \quad (6.11)$$

Thus $f^{rr} < 0$ and hence $\omega^2 > 0$. Therefore ω has two real roots and the trial solution is oscillatory and the stationary accretion solution is stable against the assumed perturbations. We have used the fact that the flow is subsonic to get $f^{rr} < 0$. Same result is also applicable for the relativistic Bernoulli's constant. It is easy to show that the conclusion also holds for the mass accretion rate.

6.2 Traveling wave analysis

Following Petterson *et al* [62], we study the traveling waves whose wavelengths are small compared to the smallest length scale in the system. In case of black hole accretion, this may be the radius of the event horizon of the black hole. Therefore, for such wave, the frequency is large and hence the trial solution may be taken as the power series of the form

$$P_\omega(r) = \exp \left[\sum_{n=-1}^{\infty} \frac{k_n(r)}{\omega^n} \right]. \quad (6.12)$$

We substitute the trail solution in Eq. (6.2) and find out leading order terms by equating the coefficients of individual power of ω to zero. Thus we get

$$\text{coefficient of } \omega^2 : f^{rr}(\partial_r k_{-1})^2 + 2if^{tr}\partial_r k_{-1} - f^{tt} = 0, \quad (6.13)$$

$$\begin{aligned} \text{coefficient of } \omega : f^{rr}[\partial_r^2 k_{-1} + 2\partial_r k_{-1}k_0] + i[2f^{tr}\partial_r k_0 \\ + \partial_r f^{tr}] + \partial_r f^{rr}\partial_r k_{-1} = 0, \end{aligned} \quad (6.14)$$

$$\begin{aligned} \text{coefficient of } \omega^0 : f^{rr}[\partial_r^2 k_0 + 2\partial_r k_{-1}\partial_r k_1 + (\partial_r k_0)^2] \\ + \partial_r f^{rr}\partial_r k_0 + 2if^{tr}\partial_r k_1 = 0. \end{aligned} \quad (6.15)$$

Eq. (6.13) gives

$$k_{-1}(r) = i \int \frac{-f^{tr} \pm \sqrt{(f^{tr})^2 - f^{tt}f^{rr}}}{f^{rr}} dr \quad (6.16)$$

using $k_{-1}(r)$ from Eq. (6.16) in Eq. (6.14) gives

$$k_0(r) = -\frac{1}{2} \ln[\sqrt{(f^{tr})^2 - f^{tt}f^{rr}}] + \text{constatnt} \quad (6.17)$$

and using Eq. (6.16) and (6.17) in Eq. (6.15) gives

$$k_1(r) = \pm \frac{i}{2} \int \frac{\partial_r(f^{rr}\partial_r k_0) + f^{rr}(\partial_r k_0)^2}{\sqrt{(f^{tr})^2 - f^{tt}f^{rr}}} dr \quad (6.18)$$

Now for the case velocity potential (Eq. (4.24)) or relativistic Bernoulli's constant ((Eq. (4.56)))

$$\det f^{\mu\nu} = f^{tt}f^{rr} - (f^{rt})^2 = \left(\frac{\sqrt{-\tilde{g}}H_0}{\rho_0^{c_s^2-1}} \right)^2 \mathcal{F} \quad (6.19)$$

and for the case of mass accretion rate (Eq. (4.43))

$$\det f^{\mu\nu} = f^{tt}f^{rr} - (f^{rt})^2 = \left(\frac{g_{rr}v_0^r c_s^2}{v_0^t v_{t0} \tilde{\Lambda}} \right)^2 \mathcal{F}, \quad (6.20)$$

where v_{t0} is the stationary value of v_t given by Eq. (4.7) and v_0^r and v_0^t are stationary values of v^r and v^t given by Eq. (4.5) and (4.6), respectively, and

$$\mathcal{F} = [-g^{tt}g^{rr} + (1 - \frac{1}{c_s^2})(-g^{tt}(v_0^r)^2 + g^{rr}(v_0^t)^2)]. \quad (6.21)$$

We can further express \mathcal{F} in terms of λ_0, u_0 and the background metric elements as

$$\mathcal{F} = -\frac{g_{\phi\phi}}{g_{rr}(g_{\phi\phi}g_{tt} + g_{\phi t}^2)} \left[1 + \frac{(1 - c_s^2)}{c_s^2(1 - u_0^2)} \left(\frac{(1 + \lambda_0 \frac{g_{\phi t}}{g_{\phi\phi}})^2}{(1 + 2\lambda_0 \frac{g_{\phi t}}{g_{\phi\phi}} - \lambda_0^2 \frac{g_{tt}}{g_{\phi\phi}})} - u_0^2 \right) \right]. \quad (6.22)$$

\mathcal{F} is negative everywhere. This can be understood in the following way: The expression of v^t from Eq. (4.6) requires $g_{\phi\phi} + 2\lambda_0 g_{\phi t} - \lambda_0^2 g_{tt} > 0$ in order that v^t is real. Which can be rewritten as

$$\left(1 + \lambda_0 \frac{g_{\phi t}}{g_{\phi\phi}}\right)^2 - \lambda_0^2 \left(\frac{g_{\phi t}^2}{g_{\phi\phi}^2} + \frac{g_{tt}}{g_{\phi\phi}}\right) > 0, \quad (6.23)$$

or

$$0 < 1 - \lambda_0^2 \left[\left(\frac{g_{\phi t}^2}{g_{\phi\phi}^2} + \frac{g_{tt}}{g_{\phi\phi}}\right) / \left(1 + \lambda_0 \frac{g_{\phi t}}{g_{\phi\phi}}\right)^2\right] < 1. \quad (6.24)$$

Therefore

$$\frac{\left(1 + \lambda_0 \frac{g_{\phi t}}{g_{\phi\phi}}\right)^2}{\left(1 + 2\lambda_0 \frac{g_{\phi t}}{g_{\phi\phi}} - \lambda_0^2 \frac{g_{tt}}{g_{\phi\phi}}\right)} = \frac{1}{1 - \lambda_0^2 \left[\left(\frac{g_{\phi t}^2}{g_{\phi\phi}^2} + \frac{g_{tt}}{g_{\phi\phi}}\right) / \left(1 + \lambda_0 \frac{g_{\phi t}}{g_{\phi\phi}}\right)^2\right]} > 1 \quad (6.25)$$

using the fact that $u_0^2 < 1$ and $c_s^2 < 1$ it is easy to see that \mathcal{F} is negative everywhere. Thus $k_{-1}(r)$ and $k_1(r)$ are purely imaginary. Therefore the leading contribution to the amplitude of the wave comes from $k_0(r)$. Thus considering the first three terms in the expansion in Eq. (6.12) the amplitude of the wave can be approximated as

$$|\psi_1| = |\xi_1| \approx \left[\frac{\rho_0^{2c_s^2-2}}{\tilde{g}H_0^2\mathcal{F}}\right]^{\frac{1}{4}}, \quad |\Psi_1| \approx \left[\left(\frac{v_0^t v_{t0} \tilde{\Lambda}}{g_{rr} v_0^r c_s^2}\right)^2 \frac{1}{-\mathcal{F}}\right]^{\frac{1}{4}} \quad (6.26)$$

The trial solution in Eq. (6.12) with the frequency $\omega \gg 1$ ensures that contribution from the higher order terms will be very small. The amplitude given by Eq. (6.26) is bounded for finite values of the stationary variables and the solution is therefore expected to be stable.

A robust way to ensure that the trial solution does not diverge and is stable, is to check whether the power series in Eq. (6.12) converge or not, i.e., we have to show $|k_n/\omega^n| \gg |k_{n+1}/\omega^{n+1}|$. As the frequency is very large $\omega \gg 1$, the contributions from higher order terms are very small. Thus it should suffice to show that $|\omega k_{-1}| \gg |k_0| \gg |k_1/\omega|$. k_{-1}, k_0, k_1 are complicated functions of the accretion variables and thus it is not possible to have an analytic form. However, we can find the spatial dependence at large distance $r \rightarrow \infty$ where the spacetime is effectively Newtonian. From the constancy of the mass accretion rate we have $v_0^r \propto 1/(\rho_0 r^2)$. At the asymptotic limit ρ_0 approaches its constant ambient value ρ_∞ and hence at $r \rightarrow \infty$,

$v_{0\infty}^r \propto 1/r^2$. The sound speed is constant for isothermal flow. $v_0^t \sim 1$ and $v_{t0} \sim -1$. Also $\tilde{\Lambda}_\infty \propto (v_0^r)^2$. We remember that for conical flow $H_0 = \text{constant}$ and $\tilde{g} = -r^4$ on the equatorial plane. Thus, In this asymptotic limit, for all the three perturbation cases, we have

$$f^{tt} \sim r^2, \quad f^{rr} \sim r^2, \quad f^{tr} \sim r^0, \quad (f^{rt})^2 - f^{tt}f^{rr} \sim r^4 \quad (6.27)$$

which gives $k_{-1} \sim r$, $k_0 \sim \ln r$ and $k_1 \sim 1/r$. Therefore, the sequence converges in the leading order at least at large r .

The perturbation equation and the $f^{\mu\nu}$ elements has exactly the same form for an adiabatic flow (which we discussed in Chap. 5 considering only the case of mass accretion rate) as those for an isothermal flow. Therefore, it is trivial to repeat the same analysis for an adiabatic accretion flow in the Kerr metric which gives the same result as discussed above.

We followed a linear perturbation scheme to obtain the perturbation equation as well as the emergent relativistic acoustic geometry embedded within the accretion flow in Chap. 4 and 5. In this chapter we used those perturbation equations to check whether the background steady state of such flow is stable. This implies that the emergent gravity phenomena are a natural outcome of the linear stability analysis of transonic accretion.

In our present work, we limit our stability analysis procedure within a purely analytical framework and did not opt for any numerical studies in this aspect. There are, however, a number of works exist in the literature (for some recent works, see [124–127]) which studies, fully numerically, the stability analysis of spherically or axially symmetric black hole accretion in two or three dimensions. We, however, did not concentrate on such approach since our main motivation was to explore how the emergent gravity phenomena can be observed through the stability analysis of steady-state solutions of hydrodynamic accretion.

7

Effective sound speed in relativistic accretion discs around Schwarzschild black holes¹

7.1 Introduction

Accretion flows onto astrophysical black holes are supposed to exhibit transonic properties in general [30, 60, 61]. For low angular momentum, practically inviscid, axially symmetric accretion, sonic transition may take place at more than one locations on the equatorial plane of the disc and such multi-transonic flow may accommodate steady, standing shock transition as discussed in Chap. 3, 4 and 5 [30, 32–59, 129]. Properties of the shocked multi-transonic accretion are usually studied for three different geometrical configurations of accreting matter. These geometric configurations have been discussed in the previous chapters (also see, e.g, [41, 92, 93, 130, 131] for the details of such geometric configurations.)

Among those three, one particular configuration, namely the accretion in hydrostatic equilibrium along the vertical direction, exhibits certain peculiar features. For such flow geometry, the Mach number at the critical points of the flow may not

¹This chapter is based on the work titled “*Effective sound speed in relativistic accretion discs around Schwarzschild black holes*” by M. A. Shaikh, S. Maity, S. Nag and T. K. Das [128].

become unity [36, 48, 53, 56, 93, 132] and hence the critical points may not be considered as sonic points. For accretion under the influence of various post-Newtonian pseudo-Schwarzschild or pseudo-Kerr black hole potentials, critical points for polytropic flow are formed at a location different from that of sonic points. For isothermal accretion under the influence of post-Newtonian black hole potentials, critical points and sonic points are, however, isomorphic. The amount of deviation of the value of the Mach number from unity, remains the same for both the saddle type sonic points for multi-transonic shocked polytropic flows under the influence of post-Newtonian potentials, and such deviations depends only on γ , where γ is the ratio of the specific heats evaluated at constant pressure and at constant volume, respectively. For general relativistic accretion in the Schwarzschild or the Kerr metric, even for the isothermal flow the sonic point and the critical point can be located at two different radial coordinates on the equatorial plane as measured from center of the accretor. The amount of deviation of the value of the Mach number (evaluated at the critical point) from unity, may be found to be different for two different sonic points for multi-transonic flows.

Such non-isomorphism of critical points and sonic points, i.e, the fact that their locations may differ, may introduce various complexities while dealing with the multi transonic flow profile and related astrophysical phenomena. While plotting the stationary transonic integral solutions onto the Mach number versus radial distance phase portrait, phase orbits corresponding to the inwardly directed accretion and outward directed wind solutions intersect at the critical point. If the location of the critical point and its corresponding sonic point form at different locations, the subsonic and supersonic branches are found not to be identical with two branches of the phase orbits located at two sides of the critical points.

The critical points are obtained using the critical point analysis method – a technique borrowed from the dynamical systems theory. For many of the accretion scenarios, it may be possible to locate the critical points analytically (see [133] and references therein). Using certain eigenvalue techniques, one becomes able to gain, completely analytically, qualitative ideas about the phase portrait of the transonic

flow structure close to the critical point [134–138]. If a sonic point is located at a distance different from that of the critical point, one needs to numerically integrate the flow equations, starting from the critical point, up to that particular point where the Mach number becomes unity. The elegance of the analytical eigenvalue-based methods is thus lost if a critical point and a sonic point are different. One needs to take recourse only to the complicated numerical techniques to have ideas about the subsonic and supersonic branches in the phase plot.

Accreting black hole systems have been studied from the perspective of emergent gravity phenomena in the previous chapters for accretion in the Schwarzschild and the Kerr metric to understand how such systems can be perceived as an interesting example of classical analogue model naturally found in the universe. Other studies could be also found, for example, in [13, 22, 52, 53, 64, 73, 74, 77, 91–93, 139]. For such work also, the non-isomorphism between the critical and the sonic point may enhance the complexity involved with the solution scheme. The Mach number at the acoustic horizons should necessarily be unity, which requires the introduction of the numerical solution scheme to obtain the integral stationary flow solutions. Had it been the situation that the Mach number would be unity at the critical point an elegant analytical method could perhaps be employed to compute the value of acoustic surface gravity and related quantities, evaluated at sonic horizons.

The aforementioned discussions demand that it is imperative to introduce certain effective sound speed for which the effective Mach number evaluated at the critical points would be unity and the critical points and sonic points will be isomorphic. This will greatly reduce the complexity involved in employing numerical solution schemes for construction of the phase portrait and many other quantities relevant to the astrophysics of transonic black hole accretion and analogue gravity phenomena. The concept of effective sound speed has been discussed in the literature for accretion flows under the influence of post-Newtonian pseudo-Schwarzschild black hole potentials [51, 132]. In the present work, we will provide a novel perturbative approach to introduce the concept of effective dynamical sound speeds embedded within the general relativistic, axially symmetric accretion flow maintained in the

hydrostatic equilibrium along the vertical direction.

We consider three different expressions for disc thickness as proposed by Novikov & Thorne [70], by Riffert & Herold [71] and by Abramowicz *et al* [72] to describe the accretion disc in hydrostatic equilibrium along the vertical direction in the Schwarzschild metric. For each of these three disc heights, we construct the time-independent Euler and the continuity equations. We solve such equations to find the corresponding first integrals of motion. For polytropic accretion, such first integrals are the total specific energy and the mass accretion rate Ψ_0 . The polytropic accretion is parametrized by the specific energy ξ_0^{ad} , the specific angular momentum λ_0 , and the adiabatic index γ . A three-parameter set $[\xi_0^{\text{ad}}, \lambda_0, \gamma]$ where $\xi_0^{\text{ad}}, \lambda_0, \gamma$ are all constants, is taken to describe the flow and to solve the corresponding flow equations. For the isothermal accretion, two first integrals of motion are quasi-specific energy ξ_0^{iso} (which is the integral solution of the time-independent part of the relativistic Euler equation) and the mass accretion rate Ψ_0 . An isothermal flow is parametrized by $[T, \lambda_0]$, where T and λ_0 are the conserved flow temperature and the constant specific angular momentum, respectively.

For all these three disc heights, we calculate for polytropic flow, the space gradient of the dynamical velocity and stationary sound speed, i.e., u'_0 and c'_{s0} , respectively. The ‘dash’ represents single derivative with respect to the radial coordinate r , as usual. From the expressions for u'_0 and c'_{s0} , we evaluate the critical point conditions and compute the value of Mach number at the critical point. We show that the value of Mach number at the critical point is not unity and write down what would be the effective sound speed for which the Mach number at the critical point would have resumed the value unity.

We then linear perturb the full time-dependent Euler and continuity equation following the same method as described in the previous chapters. Such perturbations lead to the formation of the acoustic spacetime metric. The acoustic metric governs the dynamics of propagation of linear perturbation inside the background fluid (the fluid which composes the accretion disc). We then construct the corresponding wave equation for the propagation of such linear perturbation and calculate the speed of

propagation of linear acoustic perturbation. We finally show that if we substitute the usual stationary sound speed c_s by the suitable form of the speed of propagation of linear acoustic perturbation, then the Mach number at the critical points becomes unity. Hence we establish that certain representation of the ‘dynamical sound speed’ (the speed of propagation of linear acoustic perturbation obtained through the dynamical stability analysis of the full spacetime-dependent fluid equations) should actually be considered as the effective speed of sound propagation along the equatorial plane of the black hole accretion disc. If one replaces the usual static sound speed by the aforementioned effective dynamical sound speed, the critical points always coincide with the sonic points and all the complexities originating from the non-isomorphism of the critical and the sonic points get resolved.

For isothermal flow, we perform the same operation for finding the Mach number at the critical points corresponding to the three different disc heights. We find that unlike the adiabatic accretion for which the accretion disc characterized by all three disc heights would produce a mismatch between the critical and the sonic points, for isothermal flow, accretion disc characterized by only one expression of disc height (proposed by Abramowicz *et al* [72]) produces the non-isomorphism between the critical and the sonic points. For accretion characterized by the other two expressions of disc heights (as proposed by Novikov & Thorne and Riffert & Herold [70, 71]), the location of the critical and the sonic points are found to be the same.

In section 7.2, we present the basic equations governing the general relativistic accretion flow and introduce relevant thermodynamic quantities. In section 7.3, we find out the conditions for critical points for the three different disc models of vertical equilibrium for adiabatic as well as the isothermal equation of state. In section 7.4, we derive the acoustic spacetime metric by linear perturbing the accretion flow equations. Finally in section 7.5, using the acoustic spacetime metric we obtain the effective speed, c_{s0}^{eff} , of the propagation of the acoustic perturbations. This suggests that at the critical point one always have $u_0^2 = c_{s0}^{\text{eff}2}$.

7.2 Governing equations

We consider an inviscid axially symmetric irrotational accretion flow accreting onto a Schwarzschild black hole. The background spacetime metric is given by Eq. (3.1) with the metric elements given by Eq. (3.2). The energy momentum tensor for a perfect fluid is given by Eq. (3.3). The equation of state for adiabatic flow is given by $p = k\rho^\gamma$ where k is a constant. Whereas for isothermal case $p \propto \rho$. The sound speed for adiabatic flow (isoentropic flow) is given by Eq. (5.3) and the sound speed for isothermal flow is defined by Eq. (3.8).

The mass conservation equation and the energy-momentum conservation equations are given by Eq. (3.4) and Eq. (3.5), respectively. Using the expression for the sound speed, the energy momentum conservation equation can be written in the following form

$$v^\mu \nabla_\mu v^\nu + \frac{c_s^2}{\rho} (v^\mu v^\nu + g^{\mu\nu}) \partial_\mu \rho = 0, \quad (7.1)$$

where c_s for adiabatic case and isothermal case are given by Eq. (5.3) and Eq. (3.8), respectively.

7.3 Accretion disc models and critical points

The procedure to find the critical points have been discussed in Chap. 3, 4 and 5. Here we provide a brief description of the method. To find the critical points of the accretion flow, we have to find the expression of the gradient of the advective velocity u_0 , i.e., the expression of u'_0 for stationary accretion flow. In order to do that, we need two constant integrals of the stationary flow. The first one comes from the continuity equation and the second one comes from the momentum conservation equation. For convenience, one then performs a vertical averaging of the flow equations by integrating over θ and the resultant equation is described by the flow variables defined on the equatorial plane ($\theta = \pi/2$). In addition one also integrates over ϕ which gives a factor of 2π due to the axial symmetry of the flow. Thus in case of stationary (t -independent) and axially symmetric (ϕ -independent)

flow with averaged $v^\theta \sim 0$, the continuity equation can be written as

$$\frac{\partial}{\partial r}(4\pi H_\theta \sqrt{-\tilde{g}} \rho_0 v_0^r) = 0, \quad (7.2)$$

where, as before, the factor H_θ arises due to the vertical averaging and is the local angular scale of flow. Remember that the actual local flow thickness $H(r)$ is related to the angular scale of the flow H_θ as $H_\theta = H(r)/r$, where r is the radial distance along the equatorial plane from the center of the disc. \tilde{g} is the value of the determinant of the metric $g_{\mu\nu}$ on the equatorial plane, $\tilde{g} = \det(g_{\mu\nu})|_{\theta=\pi/2} = -r^4$. The equation (7.2) gives the mass accretion rate Ψ_0 as

$$\Psi_0 = 4\pi \sqrt{-g} H_\theta \rho_0 v_0^r = 4\pi H(r) r \rho_0 v_0^r. \quad (7.3)$$

The t, r component of the four velocity, v^t, v^r , are given in terms of u_0 and $\lambda_0 = -v_{\phi 0}/v_{t0}$ in Eq. (3.116) and (3.117), respectively. λ_0 is the specific angular momentum of the fluid and is a constant for stationary flow. Thus, using $g_{rr} = r^2/\Delta$ with $\Delta = r(r-2)$, Ψ_0 can be written as

$$\Psi_0 = 4\pi H(r) \Delta^{1/2} \rho_0 \frac{u_0}{\sqrt{1-u_0^2}}. \quad (7.4)$$

For adiabatic flow, we define a new quantity $\dot{\Xi}$ from Ψ_0 by multiplying it with $(\gamma k)^{\frac{1}{\gamma-1}}$. $\dot{\Xi}$ is a measure of entropy accretion rate and typically called as the entropy accretion rate. Expressing ρ_0 in terms of γ, k and c_{s0} finally gives

$$\dot{\Xi} = \left(\frac{c_{s0}^2}{1 - n c_{s0}^2} \right)^n 4\pi H(r) \Delta^{1/2} \frac{u_0}{\sqrt{1-u_0^2}} = \text{constant}, \quad (7.5)$$

where we have used $n = 1/(\gamma-1)$. The second conserved quantity can be obtained from the time-component of the relativistic Euler equation (7.1) which for stationary adiabatic case gives

$$\xi_0^{\text{ad}} = -h_0 v_{t0} = \text{constant}, \quad (7.6)$$

and for stationary isothermal case gives

$$\xi_0^{\text{iso}} = -\rho_0 c_{s0}^2 v_{t0} = \text{constant}, \quad (7.7)$$

where c_{s0} is a constant for isothermal flow. v_{t0} can be further expressed in terms of u_0 as

$$v_{t0} = -\sqrt{\frac{\Delta}{B(1-u_0^2)}}, \quad (7.8)$$

where $B = g_{\phi\phi} - \lambda_0^2 g_{tt}$. Thus

$$\xi_0^{\text{ad}} = \frac{1}{1-nc_{s0}^2} \sqrt{\frac{\Delta}{B(1-u_0^2)}}, \quad (7.9)$$

and

$$\xi_0^{\text{iso}} = \rho_0^{c_{s0}^2} \sqrt{\frac{\Delta}{B(1-u_0^2)}}. \quad (7.10)$$

For adiabatic flow, the expression for u'_0 can be derived by using the expression of the two quantities, $\dot{\Xi}$ and ξ_0^{ad} given by equation (7.5) and (7.9), respectively. Taking logarithmic derivative of both sides of equation (7.9) gives the gradient of sound speed as

$$c_{s0}'|^{\text{ad}} = -\frac{1-nc_{s0}^2}{2nc_{s0}} \left[\frac{u_0}{1-u_0^2} \frac{du_0}{dr} + \frac{1}{2} \left(\frac{\Delta'}{\Delta} - \frac{B'}{B} \right) \right]. \quad (7.11)$$

For isothermal flow, we make use of equation (7.4) and (7.10). Taking logarithmic derivative of the equation (7.10) we can find ρ'_0/ρ_0 as

$$\frac{\rho'_0}{\rho_0} \Big|_{\text{iso}} = -\frac{1}{c_{s0}^2} \left[\frac{u_0}{1-u_0^2} \frac{du_0}{dr} + \frac{1}{2} \left(\frac{\Delta'}{\Delta} - \frac{B'}{B} \right) \right]. \quad (7.12)$$

Below we discuss different models of vertical structure of accretion disc and the corresponding critical point conditions for stationary accretion flow in such model of accretion disc.

7.3.1 Models of accretion disc under vertical equilibrium

In the beginning of the current section we mentioned that for accretion disc flow, in order for the governing equation to be written in terms of the variables evaluated at the equatorial plane, the equations are vertically averaged which introduces the disc height $H(r)$ or equivalently the local angular scale of the flow H_θ in the resulting

equations. Thus in order to solve for the accretion flow profile, we need to have an expression for the local thickness of the accretion disc. In our present work, we are concerned with accretion disc which is under hydrostatic equilibrium in the vertical direction. In Newtonian accretion flow, for accretion disc under vertical equilibrium, the disc height calculation is a rather straightforward work of balancing the pressure gradient in the vertical direction with the component of the Newtonian gravitational force in the vertical direction.

In case of a general relativistic accretion disc around a black hole, one needs to incorporate the general relativistic effects on the balancing of pressure gradient and gravitational force. Historically there have been three such general relativistic models of disc height which incorporated the general relativistic effects. The first of such prescriptions of disc height was given by Novikov & Thorne [70]. In deriving the expression for the disc height, [70] replaced the Newtonian formula for acceleration by the vertical acceleration which is calculated from the Riemann tensor R_{030}^3 given in [82] and transformed to the local tetrad. A relatively improved expression was given by Riffert & Herold [71] who derived the gravity-pressure balance equation itself by imposing two particular orthonormality condition on the vertical component of the Euler equation. However, both the disc models of [70] and that of [71] do not apply below $r = 3$ (in the units we are working with) where the disc height becomes zero. Thus the disc height expressions are not valid up to the horizon $r = 2$ (for a Schwarzschild black hole). [72] provided an expression for the disc height which is regular up to the horizon. Abramowicz *et al* [72] derived the equation directly from the relativistic Euler equation and no additional simplifying assumptions were made.

In the following, we work with the above mentioned three prescriptions of disc heights for general relativistic accretion disc under hydrostatic equilibrium in the vertical direction around Schwarzschild black holes.

7.3.2 Novikov-Thorne (NT)

The expression for the disc height as derived by [70] for accretion disc around Schwarzschild black hole could be given by

$$H_{\text{NT}}(r) = \sqrt{\frac{p_0}{\rho_0}} r^{3/2} \sqrt{\frac{r-3}{r-2}}. \quad (7.13)$$

7.3.2.1 Adiabatic case

For adiabatic equation of state, p_0/ρ_0 can be written as

$$\frac{p_0}{\rho_0} = \left(\frac{n}{n+1}\right) \left(\frac{c_{s0}^2}{1-nc_{s0}^2}\right). \quad (7.14)$$

Thus we can write $H(r)$ as

$$H_{\text{NT}}(r) = \left(\frac{n}{n+1}\right)^{1/2} \left(\frac{c_{s0}^2}{1-nc_{s0}^2}\right)^{1/2} f_{\text{NT}}(r), \quad (7.15)$$

where $f_{\text{NT}}(r) = r^{3/2} \sqrt{(r-3)/(r-2)}$. Using this expression of $H(r)$, $\dot{\Xi}$ for this model can be written as

$$\dot{\Xi}_{\text{NT}} = \sqrt{\frac{n}{n+1}} \left(\frac{c_{s0}^2}{1-nc_{s0}^2}\right)^{\frac{2n+1}{2}} 4\pi\Delta^{1/2} \frac{u_0}{\sqrt{1-u_0^2}} f_{\text{NT}}(r). \quad (7.16)$$

Taking logarithmic derivative of both sides of the above equation and substituting c'_{s0} using Eq. (7.11) gives

$$u'_0|_{\text{NT}}^{\text{ad}} = \frac{u_0(1-u_0^2) \left[\frac{2n}{2n+1} c_{s0}^2 \left(\frac{\Delta'}{2\Delta} + \frac{f'_{\text{NT}}}{f_{\text{NT}}} \right) + \frac{1}{2} \left(\frac{B'}{B} - \frac{\Delta'}{\Delta} \right) \right]}{u_0^2 - \frac{c_{s0}^2}{1+\frac{1}{2n}}} = \frac{N_{\text{NT}}^{\text{ad}}}{D_{\text{NT}}^{\text{ad}}}. \quad (7.17)$$

The critical points are obtained from the condition $D_{\text{NT}}^{\text{ad}} = 0$ which gives $u_0^2|_c = c_{s0}^2/(1+(1/2n))|_c$ or

$$u_0^2|_c = \frac{c_{s0}^2|_c}{1+\beta}, \quad \text{where } \beta = \frac{\gamma-1}{2}. \quad (7.18)$$

7.3.2.2 Isothermal case

For isothermal equation of state, $p = k_0\rho$ (k_0 is a constant), the disc height is given by

$$H_{\text{NT}}^{\text{iso}} = \sqrt{k_0} r^{3/2} \sqrt{\frac{r-3}{r-2}} = \sqrt{k_0} f_{\text{NT}}(r). \quad (7.19)$$

Therefore, the mass accretion rate is given by

$$\Psi_{\text{NT}}^{\text{iso}} = 4\pi\sqrt{k_0}\Delta^{1/2}\rho_0\frac{u_0}{\sqrt{1-u_0^2}}f_{\text{NT}}(r). \quad (7.20)$$

Taking logarithmic derivative of the above equation with respect to r and substituting ρ'_0/ρ_0 using equation (7.12) gives

$$u'_0|_{\text{NT}}^{\text{iso}} = \frac{u_0(1-u_0^2)\left[c_{s0}^2\left(\frac{f'_{\text{NT}}}{f_{\text{NT}}} + \frac{\Delta'}{2\Delta}\right) + \frac{1}{2}\left(\frac{B'}{B} - \frac{\Delta'}{\Delta}\right)\right]}{u_0^2 - c_{s0}^2} = \frac{N_{\text{NT}}^{\text{iso}}}{D_{\text{NT}}^{\text{iso}}}. \quad (7.21)$$

Thus critical points are given by the condition $D_{\text{NT}}^{\text{iso}} = 0$, which gives

$$u_0^2|_c = c_{s0}^2|_c. \quad (7.22)$$

7.3.3 Riffert-Herold (RH)

RH [71] improved the result obtained by NT. The modified expression for the disc height is given by

$$H_{\text{RH}}(r) = 2\sqrt{\frac{p}{\rho}}r^{3/2}\sqrt{\frac{r-3}{r}}. \quad (7.23)$$

7.3.3.1 Adiabatic case

$$H_{\text{RH}}(r) = \left(\frac{n}{n+1}\right)^{1/2} \left(\frac{c_{s0}^2}{1-nc_{s0}^2}\right)^{1/2} f_{\text{RH}}(r), \quad (7.24)$$

where $f_{\text{RH}} = 2r\sqrt{r-3}$. $H_{\text{RH}}(r)$ has the same form as that of H_{NT} . Therefore, the expression for u'_0 can be derived similarly which gives

$$u'_0|_{\text{RH}}^{\text{ad}} = \frac{u_0(1-u_0^2)\left[\frac{2n}{2n+1}c_{s0}^2\left(\frac{\Delta'}{2\Delta} + \frac{f'_{\text{RH}}}{f_{\text{RH}}}\right) + \frac{1}{2}\left(\frac{B'}{B} - \frac{\Delta'}{\Delta}\right)\right]}{u_0^2 - \frac{c_{s0}^2}{1+\frac{1}{2n}}} = \frac{N_{\text{RH}}^{\text{ad}}}{D_{\text{RH}}^{\text{ad}}}. \quad (7.25)$$

Setting $D_{\text{RH}}^{\text{ad}} = 0$ gives the critical point condition as

$$u_0^2|_c = \frac{c_{s0}^2|_c}{1+\beta}, \quad \text{where } \beta = \frac{\gamma-1}{2}. \quad (7.26)$$

7.3.3.2 Isothermal case

Following the same procedure as given in section 7.3.2.2, u'_0 for isothermal equation of state would be given by

$$u'_0|_{\text{RH}}^{\text{iso}} = \frac{u_0(1 - u_0^2) \left[c_{s0}^2 \left(\frac{f'_{\text{RH}}}{f_{\text{RH}}} + \frac{\Delta'}{2\Delta} \right) + \frac{1}{2} \left(\frac{B'}{B} - \frac{\Delta'}{\Delta} \right) \right]}{u_0^2 - c_{s0}^2} = \frac{N_{\text{RH}}^{\text{iso}}}{D_{\text{RH}}^{\text{iso}}}, \quad (7.27)$$

which gives the critical point condition as $u_0^2 = c_{s0}^2$.

7.3.4 Abramowicz-Lanza-Percival (ALP)

The expression for the disc height as given by [72] can be written as

$$H(r) = \sqrt{2}r^2 \sqrt{\frac{p}{\rho}} \frac{1}{|v_{\phi 0}|} = \sqrt{\frac{2}{\alpha}} \sqrt{\frac{p}{\rho}} \frac{r^2}{\lambda_0} \sqrt{1 - u_0^2}, \quad (7.28)$$

where we have used $v_{\phi 0} = -\lambda_0 v_{t0}$.

7.3.4.1 Adiabatic case

Using the above expression for the disc height the entropy accretion rate can be written as

$$\dot{\Xi}_{\text{ALP}} = \sqrt{\frac{n}{n+1}} \left(\frac{c_{s0}^2}{1 - nc_{s0}^2} \right)^{\frac{2n+1}{2}} \frac{r^2}{\lambda_0} 4\pi \sqrt{2B} u_0. \quad (7.29)$$

Taking logarithmic derivative of the above equation with respect to r and substituting c'_{s0} using equation (7.11) gives the expression for the gradient of advective velocity as

$$u'_0|_{\text{ALP}}^{\text{ad}} = \frac{c_{s0}^2 u_0 (1 - u_0^2) \left[\frac{B'}{2B} + \frac{2}{r} - \frac{2n+1}{4nc_{s0}^2} \left(\frac{\Delta'}{\Delta} - \frac{B'}{B} \right) \right]}{\left(\frac{2n+1}{2n} + c_{s0}^2 \right) \left(u_0^2 - \frac{c_{s0}^2}{1 + \frac{1}{2n} + c_{s0}^2} \right)} = \frac{N_{\text{ALP}}^{\text{ad}}}{D_{\text{ALP}}^{\text{ad}}}. \quad (7.30)$$

Setting $D_{\text{ALP}}^{\text{ad}} = 0$ gives the critical point condition as

$$u_0^2|_c = \frac{c_{s0}^2}{1 + \beta} \Big|_c, \quad \beta = \frac{\gamma - 1}{2} + c_{s0}^2. \quad (7.31)$$

7.3.4.2 Isothermal case

The disc height for isothermal case, with the equation of state $p = k_0 \rho$, would be given by

$$H(r) = \sqrt{\frac{2}{\alpha}} \sqrt{k_0} \frac{r^2}{\lambda_0} \sqrt{1 - u_0^2}. \quad (7.32)$$

For isothermal case, the mass accretion rate can be written as

$$\Psi|_{\text{ALP}}^{\text{iso}} = \rho_0 \sqrt{k} \frac{r^2}{\lambda_0} 4\pi \sqrt{2B} u_0. \quad (7.33)$$

Taking logarithmic derivative of the above equation with respect to r and substituting ρ'_0/ρ_0 using equation (7.12) gives

$$u'_0|_{\text{ALP}}^{\text{iso}} = \frac{c_{s0}^2 u_0 (1 - u_0^2) \left[\frac{B'}{2B} + \frac{2}{r} - \frac{1}{2c_{s0}^2} \left(\frac{\Delta'}{\Delta} - \frac{B'}{B} \right) \right]}{(1 + c_{s0}^2) \left(1 - \frac{c_{s0}^2}{1 + c_{s0}^2} \right)} = \frac{N|_{\text{ALP}}^{\text{iso}}}{D|_{\text{ALP}}^{\text{iso}}}. \quad (7.34)$$

Setting $D|_{\text{ALP}}^{\text{iso}}$ give the critical point condition as

$$u_0^2 = \frac{c_{s0}^2}{1 + \beta} \Big|_c, \quad \beta = c_{s0}^2. \quad (7.35)$$

Thus we summarize the results obtained for different vertical equilibrium disc models and equations of states as follows. The critical points for any disc model and equation of state are obtained from the condition

$$u_0^2|_c = \frac{c_{s0}^2}{1 + \beta} \Big|_c, \quad (7.36)$$

where β depends on the disc model and the equation state. We give the values of β in table 7.1.

7.4 Acoustic spacetime metric

In this section, we derive the acoustic spacetime metric by linear perturbing the equations governing the accretion flow. Following standard linear perturbation analysis, we write the time-dependent accretion variables, for example, the velocity

Accretion disc models	β for isothermal equation of state	β for adiabatic equation of state
Novikov & Thorne (NT)	0	$\frac{\gamma-1}{2}$
Riffert & Herold (RH)	0	$\frac{\gamma-1}{2}$
Abramowicz Lanza & Percival (ALP)	c_{s0}^2	$\frac{\gamma-1}{2} + c_{s0}^2$

Table 7.1: Values of β for different disc structure models. Critical point condition is given by $u_0^2|_c = \frac{c_{s0}^2|_c}{1+\beta}$.

components and density, as small time-dependent fluctuations about their stationary values. Therefore,

$$\begin{aligned}
 v^t(r, t) &= v_0^t(r) + v_1^t(r, t), \\
 v^r(r, t) &= v_0^r(r) + v_1^r(r, t), \\
 \rho(r, t) &= \rho_0(r) + \rho_1(r, t),
 \end{aligned} \tag{7.37}$$

where the quantities with subscript ‘1’ are the small time-dependent perturbations about the stationary quantity denoted by subscript ‘0’. We define a new variable $\Psi = 4\pi\sqrt{-g}\rho(r, t)v^r(r, t)H_\theta$ which is equal to the stationary mass accretion rate for the stationary accretion flow and hence

$$\Psi(r, t) = \Psi_0 + \Psi_1(r, t), \tag{7.38}$$

where Ψ_0 is the stationary mass accretion rate defined in equation (7.3). The geometric factor 4π is just a constant and therefore, we can redefine the mass accretion rate Ψ as simply $\Psi = \sqrt{-g}\rho(r, t)v^r(r, t)H_\theta$ without any loss of generality. Using the equations (7.37) we get

$$\Psi_1 = \sqrt{-g}[\rho_1 v_0^r H_{\theta 0} + \rho_0 v_1^r H_{\theta 0} + \rho_0 v_0^r H_{\theta 1}]. \tag{7.39}$$

It could be noticed that the perturbation Ψ_1 contains a term which is the perturbation of H_θ . We remember that H_θ is the local angular scale of the flow and is related to the local flow thickness $H(r)$ as $H_\theta = H(r)/r$. The expressions for the

disc thickness for vertical equilibrium model of Novikov-Thorne, Riffert-Herold and Abramowicz-Lanza-Percival are given by equation (7.13), (7.23) and (7.28), respectively. These expression contains p/ρ and further analysis needs an equation of state. Below we perform the analysis for adiabatic equation of state and isothermal equation of state.

7.4.1 Acoustic metric for adiabatic flow

For adiabatic flow, pressure is given by $p = k\rho^\gamma$. The enthalpy can be thus written as

$$h = 1 + \frac{\gamma}{\gamma - 1} \frac{p}{\rho}, \quad (7.40)$$

and the perturbation h_1 can be written as

$$h_1 = \frac{h_0 c_{s0}^2}{\rho_0} \rho_1. \quad (7.41)$$

We assume the accretion flow to be irrotational. Irrotationality condition provides the following equation for adiabatic flow [6]

$$\partial_\mu(hv_\nu) - \partial_\nu(hv_\mu) = 0. \quad (7.42)$$

The above equation along with the spherical symmetry of the flow (which implies $\partial_\phi = 0$) provide the conserved quantity $hv_\phi = \text{constant}$. Thus, using equation (7.41) one obtains

$$v_{\phi 1} = -\frac{v_{\phi 0} c_{s0}^2}{\rho_0} \rho_1. \quad (7.43)$$

Linear perturbing the equation given by normalization condition, i.e., $v_\mu v^\mu = -1$ and using $v_1^\phi = (1/g_{\phi\phi})v_{\phi 1}$ gives the perturbation of v^t in terms of v_1^r and ρ_1 as

$$v_1^t = \alpha_1 v_1^r + \alpha_2 \rho_1, \quad \alpha_1 = \frac{g_{rr} v_0^r}{g_{tt} v_0^t} \quad \text{and} \quad \alpha_2 = -\frac{g_{\phi\phi} (v_\phi^0)^2 c_{s0}^2}{g_{tt} v_0^t \rho_0}. \quad (7.44)$$

We express $H_{\theta 1}$ in terms of perturbations of other quantities. For Novikov-Thorne and Riffert-Herold, we get

$$\frac{H_{\theta 1}}{H_{\theta 0}} = \left(\frac{\gamma - 1}{2} \right) \frac{\rho_1}{\rho_0}, \quad (7.45)$$

and for Abramowicz-Lanza-Percival, we have

$$\frac{H_{\theta 1}}{H_{\theta 0}} = \left(c_{s0}^2 + \frac{\gamma - 1}{2} \right) \frac{\rho_1}{\rho_0}. \quad (7.46)$$

Thus the expressions for different vertical equilibrium disc models can be given by an single equation as

$$\frac{H_{\theta 1}}{H_{\theta 0}} = \beta \frac{\rho_1}{\rho_0}, \quad (7.47)$$

where β for different disc models for adiabatic equation of state are given in Table 7.1. Using this expression of $H_{\theta 1}$, we derive the acoustic metric for the three different disc models in a combined way.

The continuity equation for vertically averaged accretion flow takes the form

$$\partial_t(\sqrt{-g}\rho v^t H_\theta) + \partial_r(\sqrt{-g}\rho v^r H_\theta) = 0. \quad (7.48)$$

Using equation (7.37) and (7.38) in the above equation and further using equation (7.44) and (7.47) provides

$$\frac{\partial_r \Psi_1}{\Psi_0} = - \left[\left\{ \frac{\alpha_2}{v_0^r} + (1 + \beta) \frac{v_0^t}{\rho_0 v_0^r} \right\} \partial_t \rho_1 + \frac{\alpha_1}{v_0^r} \partial_t v_1^r \right]. \quad (7.49)$$

Differentiating equation (7.39) with respect to t and using equation (7.47) gives

$$\frac{\partial_t \Psi_1}{\Psi_0} = (1 + \beta) \frac{\partial_t \rho_1}{\rho_0} + \frac{1}{v_0^r} \partial_t v_1^r. \quad (7.50)$$

Equation (7.49) and (7.50) could be used to express $\partial_t v_1^r$ and $\partial_t \rho_1$ entirely in terms of derivatives of Ψ_1 . This provides

$$\frac{\partial_t v_1^r}{v_0^r} = \frac{1}{\Lambda} \left[\left\{ g_{tt}(v_0^t)^2(1 + \beta) - g_{\phi\phi}(v_0^\phi)^2 c_{s0}^2 \right\} \frac{\partial_t \Psi_1}{\Psi_0} + (1 + \beta) g_{tt} v_0^r v_0^t \frac{\partial_r \Psi_1}{\Psi_0} \right], \quad (7.51)$$

and

$$\frac{\partial_t \rho_1}{\rho_0} = -\frac{1}{\Lambda} \left[g_{tt}(v_0^r)^2 \frac{\partial_t \Psi_1}{\Psi_0} + g_{tt} v_0^r v_0^t \frac{\partial_r \Psi_1}{\Psi_0} \right], \quad (7.52)$$

where Λ is given by

$$\Lambda = (1 + \beta) + (1 + \beta - c_{s0}^2) g_{\phi\phi} (v_0^\phi)^2. \quad (7.53)$$

The temporal component of the Euler equation (7.1) for axially symmetric flow can be written as

$$v^t \partial_t v^t + \frac{c_{s0}^2}{\rho} \frac{\{g_{rr}(v_r)^2 + g_{\phi\phi}(v_\phi)^2\}}{g_{tt}} \partial_t \rho + v^r v^t \partial_r \{\ln(hv_t)\} = 0. \quad (7.54)$$

Differentiating the above equation with respect to t and using the perturbation equations (7.37), (7.41) and (7.44) provides

$$\partial_t \left(\frac{\alpha_1}{v_0^r} \partial_t v_1^r \right) + \partial_t \left(\frac{\alpha_1 c_s^2}{\rho_0} \partial_t \rho_1 \right) + \partial_r \left(\frac{\alpha_1}{v_0^t} \partial_t v_1^r \right) + \partial_r \left\{ \left(\frac{\alpha_2}{v_0^t} + \frac{c_s^2}{\rho_0} \right) \partial_t \rho_1 \right\} = 0. \quad (7.55)$$

Finally substituting $\partial_t v_1^r$ and $\partial_t \rho_1$ in the above equation using equation (7.51) and (7.52), respectively, gives the following equation

$$\partial_\mu (F^{\mu\nu} \partial_\nu \Psi_1) = 0, \quad (7.56)$$

where μ, ν run from 0 to 1. 0 stands for t and 1 stands for r . The matrix $F^{\mu\nu}$ is symmetric and is given by

$$F^{\mu\nu} = \frac{g_{rr} v_0 c_{s0}^2}{v_0^t \Lambda} \begin{bmatrix} -g^{tt} + (1 - \frac{1+\beta}{c_{s0}^2})(v_0^t)^2 & v_0^r v_0^t (1 - \frac{1+\beta}{c_{s0}^2}) \\ v_0^r v_0^t (1 - \frac{1+\beta}{c_{s0}^2}) & g^{rr} + (1 - \frac{1+\beta}{c_{s0}^2}) \end{bmatrix}. \quad (7.57)$$

The equation (7.56) describes the propagation of the perturbation Ψ_1 . Equation (7.56) mimics the wave equation of a massless scalar field φ in curved spacetime. Thus, following the similar procedure as discussed in the previous chapters, the acoustic metric $G_{\mu\nu}$ is obtained to be given by

$$G_{\mu\nu} = k(r) \begin{bmatrix} -g^{rr} - (1 - \frac{1+\beta}{c_{s0}^2})(v_0^r)^2 & v_0^r v_0^t (1 - \frac{1+\beta}{c_{s0}^2}) \\ v_0^r v_0^t (1 - \frac{1+\beta}{c_{s0}^2}) & g^{tt} - (1 - \frac{1+\beta}{c_{s0}^2})(v_0^t)^2 \end{bmatrix}, \quad (7.58)$$

where $k(r)$ is some conformal factor arising due to the process of inverting $G^{\mu\nu}$ in order to obtain $G_{\mu\nu}$. For our current purpose we do not need to find the exact expression for $k(r)$. In the following section we will be using equation (7.58) to solve for the null acoustic geodesic.

7.4.2 Acoustic metric for isothermal flow

The procedure to derive the acoustic metric for isothermal flow is exactly the same as laid out in the previous section 7.4.1. The differences comes from the difference in

the equation of state. For isothermal equation of state, $p/\rho = \text{constant}$. The sound speed is defined by equation (3.8). The irrotationality condition for isothermal flow is given by [64]

$$\partial_\mu(\rho^{c_s^2} v_\nu) - \partial_\nu(\rho^{c_s^2} v_\mu) = 0, \quad (7.59)$$

where the sound speed c_s is a constant for isothermal flow. Using the above equation and the axial symmetry of the flow provides

$$\rho^{c_s^2} v_\phi = \text{constant}. \quad (7.60)$$

Linear perturbation of the above equation leads to the same equation as equation (7.43) with c_s now a constant. The perturbation of H_θ gives

$$\frac{H_{\theta 1}}{H_{\theta 0}} = \beta \frac{\rho_1}{\rho_0}, \quad (7.61)$$

where β for isothermal flow for different model is given in Table 7.1. The detailed derivation of acoustic metric for isothermal flow for vertical equilibrium model of ALP could be found in [64]. The other models follow the same. This leads to the acoustic metric which has the same form as given in equation (7.58) with the only difference is that the sound speed c_s is a constant for the isothermal case.

7.5 Effective speed of acoustic perturbation

The acoustic metric for general relativistic axially symmetric disc in Schwarzschild spacetime was derived in the previous section for adiabatic and isothermal flow which is given by equation (7.58). From the acoustic metric given by equation (7.58), one can find out the location of the acoustic horizon. In analogy to the black hole event horizon in general relativity, the acoustic horizon can be defined as a null surface which acts like a one-way membrane for the acoustic perturbation. In other words, the acoustic perturbations inside the acoustic horizon cannot escape to the outside. For transonic flow, the transonic surface where bulk velocity and speed of acoustic perturbations becomes equal should act like such horizon. Because once the matter flow becomes supersonic, any acoustic perturbations will be dragged

along the medium and hence the perturbation cannot escape to the subsonic region. If a surface $r = \text{constant}$ is the horizon, then the condition that the surface is null with respect to the metric $G_{\mu\nu}$ provides

$$G_{\mu\nu}n^\mu n^\nu = 0, \quad (7.62)$$

where $n_\mu = \delta_\mu^r$ is the normal to the surface $r = \text{constant}$ [12]. Thus $G^{rr} = 0$ gives the location of the sonic horizon. Therefore, in terms of u_0 , the location of the sonic or acoustic horizon is given by $u_0^2 = c_{s0}^2/(1 + \beta)$. However, as argued earlier, the acoustic horizon is basically the transonic surface which in turn implies that the effective speed of the acoustic perturbation is $c_{s0}^{\text{eff}} = c_{s0}/\sqrt{1 + \beta}$. Now, in section 7.3, we showed that the critical point conditions for the different models and equations of state can be written in a single form as $u_0^2 = c_{s0}^2/(1 + \beta)$. Therefore, the critical point condition becomes $u_0^2 = c_{s0}^{\text{eff}2}$. Therefore, the fact that the critical points coincide with the acoustic horizon further implies that the critical points are the transonic points with effective sound speed given by $c_{s0}^{\text{eff}} = c_{s0}/\sqrt{1 + \beta}$. Hence, the apparent mismatch of the critical point and sonic point is resolved if we abandon the static sound speed c_s and use effective speed of sound c_{s0}^{eff} as the speed of propagation of acoustic perturbation and define the Mach number as the ratio of the dynamical bulk velocity u_0 and the effective sound speed c_{s0}^{eff} . In such a case, the critical point and the sonic point (where the Mach number is unity) becomes the same.

The acoustic null ray travelling in the radial direction would be given by $ds^2|_{\theta, \phi = \text{constant}} = 0$ [5]. Thus for acoustic null geodesic, which describes the path of radially travelling phonons, we have

$$G_{tt} + 2G_{rt} \left(\frac{dr}{dt} \right) + G_{rr} \left(\frac{dr}{dt} \right)^2 = 0. \quad (7.63)$$

The metric elements $G_{\mu\nu}$ are expressed in terms of u_0, λ_0 using Eq. (3.116) and

(3.117) as

$$\begin{aligned}
 G_{\mu\nu} &= \frac{k(r)}{\frac{c_{s0}^2}{1+\beta}} \tilde{G}_{\mu\nu}, \\
 \tilde{G}_{tt} &= u_0^2 - \frac{c_{s0}^2}{1+\beta}, \\
 \tilde{G}_{tr} = \tilde{G}_{rt} &= -\frac{u_0}{1-u_0^2} \left(1 - \frac{c_{s0}^2}{1+\beta}\right) \sqrt{\frac{g_{\phi\phi}}{g_{\phi\phi} - \lambda_0^2 g_{tt}}}, \\
 \tilde{G}_{rr} &= \frac{1}{g_{tt}} \frac{c_{s0}^2}{1+\beta} + \frac{1}{g_{tt}(1-u_0^2)} \left(1 - \frac{c_{s0}^2}{1+\beta}\right) \frac{g_{\phi\phi}}{g_{\phi\phi} - \lambda_0^2 g_{tt}}.
 \end{aligned} \tag{7.64}$$

The null geodesic is independent of the conformal factor and hence we can use $\tilde{G}_{\mu\nu}$ instead of $G_{\mu\nu}$ in equation (7.63). dr/dt obtained from equation (7.63) is the coordinate speed of the acoustic phonons as observed from infinity. In the large radial distance, the Schwarzschild metric becomes asymptotically flat. In the non-relativistic Newtonian limit, $g_{\mu\nu} \rightarrow \eta^{\mu\nu}$ and $u_0 \ll 1, c_{s0} \ll 1$ where $\eta^{\mu\nu} = \text{diag}(-1, 1, r^2, r^2 \sin^2 \theta)$ is the flat spacetime metric in the polar coordinate. In this limit we have

$$\begin{aligned}
 \tilde{G}_{tt} &= u_0^2 - \frac{c_{s0}^2}{1+\beta}, \\
 \tilde{G}_{tr} = \tilde{G}_{rt} &= -u_0, \\
 \tilde{G}_{rr} &= 1.
 \end{aligned} \tag{7.65}$$

Thus equation (7.63) becomes

$$\left(u_0^2 - \frac{c_{s0}^2}{1+\beta}\right) - 2u_0 \left(\frac{dr}{dt}\right) + \left(\frac{dr}{dt}\right)^2 = 0, \tag{7.66}$$

which could be rewritten as

$$\left|\frac{dr}{dt} - u_0\right| = \frac{c_{s0}}{\sqrt{1+\beta}} = c_{s0}^{\text{eff}}. \tag{7.67}$$

The above equation implies that the acoustic perturbation moves with an effective speed $c_{s0}^{\text{eff}} = c_{s0}/\sqrt{1+\beta}$ relative to the moving medium.

For the isothermal case $\beta = 0$ for NT and RH and $\beta = c_{s0}^2$ for ALP. However, $c_{s0}^2 \ll 1$ and therefore, $1+\beta \rightarrow 1$ and hence $c_{s0}^{\text{eff}} = c_{s0}$. Therefore, for isothermal case, the critical point and sonic point coincide in non-relativistic Newtonian accretion flow. For the adiabatic equation of state, $\beta = (\gamma - 1)/2$ for NT and RH and for

ALP $\beta = (\gamma - 1)/2 + c_{s0}^2$. Thus, $1 + \beta \rightarrow (\gamma + 1)/2$ as $c_{s0}^2 \ll 1$. Therefore, for adiabatic equation of state, effective sound speed is $c_{s0}^{\text{eff}} = \sqrt{2/(\gamma + 1)}c_{s0}$ for all the three disc heights.

7.6 In closing

For accretion flow maintained in hydrostatic equilibrium along the vertical direction, the Mach number does not become unity at critical points and hence the critical points and the sonic points become different (location-wise). This happens because, for such a disc model, the flow thickness contains the expression of sound speed. The deviation of Mach number from unity is always observed for polytropic accretion because the sound speed is a position dependent variable for polytropic flow. For isothermal accretion, the sound speed is a position independent constant (because of the temperature invariance). For accretion under the influence of the post-Newtonian black hole potentials, the critical and the sonic points are thus identical for isothermal flow.

The situation is observed to be completely different for complete general relativistic flow. For certain expressions of disc thickness, the Mach number deviates from unity at the critical point even for isothermal accretion. For other disc heights, the critical and the sonic points remain the same for isothermal flow. We try to explain such finding in the following way.

The expression for the flow thickness as obtained by ALP has been derived by setting an energy-momentum conservation equation along the vertical direction as well, in addition to the conservation of the Euler equation along the radial direction (for the equatorial plane). Hence the variation of the sound speed gets intrinsically included in the set of equations (written for the equatorial plane) through the process of vertical averaging, even if one considers the isothermal flow. The sound speed remains position independent constant only along radial direction if such vertical averaging would not be performed. Hence for accretion discs with flow thickness as expressed by ALP, the critical points and the sonic points are formed at different

radial distances. For two other expressions of disc heights, the relativistic Euler equation is not constructed or solved along the vertical direction.

The effective dynamical sound speed for different disc models and equation states is given by $c_{s0}^{\text{eff}} = c_{s0}/\sqrt{1 + \beta}$. As given in Table 7.1, β depends on the model as well as the equation of state. In particular, it is noticed that for isothermal equation state, β for NT and RH model are zero. For NT and RH, the disc height can be written as $H = \sqrt{p/\rho}f(r)$ where $f(r)$ is function of the radial coordinate only. For isothermal equation of state $p \propto \rho$ and therefore $H \propto f(r)$. Thus for these two models, the disc height is just a function of r for the isothermal equation of state. Thus, the height for such cases does not depend on any flow variables such as the velocity or density. Therefore, such prescription of disc height does not make the critical point different from the sonic point.

For axially symmetric accretion flow maintained in hydrostatic equilibrium along the vertical direction, the local disc thickness $H(r)$ is a function of the radial sound speed as well. Presence of the sound speed, especially when the sound speed is position dependent, is the prime reason behind the formation of the sonic point at a different location than that of the critical point. The assumption of hydrostatic equilibrium along the vertical direction demands the disc to be geometrically thin. Within the framework of the Newtonian gravity, the thickness can be evaluated using the following procedure. The pressure gradient along the vertical direction is balanced by the component of the gravitational force along that direction. From figure 7.1, this gives

$$\frac{1}{\rho} \frac{dp}{dz} = \frac{d\Phi}{dR} \times \sin \theta, \quad (7.68)$$

where $\Phi(R)$ is the gravitational potential and θ is the angle made by the disc at a distance r along the equatorial plane. Assuming the disc to be thin, i.e., $z(r) \ll r$, where $z(r)$ is the half-thickness of the disc as shown in figure 7.1, the above equation becomes

$$\frac{1}{\rho} \frac{dp}{dz} = \frac{d\Phi}{dr} \times \frac{z(r)}{r}, \quad (7.69)$$

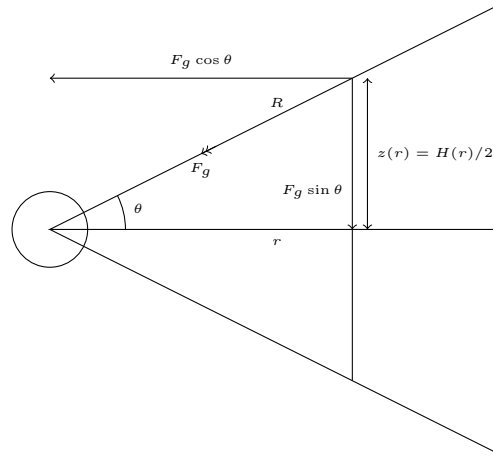


Figure 7.1: Schematic diagram showing the components of the gravitational force

$$F_g = d\Phi/dR .$$

The above equation is further approximated as

$$\frac{1}{\rho} \frac{p}{z(r)} = \frac{d\Phi}{dr} \times \frac{z(r)}{r} . \quad (7.70)$$

For adiabatic equation of state, the sound speed is given by $c_s^2 = \gamma p/\rho$. Thus the disc half-thickness is given by

$$z(r) = c_s \sqrt{\frac{r}{\gamma \frac{d\Phi}{dr}}} . \quad (7.71)$$

While writing dp/dz to be p/z , it has been assumed that a differential form can safely be approximated, at least in the present context. Such approximation assumes that the pressure is a (very) slowly varying function of the coordinate associated with the vertical direction. It is difficult to comment on how accurate such approximation is. To obtain the exact z dependence of the pressure, one needs to formulate and solve the Euler equation along the z direction. Instead of accomplishing such task, usual literature uses the value of the vertically averaged pressure evaluated on the equatorial plane only, thus makes the model effectively one dimensional. Such approximation is probably the major cause behind having a mismatch between the location of the critical and the sonic point. Had it been the case that one would solve a two-dimensional disc structure, the sonic surface would probably coincide with the critical surface. In that case, however, the problem would

not be analytically treatable, not even a semi-analytical method would suffice to address the problem, and it would be imperative to take recourse to full numerical solutions.

Also, it is important to note that a thin disc, where the hydrostatic equilibrium along the vertical direction may be assumed, would incorporate small sound crossing time, and hence, such disc model is more suitable for subsonic flow only. The aforementioned discussion indicates the possible reasons for which the sonic and the critical points are not isomorphic for one-dimensional flow solutions in Newtonian gravity. For general relativistic fluid, the governing equations look more complex and the overall solution method is rather involved. However, the overall underlying logic used to develop the solution remains the same. It is not possible to analytically/semi-analytically construct a two-dimensional disc model where the sonic points would automatically coincide with the critical points. Analytical methods restrict us to use the effective one-dimensional flow structure with vertically averaged values of accretion variables. Within such set of constraints, what best can be done is to redefine the concept of the sound speed through a dynamical approach and to introduce an effective sound speed which makes a sonic point to coincide with a critical point. We have done the same in the present work.

It is, however, important to note that it is difficult to conclude the universality of such phenomena (which kind of disc height will or will not exhibit the non-isomorphism of critical points) since the corresponding expression for flow thicknesses in the works considered here have been derived using a certain set of idealized assumptions. A more realistic flow thickness may be derived by employing the non-LTE radiative transfer [140, 141] or by taking recourse to the Grad-Shafranov equations for the MHD flows [142–144].

8

Concluding remarks

Before we summarise the results of the thesis, let us discuss some of the ongoing works on the analogue gravity phenomenon in the context of accretion astrophysics.

8.1 Non-linear perturbations and acoustic spacetime

The general procedure to obtain the analogue spacetime metric is to perform a linear perturbation analysis. However, one may ask whether the emergence of the analogue spacetime metric is a consequence of only linear perturbation or non-linear perturbation could also lead to such analogue spacetime metric. For example, instead of performing a linear order perturbation analysis, one may extend the perturbation analysis up to second order in the perturbed quantities and ask whether the resulting perturbation equations could be interpreted in a way where analogue spacetime metric could be obtained. Recently, Roy *et al* [145] has attempted such a task by performing perturbation analysis up to second order in perturbed quantities in a Newtonian fluid system. Such a task not only answers whether analogue gravity phenomenon could be found in a more general way than just in a linearized fluid system but also provides a way to test non-linear stability analysis of the accretion flow. There are two existing ways to approach the non-linear perturbation analysis— one is the way as discussed in the works of Roy *et al* [145] and another is the way which could be found in [146] by Sen *et al*. Of course, there are plenty of numerical

works which deal with non-linear stability analysis by numerical simulation of the accretion disc. However, we are more interested in the analytical approach which also addresses the analogue gravity phenomenon also.

The first approach to introduce higher-order perturbation is to expand the time-dependent fluctuations of the accretion variables about their stationary background values as a sum of higher order modes with successively diminishing amplitudes. Thus any variable $x(t, r)$ is written as

$$x(t, r) = x_0(r) + \epsilon x_1(t, r) + \epsilon^2 x_2(t, r) + \mathcal{O}(\epsilon^3), \quad (8.1)$$

where $x_2 \ll x_1$ and it is also assumed that the origin of the fluctuations are independent and they do not add up to give a single resultant perturbation. Such a perturbation scheme for inviscid, irrotational and barotropic fluid in Newtonian framework gives the following perturbation equation in terms of the perturbation of the mass accretion rate $f = \rho v r^2$

$$\partial_\mu (h^{\mu\nu} \partial_\nu f_1) = 0, \quad (8.2)$$

$$\partial_\mu (h^{\mu\nu} \partial_\nu f_2) - \partial_\mu (g^{\mu\nu} \partial_\nu f_1) = 0, \quad (8.3)$$

where the $h^{\mu\nu}$ and $g^{\mu\nu}$ metric elements are given by

$$\begin{aligned} h^{tt} &= \frac{v_0}{f_0}, \\ h^{tr} &= h^{rt} = \frac{v_0^2}{f_0}, \\ h^{rr} &= \frac{v_0}{f_0} (v_0^2 - c_{s0}^2), \\ g^{tt} &= \frac{\rho_1 v_0}{\rho_0 f_0}, \\ g^{tr} &= g^{rt} = \frac{\rho_1 v_0}{\rho_0 f_0} \left[v_0 - \frac{\rho_0}{\rho_1} v_1 \right], \\ g^{rr} &= \frac{\rho_1 v_0}{\rho_0 f_0} \left[(v_0^2 - c_{s0}^2) + (\gamma - 1) c_{s0}^2 - \frac{\rho_0}{\rho_1} 2v_0 v_1 \right], \end{aligned} \quad (8.4)$$

where ρ is the density, v is the velocity of fluid and c_{s0} is the sound speed. γ is the specific heat of the fluid. This is the approach and corresponding results obtained in [145]. Eq. (8.2) can be interpreted in the usual way that the perturbation f_1 is governed by the curved spacetime metric related to $h^{\mu\nu}$. However, in the wave

equation for f_2 there is a source term which is coupled to $h^{\mu\nu}$ and we can not use the usual method to find out and associate an analogue metric to $g^{\mu\nu}$ which governs the propagation of the second order mode f_2 .

The second approach to study non-linear perturbation in accretion flow, a variable $x(t, r)$ is written as $x(t, r) = x_0(r) + x'(t, r)$ and then the perturbation equation is obtained in terms of the fluctuations without neglecting any higher order terms like $\rho'v'$ or ρ'^2 and v'^2 . For example, the fluctuation of the mass accretion rate (defined as $f = \rho v r^2$) is expressed as

$$\frac{f'}{f_0} = \frac{\rho'}{\rho_0} + \frac{v'}{v_0} + \frac{\rho' v'}{\rho_0 v_0}. \quad (8.5)$$

Using such perturbation scheme to the continuity equation and Euler equation, the perturbation equation could be found in terms of f' as

$$\partial_\mu (h^{\mu\nu} \partial_\nu f') = 0, \quad (8.6)$$

where $h^{\mu\nu}$ elements are given by

$$\begin{aligned} h^{tt} &= \frac{v}{f}, \\ h^{tr} &= h^{rt} = \frac{v^2}{f}, \\ h^{rr} &= \frac{v}{f}(v^2 - c_s^2). \end{aligned} \quad (8.7)$$

The metric elements $h^{\mu\nu}$ contains the full variables v, f, c_s and not only the stationary values. Thus the Eq. (8.6) becomes the usual linear perturbation equation if the in the metric elements the variables are replaced by their stationary values. In fact, we can expand the variables upto any higher order to get non-linear perturbation equation. However, unlike the linear case, $h^{\mu\nu}$ in Eq. (8.6) is time-dependent and not stationary. Thus we are unable to compare it to the wave equation of massless scalar field propagating in stationary curved spacetime. Therefore, the usual method to obtain the acoustic metric fails. This fact is complemented by numerical simulation done by Mach and Malec [147] where it is shown that introducing non-linear perturbation would force the acoustic horizons to suffer a shift about their stationary values and thus the comparison between the acoustic horizon and the event horizon of the black hole would appear limited.

8.2 Effective sound speed in accretion disc around Kerr black holes

In Chap. 7, we discussed an effective sound speed obtained through the study of acoustic perturbation and corresponding acoustic metric in accretion discs under hydrostatic equilibrium along the vertical direction in the Schwarzschild spacetime. The next step is to study whether such an effective sound speed could be defined also in accretion disc around Kerr black holes to remove the non-isomorphism of the critical points and the transonic points of the accretion flow under hydrostatic equilibrium along the vertical direction. Such an attempt could be found in recent work by Maity *et al* [148].

8.3 Brief summary

The underlying theme of our work was to show how the linear perturbation analysis of the accretion flow gives rise to the acoustic spacetime metric. First, we showed that this emergence of the curved acoustic metric is independent of the physical quantity which is being linearly perturbed. In other words, we showed that the linear perturbation of the velocity potential, mass accretion rate and the relativistic Bernoulli's constant give rise to the same acoustic spacetime metric up to a conformal factor. However, the acoustic spacetime time metric obtained by linear perturbation depends sensitively on the geometry of the accretion disc, i.e., the geometrical configuration of accreting matter. It was shown that while the acoustic metric for accretion disc with conical and constant height geometry are identical, it differs in the case of accretion flow in hydrostatic equilibrium along the vertical direction.

Acoustic event horizon have been identified by using the analogy borrowed from the general relativity. For a stationary, asymptotically flat spacetime with the event horizon of spherical topology, the event horizon could be defined as $r = \text{constant}$ null hypersurface. In the corotating frame, we found that the event horizon of the

acoustic spacetime metric for an accretion flow is located at the critical points of the stationary accretion flow. For accretion flow with conical or constant height disc models, the critical points are the transonic points. Thus for these models of the accretion disc, the transonic surface and the acoustic horizon coincide. However, for an accretion flow in hydrostatic equilibrium along the vertical direction, the transonic points and the critical points are not isomorphic and therefore the acoustic horizon and the transonic surface for this particular model of accretion disc are not the same surfaces. This apparent non-isomorphism of the critical points and the transonic points could be removed by defining an “effective” sound speed which is the speed of propagation of the acoustic perturbations. The transonic point defined in terms of the “effective” sound speed coincide with the critical point and hence coincide also with the acoustic horizon of the acoustic spacetime.

The event horizon of an acoustic black hole is basically the boundary of the region from which null geodesics cannot escape to the outside. In terms of the sound-cones, this is the surface where the sound-cone tilts past the vertical. This is best visualized by constructing the causal structure of the acoustic spacetime. For illustration, we have constructed the causal structure for radially travelling null geodesics. By numerically integrating the stationary accretion flow equation, we constructed the causal structure which showed the existence of an acoustic horizon at the critical points of the flow where the sound-cones tilt past the vertical.

Depending on the physical parameters governing the stationary flow, there could be more than one critical points of the flow. We showed that for a particular set of values of the governing parameters, the accretion flow could be multi transonic by encountering a stationary shock. We showed by drawing the causal structure that the shock location indicates the presence of an acoustic white hole.

Astrophysical black holes are supposed to possess non-zero spin a . Thus it is important to understand how the black hole spin influences the properties of the acoustic black hole. The influence of the black hole spin was studied in details by performing the linear perturbation of the accretion flow on to a rotating black hole. We studied the dependence of the location of the acoustic event horizon (both

inner and outer for multi transonic flow) on the black hole spin for fixed values of the other parameters. Similarly, the dependence of the causal structure and the acoustic surface gravity on the black hole spin was studied in details.

Our analysis was done for Schwarzschild and Kerr spacetime using both isothermal as well as the adiabatic equation of state. Thus our work provides the necessary elements to complete a set of work on the analogue gravity phenomenon arising in accretion flow in general relativistic spacetime metric. We showed how the linear perturbation equation could be used to perform a linear stability analysis of the stationary accretion solutions and in this way, our work combines these two apparently disjoint phenomena—the emergence of analogue gravity metric and the linear stability analysis of the stationary accretion solutions.

Bibliography

- [1] W. G. Unruh. In: *Phys. Rev. Lett.* 46 (21 1981), pp. 1351–1353. DOI: [10.1103/PhysRevLett.46.1351](https://doi.org/10.1103/PhysRevLett.46.1351) (cit. on pp. 7, 8, 12, 21, 39, 66).
- [2] W. G. Unruh. In: *Phys. Rev. D* 51 (6 1995), pp. 2827–2838. DOI: [10.1103/PhysRevD.51.2827](https://doi.org/10.1103/PhysRevD.51.2827) (cit. on pp. 7, 11).
- [3] S. W. Hawking. In: *Communications in Mathematical Physics* 43.3 (1975), pp. 199–220 (cit. on pp. 7, 66).
- [4] MATT VISSER. In: *International Journal of Modern Physics D* 12.04 (2003), pp. 649–661. DOI: [10.1142/S0218271803003190](https://doi.org/10.1142/S0218271803003190) (cit. on p. 8).
- [5] Matt Visser. In: *Classical and Quantum Gravity* 15.6 (1998), p. 1767. DOI: [10.1088/0264-9381/15/6/024](https://doi.org/10.1088/0264-9381/15/6/024) (cit. on pp. 8, 11, 20, 28, 39, 98, 147).
- [6] Neven Bilic. In: *Classical and Quantum Gravity* 16.12 (1999), p. 3953. DOI: [10.1088/0264-9381/16/12/312](https://doi.org/10.1088/0264-9381/16/12/312) (cit. on pp. 12, 33, 41, 101, 143).
- [7] S.M. Carroll. Addison Wesley, 2004 (cit. on pp. 12, 54).
- [8] Carlos Barcelo, Stefano Liberati, and Matt Visser. In: *Living Reviews in Relativity* 8.1 (2005), p. 12. DOI: [10.1007/lrr-2005-12](https://doi.org/10.1007/lrr-2005-12) (cit. on pp. 13, 14, 51).
- [9] Carlos Barceló et al. In: *New Journal of Physics* 6.1 (2004), p. 186. DOI: [10.1088/1367-2630/6/1/186](https://doi.org/10.1088/1367-2630/6/1/186) (cit. on pp. 13, 15, 16, 18, 51).
- [10] Eric Poisson. Cambridge University Press, 2004 (cit. on p. 20).
- [11] Robert M Wald. Chicago, IL: Chicago Univ. Press, 1984 (cit. on pp. 20, 67).

-
- [12] V. Moncrief. In: *Astrophysical Journal* 235 (Feb. 1980), pp. 1038–1046. DOI: [10.1086/157707](https://doi.org/10.1086/157707) (cit. on pp. 21, 29, 30, 39, 54, 147).
- [13] Tapas K Das. In: *Classical and Quantum Gravity* 21.22 (2004), p. 5253. DOI: [10.1088/0264-9381/21/22/016](https://doi.org/10.1088/0264-9381/21/22/016) (cit. on pp. 21, 39, 119, 131).
- [14] Germain Rousseaux et al. In: *New Journal of Physics* 10.5 (2008), p. 053015. DOI: [10.1088/1367-2630/10/5/053015](https://doi.org/10.1088/1367-2630/10/5/053015) (cit. on p. 22).
- [15] Germain Rousseaux et al. In: *New Journal of Physics* 12.9 (2010), p. 095018. DOI: [10.1088/1367-2630/12/9/095018](https://doi.org/10.1088/1367-2630/12/9/095018) (cit. on p. 22).
- [16] G. Jannes et al. In: *Phys. Rev. E* 83 (5 2011), p. 056312. DOI: [10.1103/PhysRevE.83.056312](https://doi.org/10.1103/PhysRevE.83.056312) (cit. on p. 22).
- [17] Silke Weinfurtner et al. In: *Phys. Rev. Lett.* 106 (2 2011), p. 021302. DOI: [10.1103/PhysRevLett.106.021302](https://doi.org/10.1103/PhysRevLett.106.021302) (cit. on p. 22).
- [18] Ulf Leonhardt and Scott Robertson. In: *New Journal of Physics* 14.5 (2012), p. 053003. DOI: [10.1088/1367-2630/14/5/053003](https://doi.org/10.1088/1367-2630/14/5/053003) (cit. on p. 22).
- [19] Scott J Robertson. In: *Journal of Physics B: Atomic, Molecular and Optical Physics* 45.16 (2012), p. 163001. DOI: [10.1088/0953-4075/45/16/163001](https://doi.org/10.1088/0953-4075/45/16/163001) (cit. on p. 22).
- [20] H. Bondi. In: *Monthly Notices of the Royal Astronomical Society* 112.2 (1952), pp. 195–204 (cit. on pp. 25, 26).
- [21] F. Curtis Michel. In: *Astrophysics and Space Science* 15.1 (1972), pp. 153–160 (cit. on pp. 25, 26, 35).
- [22] Neven Bilic et al. In: *Classical and Quantum Gravity* 31.3 (2014), p. 035002. DOI: [10.1088/0264-9381/31/3/035002](https://doi.org/10.1088/0264-9381/31/3/035002) (cit. on pp. 25, 39, 119, 131).
- [23] Monika Mościbrodzka, Tapas K. Das, and Bożena Czerny. In: *Monthly Notices of the Royal Astronomical Society* 370.1 (2006), pp. 219–228. DOI: [10.1111/j.1365-2966.2006.10470.x](https://doi.org/10.1111/j.1365-2966.2006.10470.x) (cit. on p. 28).
- [24] A. F. Illarionov and R. A. Sunyaev. In: *Astronomy & Astrophysics* 39 (1975), p. 205 (cit. on p. 28).

- [25] E. P. Liang and P. L. Nolan. In: *Space Science Reviews* 38.3 (1984), pp. 353–384. DOI: [10.1007/BF00176834](https://doi.org/10.1007/BF00176834) (cit. on p. 28).
- [26] D. V. Bisikalo et al. In: *Monthly Notices of the Royal Astronomical Society* 300.1 (1998), pp. 39–48. DOI: [10.1046/j.1365-8711.1998.01815.x](https://doi.org/10.1046/j.1365-8711.1998.01815.x) (cit. on p. 28).
- [27] A. F. Illarionov. In: *Soviet Astron.* 31 (1988), p. 618 (cit. on p. 28).
- [28] Luis C. Ho. In: *Observational Evidence for Black Holes in the Universe*. Ed. by Sandip K. Chakrabarti. Dordrecht: Springer Netherlands, 1999, pp. 157–186 (cit. on p. 28).
- [29] Igor V. Igumenshchev and Marek A. Abramowicz. In: *Monthly Notices of the Royal Astronomical Society* 303.2 (1999), pp. 309–320. DOI: [10.1046/j.1365-8711.1999.02220.x](https://doi.org/10.1046/j.1365-8711.1999.02220.x) (cit. on p. 28).
- [30] EPT Liang and KA Thompson. In: *The Astrophysical Journal* 240 (1980), pp. 271–274. DOI: [10.1086/158231](https://doi.org/10.1086/158231) (cit. on pp. 28, 29, 123, 129).
- [31] M. Morris and E. Serabyn. In: *Annual Review of Astronomy and Astrophysics* 34 (1996), pp. 645–702. DOI: [10.1146/annurev.astro.34.1.645](https://doi.org/10.1146/annurev.astro.34.1.645) (cit. on p. 28).
- [32] M. A. Abramowicz and W. H. Zurek. In: *The Astrophysical Journal* 246 (May 1981), pp. 314–320. DOI: [10.1086/158924](https://doi.org/10.1086/158924) (cit. on pp. 29, 129).
- [33] B. Muchotrzeb and B. Paczynski. In: *Acta Astronomica* 32 (1982), pp. 1–11 (cit. on pp. 29, 129).
- [34] B. Muchotrzeb. In: *Acta Astronomica* 33 (1983), pp. 79–87 (cit. on pp. 29, 129).
- [35] J. Fukue. In: *Publications of the Astronomical Society of Japan* 35 (1983), pp. 355–364 (cit. on pp. 29, 129).
- [36] J. Fukue. In: *PASJ* 39 (1987), pp. 309–327 (cit. on pp. 29, 129, 130).
- [37] J. F. Lu. In: *Astronomy and Astrophysics* 148 (July 1985), pp. 176–178 (cit. on pp. 29, 129).

-
- [38] J. F. Lu. In: *General Relativity and Gravitation* 18.1 (1986), pp. 45–51. DOI: [10.1007/BF00843747](https://doi.org/10.1007/BF00843747) (cit. on pp. 29, 129).
- [39] B. Muchotrzeb and Czerny B. In: *Acta Astronomica* 36 (1986) (cit. on pp. 29, 129).
- [40] M. A. Abramowicz and S. Kato. In: *Astrophysical Journal* 336 (Jan. 1989), pp. 304–312. DOI: [10.1086/167012](https://doi.org/10.1086/167012) (cit. on pp. 29, 129).
- [41] M. A. Abramowicz and S. K. Chakrabarti. In: *Astrophysical Journal* 350 (Feb. 1990), pp. 281–287. DOI: [10.1086/168380](https://doi.org/10.1086/168380) (cit. on pp. 29, 129).
- [42] Sandip K. Chakrabarti. In: *Physics Reports* 266.5 (1996), pp. 229–390. DOI: [https://doi.org/10.1016/0370-1573\(95\)00057-7](https://doi.org/10.1016/0370-1573(95)00057-7) (cit. on pp. 29, 123, 129).
- [43] M. Kafatos and R. X. Yang. In: *Monthly Notices of the Royal Astronomical Society* 268 (June 1994), p. 925. DOI: [10.1093/mnras/268.4.925](https://doi.org/10.1093/mnras/268.4.925) (cit. on pp. 29, 129).
- [44] R. Yang and M. Kafatos. In: *Astronomy and Astrophysics* 295 (Mar. 1995), pp. 238–244 (cit. on pp. 29, 116, 129).
- [45] V. I. Pariev. In: *Monthly Notices of the Royal Astronomical Society* 283.4 (1996), pp. 1264–1280. DOI: [10.1093/mnras/283.4.1264](https://doi.org/10.1093/mnras/283.4.1264) (cit. on pp. 29, 129).
- [46] J. Peitz and S. Appl. In: *Monthly Notices of the Royal Astronomical Society* 286 (Apr. 1997), pp. 681–695. DOI: [10.1093/mnras/286.3.681](https://doi.org/10.1093/mnras/286.3.681) (cit. on pp. 29, 129).
- [47] David M. Caditz and Sachiko Tsuruta. In: *The Astrophysical Journal* 501.1 (1998), p. 242 (cit. on pp. 29, 129).
- [48] Tapas K. Das. In: *The Astrophysical Journal* 577.2 (2002), p. 880. DOI: [10.1086/342114](https://doi.org/10.1086/342114) (cit. on pp. 29, 129, 130).
- [49] Tapas K. Das, Jayant K. Pendharkar, and Sanjit Mitra. In: *The Astrophysical Journal* 592.2 (2003), p. 1078. DOI: [10.1086/375732](https://doi.org/10.1086/375732) (cit. on pp. 29, 129).

- [50] Paramita Barai, Tapas K. Das, and Paul J. Wiita. In: *The Astrophysical Journal Letters* 613.1 (2004), p. L49. DOI: [10.1086/424875](https://doi.org/10.1086/424875) (cit. on pp. 29, 129).
- [51] J. Fukue. In: *Publications of the Astronomical Society of Japan* (2004) (cit. on pp. 29, 129, 131).
- [52] Hrvoje Abraham, Neven Bilic, and Tapas K Das. In: *Classical and Quantum Gravity* 23.7 (2006), p. 2371. DOI: [10.1088/0264-9381/23/7/010](https://doi.org/10.1088/0264-9381/23/7/010) (cit. on pp. 29, 65, 113, 119, 129, 131).
- [53] Tapas Kumar Das, Neven Bilić, and Surajit Dasgupta. In: *Journal of Cosmology and Astroparticle Physics* 2007.06 (2007), pp. 009–009. DOI: [10.1088/1475-7516/2007/06/009](https://doi.org/10.1088/1475-7516/2007/06/009) (cit. on pp. 29, 39, 119, 129–131).
- [54] Toru Okuda et al. In: *Publications of the Astronomical Society of Japan* 56.3 (2004), pp. 547–552. DOI: [10.1093/pasj/56.3.547](https://doi.org/10.1093/pasj/56.3.547) (cit. on pp. 29, 129).
- [55] T. Okuda, V. Teresi, and D. Molteni. In: *Monthly Notices of the Royal Astronomical Society* 377 (June 2007), pp. 1431–1438. DOI: [10.1111/j.1365-2966.2007.11736.x](https://doi.org/10.1111/j.1365-2966.2007.11736.x) (cit. on pp. 29, 129).
- [56] Tapas K. Das and B. Czerny. In: *New Astronomy* 17.3 (2012), pp. 254–271. DOI: <https://doi.org/10.1016/j.newast.2011.08.002> (cit. on pp. 29, 113, 129, 130).
- [57] Petra Suková and Agnieszka Janiuk. In: *Journal of Physics: Conference Series* 600.1 (2015), p. 012012 (cit. on pp. 29, 129).
- [58] P. Suková and A. Janiuk. In: *Monthly Notices of the Royal Astronomical Society* 447.2 (2015), pp. 1565–1579. DOI: [10.1093/mnras/stu2544](https://doi.org/10.1093/mnras/stu2544) (cit. on pp. 29, 119, 129).
- [59] P. Suková, S. Charzyński, and A. Janiuk. In: *Monthly Notices of the Royal Astronomical Society* 472.4 (2017), pp. 4327–4342. DOI: [10.1093/mnras/stx2254](https://doi.org/10.1093/mnras/stx2254) (cit. on pp. 29, 119, 129).

-
- [60] J.R. Frank, A.R. King, and D.J. Raine. Cambridge astrophysics series. Cambridge University Press, 1985 (cit. on pp. 29, 123, 129).
- [61] Shoji Kato, Jun Fukue, and Shin Mineshige. Kyoto University Press, 2008 (cit. on pp. 29, 129).
- [62] Jacobus A. Petterson, Joseph Silk, and Jeremiah P. Ostriker. In: *Monthly Notices of the Royal Astronomical Society* 191.3 (1980), p. 571. DOI: [10.1093/mnras/191.3.571](https://doi.org/10.1093/mnras/191.3.571) (cit. on pp. 29, 123, 124).
- [63] Satadal Datta, Md Arif Shaikh, and Tapas Kumar Das. In: *New Astronomy* 63 (2018), pp. 65–74. DOI: <https://doi.org/10.1016/j.newast.2018.03.003> (cit. on pp. 29, 39).
- [64] Md Arif Shaikh, Ivleena Firdousi, and Tapas Kumar Das. In: *Classical and Quantum Gravity* 34.15 (2017), p. 155008. DOI: [10.1088/1361-6382/aa7b19](https://doi.org/10.1088/1361-6382/aa7b19) (cit. on pp. 29, 31, 39, 95, 102, 131, 146).
- [65] Feng Yuan, Shawfeng Dong, and Ju-Fu Lu. In: *Astrophysics and Space Science* 246.2 (1996), pp. 197–210. DOI: [10.1007/BF00645640](https://doi.org/10.1007/BF00645640) (cit. on pp. 33, 93).
- [66] L.D. Landau and E.M. Lifshitz. v. 6. Pergamon, 1987 (cit. on p. 33).
- [67] Wei Chieh Liang and Si Chen Lee. In: *Phys. Rev. D* 87 (4 2013), p. 044024 (cit. on p. 33).
- [68] B. R. Iyer and C. V. Vishveshwara. In: *Phys. Rev. D* 48 (12 1993), pp. 5706–5720 (cit. on p. 34).
- [69] Charles F. Gammie and Robert Popham. In: *The Astrophysical Journal* 498.1 (1998), p. 313. DOI: [10.1086/305521](https://doi.org/10.1086/305521) (cit. on pp. 37, 73, 74, 108).
- [70] I. D. Novikov and K. S. Thorne. In: *Black Holes (Les Astres Occlus)*. Ed. by C. Dewitt and B. S. Dewitt. 1973, pp. 343–450 (cit. on pp. 38, 132, 133, 137, 138).
- [71] H. Riffert and H. Herold. In: *The Astrophysical Journal* 450 (Sept. 1995), p. 508. DOI: [10.1086/176161](https://doi.org/10.1086/176161) (cit. on pp. 38, 132, 133, 137, 139).

- [72] M. A. Abramowicz, A. Lanza, and M. J. Percival. In: *The Astrophysical Journal* 479.1 (1997), p. 179. DOI: [10.1086/303869](https://doi.org/10.1086/303869) (cit. on pp. 38, 65, 132, 133, 137, 140).
- [73] Md Arif Shaikh. In: *Classical and Quantum Gravity* 35.5 (2018), p. 055002 (cit. on pp. 39, 65, 71, 121, 131).
- [74] Surajit Dasgupta, Neven Bilic, and Tapas K. Das. In: *General Relativity and Gravitation* 37.11 (2005), pp. 1877–1890. DOI: [10.1007/s10714-005-0194-9](https://doi.org/10.1007/s10714-005-0194-9) (cit. on pp. 39, 119, 131).
- [75] Deepika B. Ananda, Sourav Bhattacharya, and Tapas K. Das. In: *General Relativity and Gravitation* 47.9 (2015), p. 96 (cit. on pp. 39, 58).
- [76] Deepika A. Bollimpalli, Sourav Bhattacharya, and Tapas K. Das. In: *New Astronomy* 51 (2017), pp. 153–160. DOI: <http://dx.doi.org/10.1016/j.newast.2016.09.001> (cit. on pp. 39, 102, 106).
- [77] Md Arif Shaikh and Tapas Kumar Das. In: *Phys. Rev. D* 98 (12 2018), p. 123022. DOI: [10.1103/PhysRevD.98.123022](https://doi.org/10.1103/PhysRevD.98.123022) (cit. on pp. 39, 65, 99, 121, 131).
- [78] I.P. Bazarov. Pergamon Press, 1964 (cit. on p. 58).
- [79] J.W. Gibbs. Dover Books on Physics. Dover Publications, 2014 (cit. on p. 58).
- [80] S. W. Hawking. In: *Nature* 248 (1974), pp. 30–31 (cit. on p. 66).
- [81] Robert H. Boyer and Richard W. Lindquist. In: 8.265 (2 1967) (cit. on p. 72).
- [82] J. M. Bardeen, W. H. Press, and S. A. Teukolsky. In: *The Astrophysical Journal* 178 (Dec. 1972), pp. 347–370 (cit. on pp. 73, 86, 137).
- [83] S. Chandrasekhar. International series of monographs on physics. Oxford, 1983 (cit. on p. 86).
- [84] V. Frolov and I. Novikov. Fundamental Theories of Physics. Springer Netherlands, 2012 (cit. on p. 86).
- [85] Carl Eckart. In: *Phys. Rev.* 58 (10 1940), pp. 919–924. DOI: [10.1103/PhysRev.58.919](https://doi.org/10.1103/PhysRev.58.919) (cit. on p. 113).

-
- [86] A. H. Taub. In: *Phys. Rev.* 74 (3 1948), pp. 328–334. DOI: [10.1103/PhysRev.74.328](https://doi.org/10.1103/PhysRev.74.328) (cit. on p. 113).
- [87] A. Lichnerowicz. W.A. Benjamin Mathematical Physics Monograph Series. W.A Benjamin, 1967 (cit. on p. 113).
- [88] K. S. Thorne. In: *The Astrophysical Journal* 179 (Feb. 1973), pp. 897–908. DOI: [10.1086/151927](https://doi.org/10.1086/151927) (cit. on p. 113).
- [89] A H Taub. In: *Annual Review of Fluid Mechanics* 10.1 (1978), pp. 301–332. DOI: [10.1146/annurev.fl.10.010178.001505](https://doi.org/10.1146/annurev.fl.10.010178.001505). eprint: <https://doi.org/10.1146/annurev.fl.10.010178.001505> (cit. on p. 113).
- [90] S. Hacyan. In: *General Relativity and Gravitation* 14.4 (1982), pp. 399–410. DOI: [10.1007/BF00756273](https://doi.org/10.1007/BF00756273) (cit. on p. 113).
- [91] Hung-Yi Pu et al. In: *Classical and Quantum Gravity* 29.24 (2012), p. 245020. DOI: [10.1088/0264-9381/29/24/245020](https://doi.org/10.1088/0264-9381/29/24/245020) (cit. on pp. 119, 131).
- [92] Pratik Tarafdar and Tapas K. Das. In: *International Journal of Modern Physics D* 24.14 (2015), p. 1550096. DOI: [10.1142/S0218271815500960](https://doi.org/10.1142/S0218271815500960) (cit. on pp. 119, 129, 131).
- [93] Pratik Tarafdar and Tapas K. Das. In: *International Journal of Modern Physics D* 27.03 (2018), p. 1850023. DOI: [10.1142/S0218271818500232](https://doi.org/10.1142/S0218271818500232) (cit. on pp. 119, 129–131).
- [94] J. F. Hawley, L. L. Smarr, and J. R. Wilson. In: *The Astrophysical Journal* 277 (Feb. 1984), pp. 296–311. DOI: [10.1086/161696](https://doi.org/10.1086/161696) (cit. on p. 119).
- [95] J. F. Hawley, L. L. Smarr, and J. R. Wilson. In: *The Astrophysical Journal* 55 (June 1984), pp. 211–246. DOI: [10.1086/190953](https://doi.org/10.1086/190953) (cit. on p. 119).
- [96] A. Kheyfets, W. A. Miller, and W. H. Zurek. In: *Physical Review D* 41 (Jan. 1990), pp. 451–454. DOI: [10.1103/PhysRevD.41.451](https://doi.org/10.1103/PhysRevD.41.451) (cit. on p. 119).
- [97] J. F. Hawley. In: *The Astrophysical Journal* 381 (Nov. 1991), pp. 496–507. DOI: [10.1086/170673](https://doi.org/10.1086/170673) (cit. on p. 119).

- [98] M. Yokosawa. In: *Publications of the Astronomical Society of Japan* 47 (Oct. 1995), pp. 605–615 (cit. on p. 119).
- [99] I. V. Igumenshchev, X. Chen, and M. A. Abramowicz. In: *Monthly Notices of the Royal Astronomical Society* 278 (Jan. 1996), pp. 236–250. DOI: [10.1093/mnras/278.1.236](https://doi.org/10.1093/mnras/278.1.236). eprint: [astro-ph/9509070](https://arxiv.org/abs/astro-ph/9509070) (cit. on p. 119).
- [100] Igor V. Igumenshchev and Andrei M. Beloborodov. In: *Monthly Notices of the Royal Astronomical Society* 284.3 (1997), p. 767. DOI: [10.1093/mnras/284.3.767](https://doi.org/10.1093/mnras/284.3.767) (cit. on p. 119).
- [101] K. Nobuta and T. Hanawa. In: *The Astrophysical Journal* 510 (Jan. 1999), pp. 614–630. DOI: [10.1086/306591](https://doi.org/10.1086/306591). eprint: [astro-ph/9808254](https://arxiv.org/abs/astro-ph/9808254) (cit. on p. 119).
- [102] D. Molteni, G. Tóth, and O. A. Kuznetsov. In: *The Astrophysical Journal* 516 (May 1999), pp. 411–419. DOI: [10.1086/307079](https://doi.org/10.1086/307079). eprint: [astro-ph/9812453](https://arxiv.org/abs/astro-ph/9812453) (cit. on p. 119).
- [103] J. M. Stone, J. E. Pringle, and M. C. Begelman. In: *Monthly Notices of the Royal Astronomical Society* 310 (Dec. 1999), pp. 1002–1016. DOI: [10.1046/j.1365-8711.1999.03024.x](https://doi.org/10.1046/j.1365-8711.1999.03024.x). eprint: [astro-ph/9908185](https://arxiv.org/abs/astro-ph/9908185) (cit. on p. 119).
- [104] S. E. Caunt and M. J. Korpi. In: *Astronomy and Astrophysics* 369 (Apr. 2001), pp. 706–728. DOI: [10.1051/0004-6361:20010157](https://doi.org/10.1051/0004-6361:20010157). eprint: [astro-ph/0102068](https://arxiv.org/abs/astro-ph/0102068) (cit. on p. 119).
- [105] J. P. De Villiers and J. F. Hawley. In: *The Astrophysical Journal* 577 (Oct. 2002), pp. 866–879. DOI: [10.1086/342238](https://doi.org/10.1086/342238). eprint: [astro-ph/0204163](https://arxiv.org/abs/astro-ph/0204163) (cit. on p. 119).
- [106] Daniel Proga and Mitchell C. Begelman. In: *The Astrophysical Journal* 582.1 (2003), p. 69. DOI: [10.1086/344537](https://doi.org/10.1086/344537) (cit. on p. 119).
- [107] G. Gerardi, D. Molteni, and V. Teresi. In: *ArXiv Astrophysics e-prints* [astro-ph/0501549](https://arxiv.org/abs/astro-ph/0501549) (Jan. 2005). eprint: [astro-ph/0501549](https://arxiv.org/abs/astro-ph/0501549) (cit. on p. 119).

-
- [108] M. Moscibrodzka and D. Proga. In: *The Astrophysical Journal* 679, 626–638 (May 2008), pp. 626–638. DOI: [10.1086/529372](https://doi.org/10.1086/529372). arXiv: [0801.1076](https://arxiv.org/abs/0801.1076) (cit. on p. 119).
- [109] Hiroki Nagakura and Shoichi Yamada. In: *The Astrophysical Journal* 689.1 (2008), pp. 391–406. DOI: [10.1086/590325](https://doi.org/10.1086/590325) (cit. on p. 119).
- [110] Hiroki Nagakura and Shoichi Yamada. In: *The Astrophysical Journal* 696.2 (2009), pp. 2026–2035. DOI: [10.1088/0004-637X/696/2/2026](https://doi.org/10.1088/0004-637X/696/2/2026) (cit. on p. 119).
- [111] Agnieszka Janiuk et al. In: *The Astrophysical Journal* 705.2 (2009), pp. 1503–1521. DOI: [10.1088/0004-637X/705/2/1503](https://doi.org/10.1088/0004-637X/705/2/1503) (cit. on p. 119).
- [112] C. Bambi and N. Yoshida. In: *Physical Review D* 82.6, 064002 (Sept. 2010), p. 064002. DOI: [10.1103/PhysRevD.82.064002](https://doi.org/10.1103/PhysRevD.82.064002). arXiv: [1006.4296](https://arxiv.org/abs/1006.4296) [gr-qc] (cit. on p. 119).
- [113] C. Bambi and N. Yoshida. In: *Physical Review D* 82.12, 124037 (Dec. 2010), p. 124037. DOI: [10.1103/PhysRevD.82.124037](https://doi.org/10.1103/PhysRevD.82.124037). arXiv: [1009.5080](https://arxiv.org/abs/1009.5080) [gr-qc] (cit. on p. 119).
- [114] P. Barai, D. Proga, and K. Nagamine. In: *Monthly Notices of the Royal Astronomical Society* 418 (Nov. 2011), pp. 591–611. DOI: [10.1111/j.1365-2966.2011.19508.x](https://doi.org/10.1111/j.1365-2966.2011.19508.x). arXiv: [1102.3925](https://arxiv.org/abs/1102.3925) [astro-ph.CO] (cit. on p. 119).
- [115] P. Barai, D. Proga, and K. Nagamine. In: *Monthly Notices of the Royal Astronomical Society* 424 (July 2012), pp. 728–746. DOI: [10.1111/j.1365-2966.2012.21260.x](https://doi.org/10.1111/j.1365-2966.2012.21260.x). arXiv: [1112.5483](https://arxiv.org/abs/1112.5483) [astro-ph.CO] (cit. on p. 119).
- [116] Y. Zhu et al. In: *Monthly Notices of the Royal Astronomical Society* 451 (Aug. 2015), pp. 1661–1681. DOI: [10.1093/mnras/stv1046](https://doi.org/10.1093/mnras/stv1046). arXiv: [1505.04838](https://arxiv.org/abs/1505.04838) [astro-ph.HE] (cit. on p. 119).
- [117] R. Narayan et al. In: *Monthly Notices of the Royal Astronomical Society* 457 (Mar. 2016), pp. 608–628. DOI: [10.1093/mnras/stv2979](https://doi.org/10.1093/mnras/stv2979). arXiv: [1510.04208](https://arxiv.org/abs/1510.04208) [astro-ph.HE] (cit. on p. 119).

- [118] M. Mościbrodzka, H. Falcke, and H. Shiokawa. In: *Astronomy & Astrophysics* 586, A38 (Feb. 2016), A38. DOI: [10.1051/0004-6361/201526630](https://doi.org/10.1051/0004-6361/201526630). arXiv: [1510.07243](https://arxiv.org/abs/1510.07243) [astro-ph.HE] (cit. on p. 119).
- [119] A. Sadowski et al. In: *Monthly Notices of the Royal Astronomical Society* 466 (Apr. 2017), pp. 705–725. DOI: [10.1093/mnras/stw3116](https://doi.org/10.1093/mnras/stw3116). arXiv: [1605.03184](https://arxiv.org/abs/1605.03184) [astro-ph.HE] (cit. on p. 119).
- [120] P. Mach, M. Piróg, and J. A. Font. In: *ArXiv e-prints gr-qc:1803.04032* (Mar. 2018). arXiv: [1803.04032](https://arxiv.org/abs/1803.04032) [gr-qc] (cit. on p. 119).
- [121] J. Karkowski et al. In: *ArXiv e-prints gr-qc:1802.02848* (Feb. 2018). arXiv: [1802.02848](https://arxiv.org/abs/1802.02848) [gr-qc] (cit. on p. 119).
- [122] K. Inayoshi et al. In: *Monthly Notices of the Royal Astronomical Society* 476 (May 2018), pp. 1412–1426. DOI: [10.1093/mnras/sty276](https://doi.org/10.1093/mnras/sty276). arXiv: [1709.07452](https://arxiv.org/abs/1709.07452) (cit. on p. 119).
- [123] P. C. Fragile et al. In: *ArXiv e-prints astro-ph.HE : 1803.06423* (Mar. 2018). arXiv: [1803.06423](https://arxiv.org/abs/1803.06423) [astro-ph.HE] (cit. on p. 119).
- [124] A. J. Penner. In: *Monthly Notices of the Royal Astronomical Society* 414.2 (2011), pp. 1467–1482. DOI: [10.1111/j.1365-2966.2011.18480.x](https://doi.org/10.1111/j.1365-2966.2011.18480.x) (cit. on p. 127).
- [125] F. D. Lora-Clavijo and F. S. Guzmán. In: *Monthly Notices of the Royal Astronomical Society* 429.4 (2013), pp. 3144–3154. DOI: [10.1093/mnras/sts573](https://doi.org/10.1093/mnras/sts573) (cit. on p. 127).
- [126] M. Gracia-Linares and F. S. Guzmán. In: *The Astrophysical Journal* 812.1 (2015), p. 23 (cit. on p. 127).
- [127] J. A. González and F. S. Guzmán. In: *Phys. Rev. D* 97 (6 2018), p. 063001. DOI: [10.1103/PhysRevD.97.063001](https://doi.org/10.1103/PhysRevD.97.063001) (cit. on p. 127).
- [128] Md Arif Shaikh et al. In: *New Astronomy* 69 (2019), pp. 48–57. DOI: <https://doi.org/10.1016/j.newast.2018.12.001> (cit. on p. 129).

-
- [129] S. K. Chakrabarti. In: *Astrophysical Journal* 347 (Dec. 1989), pp. 365–372. DOI: [10.1086/168125](https://doi.org/10.1086/168125) (cit. on p. 129).
- [130] Sandip K. Chakrabarti and Santabrata Das. In: *Monthly Notices of the Royal Astronomical Society* 327.3 (2001), pp. 808–812 (cit. on p. 129).
- [131] Sankhasubhra Nag et al. In: *New Astronomy* 17.3 (2012), pp. 285–295 (cit. on p. 129).
- [132] Ryoji Matsumoto et al. In: *Publications of the Astronomical Society of Japan* 36 (1984), pp. 71–85 (cit. on pp. 130, 131).
- [133] Shilpi Agarwal et al. In: *General Relativity and Gravitation* 44.7 (2012), pp. 1637–1655 (cit. on p. 130).
- [134] A. K. Ray. In: *Monthly Notices of the Royal Astronomical Society* 344 (Oct. 2003), pp. 1085–1090. DOI: [10.1046/j.1365-8711.2003.06992.x](https://doi.org/10.1046/j.1365-8711.2003.06992.x) (cit. on p. 131).
- [135] Soumini Chaudhury, Arnab K. Ray, and Tapas K. Das. In: *Monthly Notices of the Royal Astronomical Society* 373.1 (2006), pp. 146–156 (cit. on p. 131).
- [136] Sanghamitra Goswami et al. In: *Monthly Notices of the Royal Astronomical Society* 378.4 (2007), pp. 1407–1417. DOI: [10.1111/j.1365-2966.2007.11869.x](https://doi.org/10.1111/j.1365-2966.2007.11869.x). eprint: [/oup/backfile/content_public/journal/mnras/378/4/10.1111_j.1365-2966.2007.11869.x/1/mnras0378-1407.pdf](https://oup/backfile/content_public/journal/mnras/378/4/10.1111_j.1365-2966.2007.11869.x/1/mnras0378-1407.pdf) (cit. on p. 131).
- [137] Eliana Chaverra, Patryk Mach, and Olivier Sarbach. In: *Classical and Quantum Gravity* 33.10 (2016), p. 105016 (cit. on p. 131).
- [138] Ipsita Mandal, Arnab K. Ray, and Tapas K. Das. In: *Monthly Notices of the Royal Astronomical Society* 378.4 (2007), pp. 1400–1406. DOI: [10.1111/j.1365-2966.2007.11898.x](https://doi.org/10.1111/j.1365-2966.2007.11898.x). eprint: [/oup/backfile/content_public/journal/mnras/378/4/10.1111_j.1365-2966.2007.11898.x/1/mnras0378-1400.pdf](https://oup/backfile/content_public/journal/mnras/378/4/10.1111_j.1365-2966.2007.11898.x/1/mnras0378-1400.pdf) (cit. on p. 131).

- [139] Sonali Saha et al. In: *New Astronomy* 43 (2016), pp. 10–21. DOI: <http://dx.doi.org/10.1016/j.newast.2015.07.007> (cit. on p. 131).
- [140] I. Hubeny and V. Hubeny. In: *The Astrophysical Journal* 505 (Oct. 1998), pp. 558–576. DOI: [10.1086/306207](https://doi.org/10.1086/306207). eprint: [astro-ph/9804288](https://arxiv.org/abs/astro-ph/9804288) (cit. on p. 152).
- [141] S. W. Davis and I. Hubeny. In: *The Astrophysical Journal Supplement Series* 164 (June 2006), pp. 530–535. DOI: [10.1086/503549](https://doi.org/10.1086/503549). eprint: [astro-ph/0602499](https://arxiv.org/abs/astro-ph/0602499) (cit. on p. 152).
- [142] V. S. Beskin. In: *Physics Uspekhi* 40 (July 1997), pp. 659–688. DOI: [10.1070/PU1997v040n07ABEH000250](https://doi.org/10.1070/PU1997v040n07ABEH000250) (cit. on p. 152).
- [143] V. Beskin and A. Tchekhovskoy. In: *Astronomy and Astrophysics* 433 (Apr. 2005), pp. 619–628. DOI: [10.1051/0004-6361:20041592](https://doi.org/10.1051/0004-6361:20041592). eprint: [astro-ph/0412027](https://arxiv.org/abs/astro-ph/0412027) (cit. on p. 152).
- [144] V. S. Beskin. 2010. DOI: [10.1007/978-3-642-01290-7](https://doi.org/10.1007/978-3-642-01290-7) (cit. on p. 152).
- [145] Nandan Roy et al. In: (2018). arXiv: [1803.05312 \[gr-qc\]](https://arxiv.org/abs/1803.05312) (cit. on pp. 153, 154).
- [146] Sourav Sen and Arnab K. Ray. In: *Phys. Rev. D* 89 (6 2014), p. 063004. DOI: [10.1103/PhysRevD.89.063004](https://doi.org/10.1103/PhysRevD.89.063004) (cit. on p. 153).
- [147] P. Mach and E. Malec. In: *Physical Review D* 78.12, 124016 (Dec. 2008), p. 124016. DOI: [10.1103/PhysRevD.78.124016](https://doi.org/10.1103/PhysRevD.78.124016) (cit. on p. 155).
- [148] Susovan Maity, Md Arif Shaikh, and Tapas Kumar Das. In: (2018). arXiv: [1811.04975 \[astro-ph.HE\]](https://arxiv.org/abs/1811.04975) (cit. on p. 156).